Copyright Warning & Restrictions

The copyright law of the United States (Title 17, United States Code) governs the making of photocopies or other reproductions of copyrighted material.

Under certain conditions specified in the law, libraries and archives are authorized to furnish a photocopy or other reproduction. One of these specified conditions is that the photocopy or reproduction is not to be "used for any purpose other than private study, scholarship, or research." If a, user makes a request for, or later uses, a photocopy or reproduction for purposes in excess of "fair use" that user may be liable for copyright infringement,

This institution reserves the right to refuse to accept a copying order if, in its judgment, fulfillment of the order would involve violation of copyright law.

Please Note: The author retains the copyright while the New Jersey Institute of Technology reserves the right to distribute this thesis or dissertation

Printing note: If you do not wish to print this page, then select "Pages from: first page # to: last page #" on the print dialog screen

ABSTRACT

APPLICATION OF THE WAVELET TRANSFORM TO BIOMEDICAL SIGNALS

by
Karl O. Hauck

The basic concepts and fundamentals of the wavelet signal representation were examined. The orthonormal wavelet was selected for this project after being compared to various types of wavelets. The orthonormal wavelet was chosen due to the equal time and frequency resolution exhibited in the wavelet coefficients. Programs were written in Matlab to implement the orthonormal wavelet in developing wavelet coefficients for a given signal. The programs include the conditions for an orthonormal wavelet in and which produce the wavelet filters $g(n)$ and $h(n)$. The wavelet filters were then incorporated into another program that applied Mallat's multiresolution algorithm for a given signal. The resulting wavelet coefficients were obtained and interpreted. The orthonormal wavelet was applied to various types of biomedical signals. The wavelet transform was applied to motor evoked potentials (MEPs) created cortical magnetic stimulation. The wavelet was also applied to evoked potentials (EPs) and to various types of EKG signals. The wavelet representation exposed new ways of observing biomedical signals by bringing out details and structures not present in the original waveforms.

APPLICATION OF THE WAVELET TRANSFORM TO BIOMEDICAL SIGNALS

by
Karl O. Hauck

A Thesis
Submitted to the Faculty of
New Jersey Institute of Technology
in Partial Fulfillment of the Requirements for the Degree of
Master of Science in Electrical Engineering

Department of Electrical and Computer Engineering

January 1994

APPROVAL PAGE

Application of the Wavelet Transform to Biomedical Signals

Karl O. Hauck

Dr. Stanley Reisman, Thesis Advisor — Date
Professor of Electrical Engineering
New Jersey Institute of Technology

Dr. Peter Engler, Committee Member — Date
Associate Professor of Electrical Engineering
New Jersey Institute of Technology

Dr. Thomas Findley, Committee Member — Date
Director of Research
Kessler Institute for Rehabilitation

BIOGRAPHICAL SKETCH

Author: Karl O. Hauck

Degree: Master of Science in Electrical Engineering

Date: January 1994

Undergraduate and Graduate Education:

- Master of Science in Electrical Engineering,
  New Jersey Institute of Technology, Newark, NJ, 1994
- Bachelor of Science in Electrical Engineering,
  New Jersey Institute of Technology, Newark, NJ, 1993

Major: Electrical Engineering

This work is dedicated to my parents, Otto and Lucia Hauck,
and to my fiancee Susan.

ACKNOWLEDGMENT

I would like to express my thanks to my thesis advisor, Professor Stanley Reisman, for his selection of this topic, guidance and support throughout the process of this work.

I would also like to express my appreciation to the distinguished members of my thesis committee, Professor Peter Engler and Dr. Thomas Findley, and to the Kessler Institute of Rehabilitation Research Department for allowing me to use their facilities.

TABLE OF CONTENTS

TABLE OF CONTENTS
(continued)

Chapter **Page**

TABLE OF CONTENTS
(continued)

LIST OF TABLES

Table **Page**

LIST OF FIGURES

Figure **Page**

CHAPTER 1

WAVELETS

1.1 Introduction

The Fourier transform has been the most widely used mathematical tool for signal analysis in science and engineering. Fourier methods allow the transformation of a signal from the time to the frequency domain and enable one to view the properties and features of the signal.

Recently, a new signal processing tool known as wavelets, has been developed. The wavelet transform of a signal is a decomposition of the signal into a set of frequency channels of equal bandwidth [1]. In signal processing terms, the wavelet is essentially an ideal bandpass filter, allowing certain frequency components to pass through without losing any signal information [3]. The bandpass filtering is performed by the successive convolution of the signal with a highpass and lowpass filter, where the combination of the filters produce the bandpass filter. Once these filters are applied, the different scales of the signal, known as the wavelet coefficients, are then obtained.

Each of the different scales pertains to a specific frequency channel [2]. The various scales of the signal bring out the details not present in the original signal. The original signal might seem stationary and smooth but the wavelet representation of the signal brings out components that are not apparent and even transient in nature. Unlike the Fourier transform, the wavelet transform allows one to see the different frequency properties of the signal in the time domain.

1.2 Basic Concepts and Transform Definitions

The wavelet representation of a signal is achieved by a family of functions that is created by sweeping the wavelet along the time axis giving the wavelet a specific location in time.

The basic analyzing wavelet is known as $\Psi(t)$ and the corresponding family of basis functions (Appendix B.2) is defined by integer translations in the time domain [5] by

$$\Psi(t) = \Psi(t-k) \qquad k \in Z \tag{1.1}$$

where Z is an integer vector field (Appendix B.1). The space spanned (Appendix B.2) by $\Psi(t)$ is

$$S = span_k\{\Psi(t-k)\} \tag{1.2}$$

For a given signal *s(t)*, the elements of the space spanned by $\Psi(t)$ are related by

$$s(t) \in S \quad \Rightarrow \quad s(t) = \sum_k a_k \cdot \Psi_k(t) = \sum_k a_k \cdot \Psi(t-k) \tag{1.3}$$

where the space mentioned pertains to the frequency span of the wavelet filters [5]. The wavelet transform previously described will be implemented in discrete translations, decompostions, and interpretations. Therefore, the rest of this discussion and theory developed will remain in the discrete time case.

The wavelet $\Psi(t)$ must next be modified by scaling the time variable to localize the wavelet in scale and frequency and is denoted by

$$\Psi_{j,k}(t) = 2^{-j/2}\Psi(2^{-j}t - k) \qquad j,k \in Z \tag{1.4}$$

where j, also referred to as the dilation, is an integer measure of the scaling of the signal for the jth scale, $2^{-j/2}$ maintains the normalization for the resulting wavelet coefficient at the different scales, and k locates the wavelet in time [5].

A set of wavelet expansion functions can be generated for any signal in the space spanned by $L^2(R)$ by

$$s(t) = \sum_{j,k} a_{j,k} \cdot 2^{-j/2}\Psi(2^{-j}t - k) \tag{1.5}$$

or

$$s(t) = \sum_{j,k} a_{j,k} \cdot \Psi_{j,k}(t) \tag{1.6}$$

where $L^2(R)$ is the space of square-integral functions (Appendix C) and $a_{j,k}$ are the discrete wavelet transforms (DWT) of the signal *s(t)* for scale *j*. If the wavelets, $\Psi_{j,k}(t)$, form an orthonormal basis for the signal *s(t)*, the DWT can be calculated by using inner products (Appendix B.3) where

$$s(t) = \sum_{j,k} \langle \Psi_{j,k}(t), s(t) \rangle \Psi_{j,k}(t). \tag{1.7}$$

To fully understand the effect of the integer *j*, let us take the Fourier transform of 1.4 resulting in

$$\Psi_{j,k}(w) = \Psi(2^{+j} w) e^{-kwi} \tag{1.8}$$

From equation 1.8, it can be observed that as *j* increases one has a finer frequency resolution of detail in the space of functions spanned by the wavelet function $\Psi_{j,k}(t)$ given in 1.4 [5]. It can also be seen from equation 1.4 that the time resolution decreases with *j*. This is clearly shown in figure 1.2.1 which is a plot of time resolution verses frequency resolution [2].

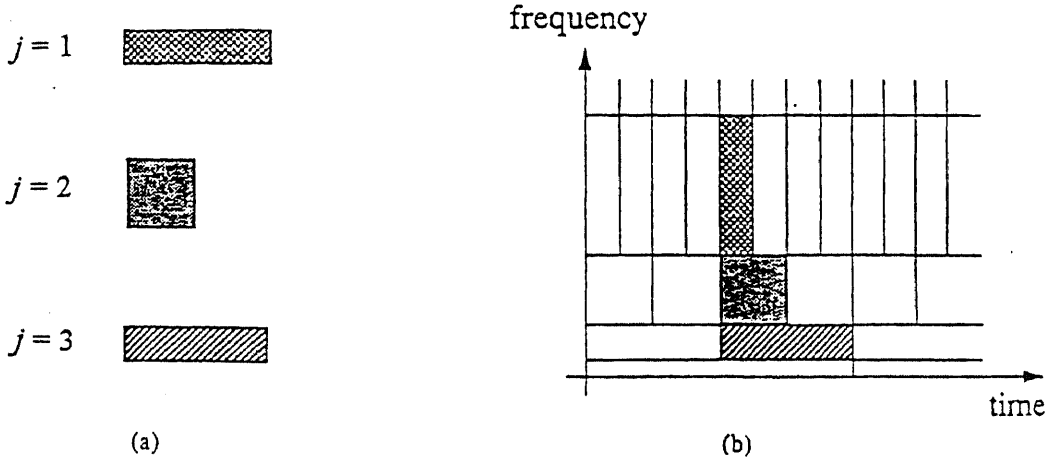

Figure 1.2.1 Plot of time verses frequency resolution

Mallat [1] introduced this concept of multiresolution signal analysis and used it to construct an orthonormal basis of wavelets. The following section will develop an orthonormal wavelet basis and relate the wavelet representation directly to the changes in scale. This section is based on the work of Mallat [1] and Daubechies [5].

1.3 Derivation of the Scaling and Wavelet Coefficients

A set of scaling functions in terms of an integer translation in time is derived as

$$\varphi_k(t) = \varphi(t-k) \tag{1.9}$$

The subspace $L^2(\mathrm{R})$ spanned by these functions is defined as $V_o = span_k\{\varphi_k(t)\}$ (Appendix B.2). Let V_o be the space of all the frequencies in the interval (-π, π) [3]. The set of functions that forms an orthonormal basis (Appendix B.3) for V_o is

$$\varphi(t-k) = \mathrm{sinc}(t-k) = \frac{\sin(\pi(t-k))}{\pi(t-k)} \qquad k \in Z. \tag{1.10}$$

Next let V_{-1} be the space spanned by functions in the frequency interval (-2π, 2π) [3]. The set of functions that forms an orthonormal basis for V_{-1} is

$$\sqrt{2}\cdot\varphi(t-k) = \sqrt{2}\cdot\mathrm{sinc}(t-k) = \sqrt{2}\cdot\frac{\sin(\pi(t-k))}{\pi(t-k)} \tag{1.11}$$

It can then be deduced that $V_o \subset V_{-1}$ or that V_o is in the space spanned by V_{-1}.

To develop a relationship between V_o and V_{-1} we will call W_o the space that spans the functions in the frequency band of (-2π, -π) ⊂ (π, 2π) which results in the following relation

$$V_{-1} = V_o \oplus W_o \tag{1.12}$$

where ⊕ denotes that the wavelet spanned by W_o is the orthogonal complement of V_{-1} in V_o (Appendix B.4). In other words, V_{-1} is equivalent to V_o plus some added detail

contained in W_o [2]. For resolution or signal details up to a scale 2^{-i}, if V_o is the space of functions with frequencies in the interval $(-2^{-i}\pi, 2^{-i}\pi)$, then

$$V_i \subset V_{i-1} \quad i \in Z \tag{1.13}$$

and

$$V_{i-1} = V_i \oplus W_i \quad i \in Z \tag{1.14}$$

where W_o is the space of functions with the frequencies in the interval $(-2^{-i+1}\pi, -2^{-i}\pi) \cup (2^{-i}\pi, 2^{-i+1}\pi)$ [2]. The relationship of the various subspaces can be seen from the following expressions.

$$\cdots\cdots V_2 \subset V_1 \subset V_0 \subset V_{-1} \subset V_{-2} \cdots\cdots L^2(R) \tag{1.15}$$

and

$$V_i = W_{i+1} \oplus W_{i+2} \oplus W_{i+3} \oplus W_{i+4} \cdots\cdots. \tag{1.16}$$

where V_i is in the frequency space of $(-2^{-i+1}\pi, 0) \cup (0, 2^{-i+1}\pi)$ [2]. This is clearly shown in figure 1.3.1.

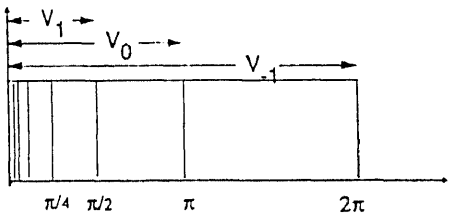

(a)

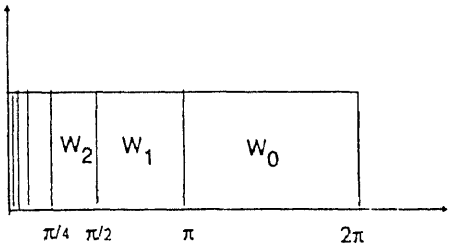

(b)

Figure 1.3.1 Relation of various subspaces

Essentially, the objective of the wavelet is to obtain the signal components in the space spanned by W_o. The various levels of W_i are the wavelet coefficients. To obtain the wavelet coefficients, a wavelet that will span W_o must be constructed. This is achieved by first noticing that the set of functions $\{\varphi(t-k), k \in Z\}$ given by 1.10 form a basis for V_o. Therefore $\{\sqrt{2}\varphi(t-k), k \in Z\}$ forms a basis for V_{-1}. To obtain the upper half of the spectrum of V_{-1}, which is V_o, a lowpass filter, passing the lower half of the frequency spanned, is applied with impulse response

$$\sqrt{2}h(n) = \frac{\sin(\pi(n/2))}{\pi(n/2)}. \tag{1.17}$$

The function $\varphi(t)$ can now be written as

$$\varphi(t) = \sum_n h(n)\varphi(2t-n) \tag{1.18}$$

where $\varphi(t)$ is referred to as the scaling function because it produces an approximation in V_{j+1} of the signal components in V_j. [3]. The sequence $h(n)$ is a set of coefficients referred to as the scaling coefficients. This sequence is a filter of finite length derived from the conditions of orthonormality in [5]. Now to obtain the span of frequencies between the various scales of the scaling function the wavelet coefficients are found.

The wavelet coefficients reside in the space spanned by the next narrower scaling functions represented by W_j [2]. The orthogonal complement W_j to V_j is obtained by highpass filtering the upper half of the signals. The wavelet function can then be derived in terms of the scaling function by

$$\Psi(t) = \sum_n g(n)\varphi(2t-n). \tag{1.19}$$

From the condition that the wavelets span the different spaces, the wavelet coefficients are related to the scaling coefficients by

$$g(n) = (-1)^n h(N-1-n) \tag{1.20}$$

for the filter lengths of *g(n)* and *h(n)* equal to *N*. This relation is based on the requirements of orthonormality in [1]. The process of obtaining the scaling and wavelet coefficients from filters *g(n)* and *h(n)* is best described by figure 1.3.2 (facing 7).

The wavelet that will span all of the subspaces in W_j is in the form

$$\Psi_{j,k}(t) = 2^{j/2}\Psi(2^j t - k) \tag{1.21}$$

where 2^j is the scaling of *t*, *k* is the time translation in *t* and $2^{j/2}$ maintains the normalization for the wavelet. The set of functions formed from the scaling function $\varphi_k(t)$ and the wavelet function $\Psi_{j,k}(t)$ spans the entire space of the signal denoted by $L^2(\mathrm{R})$. Therefore, any signal *f(t)* can be written in terms of the scaling and wavelet coefficients [5] by

$$f(t) = \sum_{k=-\infty}^{\infty} S(k)\varphi_k(t) + \sum_{j=1}^{\infty}\sum_{k=-\infty}^{\infty} W(j,k)\Psi_{j,k}(t) \tag{1.22}$$

where *S(k)* are the scaling coefficients and *W(j,k)* are the wavelet coefficients for scales *j*. Since these expansion functions form an orthonormal basis, the scaling coefficients can be derived as inner products (Appendix B.3)

$$S(j) = \langle f(t), \varphi_k(t) \rangle \tag{1.23}$$

and similarly for the wavelet coefficients we have

$$W(j,k) = \langle f(t), \Psi_{j,k}(t) \rangle. \tag{1.24}$$

The wavelet coefficients are called the discrete wavelet transform (DWT) of the signal *f(t)*. The wavelet coefficients are similar to the Fourier coefficients when taking the Fourier transform of a signal.

1.4 Signal Decomposition

The orthonormal wavelet used for the wavelet transform (WT) has been developed according to the multiresolution signal analysis ideas presented by Mallat [2]. The procedure implemented to perform the WT is known as the Mallat tree algorithm outlined in figure 1.4.1 [2].

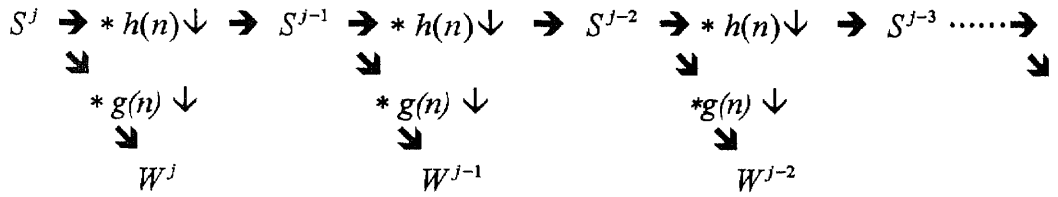

Figure 1.4.1 Mallat tree algorithm

The resulting W^js correspond to the wavelet coefficients and the S^js correspond to the scaling coefficients. The scaling and wavelet coefficients at different levels of scale j are be obtained by convolving the coefficients at scale j by the $h(n)$ and $g(n)$ filters and then downsampling or taking every other term, which is represented by $\downarrow$ [1]. Downsampling is required since the number of data points is doubled when convolving one of the filters with the signal, where convolution is represented by the symbol $*$. The convolution results in the coefficients at the next lower level. In other words, the scale j coefficients are filtered by two finite digital filters with coefficients $h(n)$ and $g(n)$ which after downsampling give the next lower level of scaling coefficients [3].

The levels or the scaling of j refers to the amplitude of the signal's wavelet coefficients, where $0 < j \leq N$ and N is the length of $h(n)$. For example, if the original signal has an amplitude of 100 the first wavelet coefficient, $j = 1$, will have an amplitude of $100 * 2^{-1}$ or 50. Similarly, the second wavelet coefficient will have an amplitude of

25 ($100* 2^{-2}$). It is also important to remember that the length of the filters is equal to the number of wavelet coefficients obtained.

The two finite filters, *h(n)* and *g(n)*, are an ideal lowpass filter and an ideal highpass filter, respectively. The successive filtering of both filters to a given signal results in a bandpass filter passing only the upper half of the spectrum (see figure 1.3.2). It is important to remember that the change in scale and time translation is done simultaneously while the frequency components of the signal are being bandpass filtered. This is all performed by the two filters.

For example, a signal is given with frequencies in the range of 0-100 Hz, where the original signal is represented by S^j. The first scaling coefficient denoted by S^{j-1} contains the frequency components from 0-50 Hz. S^{j-1} is obtained by low pass filtering S^j by *h(n)*. The first wavelet coefficient, W^j, is obtained after high pass filtering S^j by *g(n)* and contains frequency components between 50-100 Hz. Similarly, the second scaling coefficient, S^{j-2}, contains frequencies in the interval of 0-25 Hz and the second wavelet coefficients contains frequencies in the range of 25-50 Hz. As you can see, this successive filtering process continuously cuts the frequency spectrum in half and displays the upper half of the spectrum in the wavelet coefficients. This shown in figures 1.4.1 and 1.3.2.

Also, zeroes must be inserted between the filter coefficients to set the length of the filter to the length of the original signal. For example, if the length of *h(n)* is 10 and the signal length is 100, 10 zeroes must be inserted between each coefficient of *h(n)*. This process of inserting zeroes between the filter coefficients is known as upsampling, which is performed on the filters before each successive convolution. (for an elaboration on upsampling and downsampling see Appendix A)

In detail, the Mallat tree algorithm is as follows:

1) The filter *g(n)* is upsampled to match the signal length.

2) High frequency components are then obtained by convolving the filter *g(n)* with the

upper half of the spectrum of S^j.

3) The filter output is then downsampled to obtain the original signal length. The resultant is the wavelet coefficient W^j.

4) The filter *h(n)* is upsampled to match the signal length.

5) S^j is then low-pass filtered by *h(n)* to obtain the next signal level. The low frequency components are obtained while preventing the upper half of the spectrum from aliasing.

6) The filter output is then downsampled to obtain the original signal length. The resultant is the next decomposition level with the scaling coefficient S^{j-1}.

7) The entire procedure is repeated. S^{j-1} is bandpass filtered to get the spectral contents at frequencies which are one half the frequencies of the previous level. The frequency bandwidth is relative to the maximum frequency of the original signal.

This process is shown in figure 1.3.2 for the first level of the wavelet decomposition of a signal with relative bandwidth equal to π. This figure shows that the frequency spectrum is cut in half for each level of the wavelet representation. The upper half of the spectrum is the wavelet coefficient. This process is similar to the concept of the scaling function where the scale is halved for each wavelet level. It is important to understand that when convolving the signal with filters *h(n)* and *g(n)*, both the scale of the signal in time and the frequency is halved.

Also, the number of data points at the output of the system is the same as the number at the input of the system. The number is first doubled by the two filters and is then cut in half by the decimation back to the original length of the data sequence. This means that there is no information lost and that the original signal can be completely recovered [5]. This idea of not losing any information is the basic concepts behind QMF filter bank theory [3].

To calculate the scaling and wavelet coefficients the corresponding *g(n)* and *h(n)* filter coefficients must be obtained. The filter coefficients were derived from the conditions for orthonormal wavelets in [2] and [5]. A program was written in Matlab and used to calculate the *g(n)* and *h(n)* filter coefficients. This program along with the program to perform the Mallat multiresolution algorithm to generate the wavelet coefficients is listed in Appendix C.

1.5 A Comparison of Orthonormal to Cubic B-Spline and Lemarie-Battle Wavelets

1.5.1 Introduction

Orthonormal wavelets were used primarily due to the equal localization of the wavelet coefficients in both time and frequency. To demonstrate the effectiveness of the orthonormal wavelet a comparison was made with the wavelet coefficients of two other wavelets. The wavelets chosen were the Cubic B-Spline [15] and the Lemarie- Battle [16] wavelet. The actual wavelets themselves were not calculated or displayed since it is the filter sequences, $h(n)$ and $g(n)$, and the wavelet coefficients which are of interest.

1.5.2 Results and Discussion

A filter length of six was chosen for each of the wavelet filter sequences for demonstrative purposes. The corresponding filter coefficients for the wavelets are displayed in table 1.5.1. Wavelet analysis was performed with each wavelet and applied to the waveform in figure 1.5.1. This particular waveform was chosen because it clearly demonstrates the properties of the wavelet such as time dilation and the changes in scale. The filters were implemented using the Matlab program listed in Appendix C to obtain the wavelet coefficients for the various levels of the wavelet representation.

The first set of wavelet coefficients are displayed in figure 1.5.2. The orthonormal wavelet coefficient in figure 1.5.2a is symmetrical and is apparently derived from the signal in figure 1.5.1. Notice how the scale of the wavelet coefficient is dilated (compressed) in time compared to the original signal. Similar results were obtained for the Lemarie-Battle wavelet coefficient in figure 1.5.2b except that the time dilation is more compressed. The Cubic B-Spline, in figure 1.5.2c, displayed the basic signal shape but also added components which are repetitive and obviously obtained from the original signal.

The second set of wavelet coefficients are displayed in figure 1.5.3 (Note: wavelet coefficients two through six are in Appendix D). First, it can be seen that the time dilation orthonormal wavelet coefficient is becoming more compressed when compared to the first wavelet coefficient. Also, higher frequency components of the signal are becoming apparent. This agrees with the theory earlier presented in section 1.3 that as one decreases the scale given by integer j, the time resolution is decreased while the frequency resolution is increased . In this case, the first wavelet coefficient is represented by $j = 1$ with the second is represented by $j = 2$. Remember the scale is decreased as j increases.

Secondly, the orthonormal wavelet (figure 1.5.3a) maintains the basic form of the original signal in the center with lobes at the end. The lobes are a result of the integer time translations for each level of scale. The Lemarie-Battle wavelet coefficient (figure 1.5.3b) does not separate the actual contents of the wavelet representation from the resulting side lobes as well as the orthonormal wavelet. The side lobes are also not as attenuated as they were for the orthonormal coefficient. The time resolution is also decreased.

Similar results were obtained for the Cubic B-Spline wavelet coefficient (figure 1.5.3c). The side lobes are not as attenuated and the time resolution is dramatically decreased. The frequency components are not as apparent in this wavelet as they were for the Lemarie-Battle and orthonormal wavelet coefficients. Also, the time translation is not centered when compared to the coefficients of the other wavelets.

Table 1.5.1 Table of wavelet filters

Orthonormal		Lemarie-Battle		Cubic B-Spline	
$h(n)$	$g(n)$	$h(n)$	$g(n)$	$h(n)$	$g(n)$
0.235	0.025	0.542	0.030	0.890	1.475
0.571	0.060	0.307	-0.023	0.401	-0.468
0.325	-0.096	-0.035	0.078	-0.282	-0.742
-0.096	-0.325	-0.078	0.035	-0.233	0.346
-0.060	0.571	0.023	-0.307	0.129	0.390
0.025	-0.235	-0.030	-0.542	0.127	-0.197

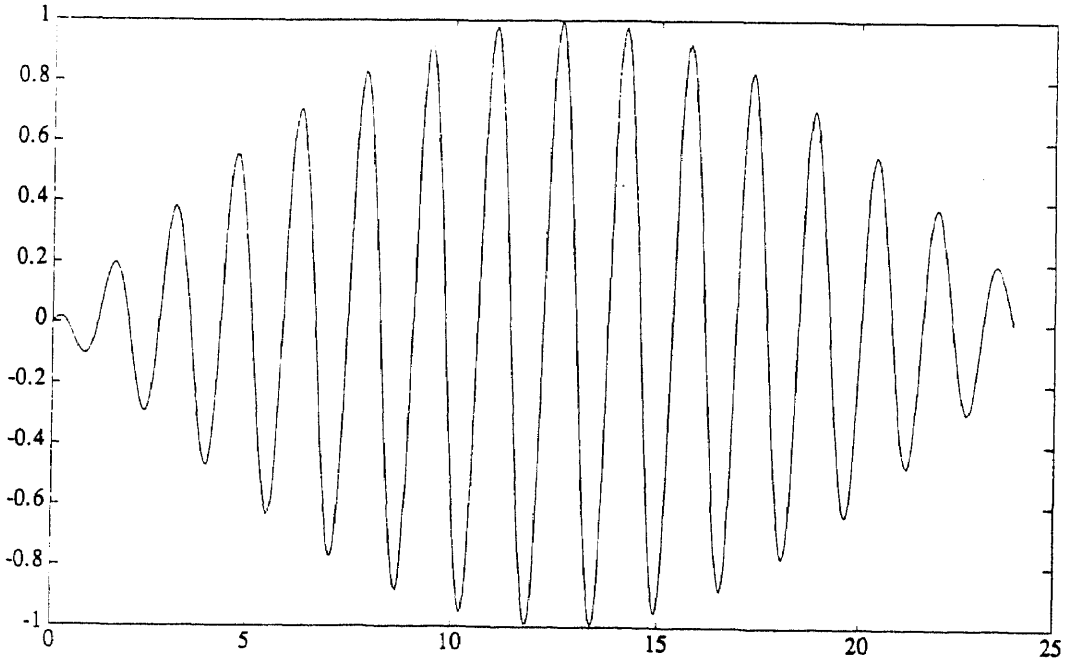

Figure 1.5.1 Waveform used for wavelet comparison

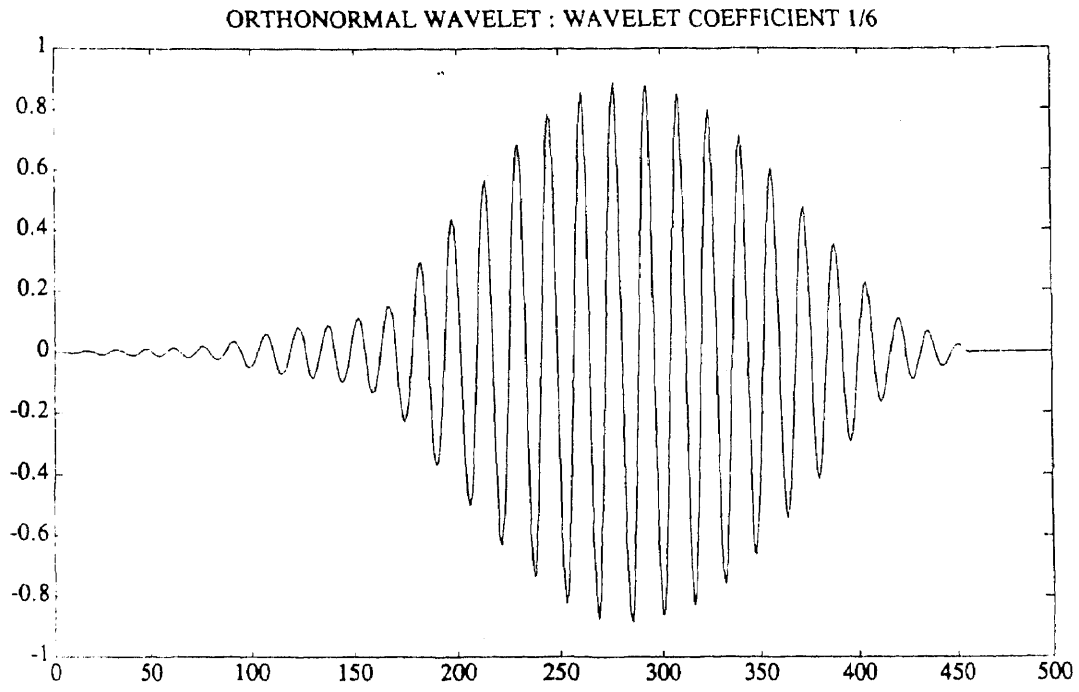

(a)

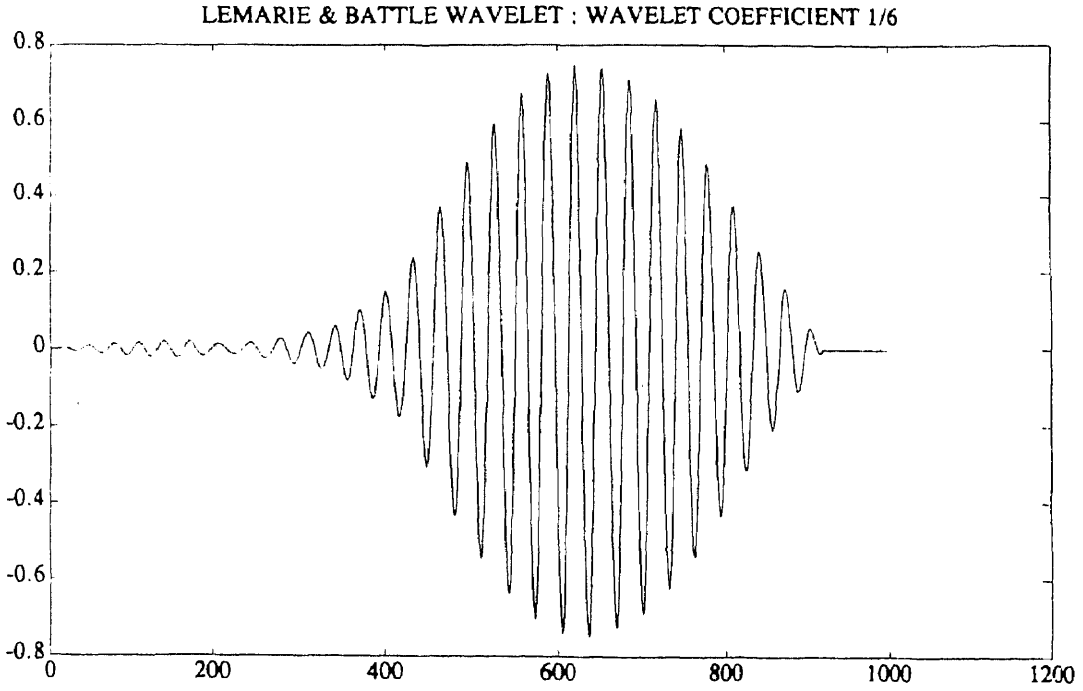

(b)

Figure 1.5.2 First set of wavelet coefficients

The lower level wavelet coefficients 3 through 6 (figures 1.5.4 to 1.5.7, respectively) exhibit similar results as in the first and second wavelet coefficients. It becomes more apparent that the time dilation is increased dramatically for the Lemarie-Battle and the Cubic B-Spline wavelet while the orthonormal wavelet maintains a better time resolution. Also, the orthonormal wavelet brings out other frequency components sooner.

The orthonormal representation brought out separate frequency components, or the details of the signal, in the second wavelet coefficient and continued to do so for each level of the representation. The Lemarie-Battle and Cubic B-Spline did not bring out the details of the signal until the final level of the decomposition (figure 1.5.7).

1.5.3 Conclusion

It is apparent from the various levels of the wavelet coefficients that the orthonormal wavelet has a better localization in time and frequency. This was not the case with the Lemarie-Battle and Cubic B-Spline wavelets which generated larger side lobes and did not exhibit an equal time and frequency localization. It is difficult to interpret the results for the Lemarie-Battle and Cubic B-Spline since the time resolution is restricted to a very small area along the time axis. It can be deduced that the Lemarie-Battle and Cubic B-Spline wavelets do not contain the desired time and frequency resolution needed.

1.6 Scope of Thesis

The basic concepts and fundamentals of the wavelet signal representation have been introduced. The theory and background presented provides an overview of the concepts of wavelets. The objective of this paper was to gather the available theory and create a method for observing the discrete wavelet transform of discrete time signals. The method developed is based on Mallat's multiresolution tree algorithm. [3]

Programs to implement Mallat's algorithm were written in Matlab for discrete time signals. The programs include the filters $h(n)$ and $g(n)$, which represent the orthonormal wavelet created by Daubechies. [5] The program outputs are the wavelet coefficients which are displayed along the original time axis. All programs are listed in Appendix C.

The orthonormal wavelet was applied to various types of bioelectric signals. Chapter 2 is essentially the wavelet representation of recorded motor evoked potentials (MEPs) created by a new method of stimulation known as magnetic stimulation. In Chapter 3, the wavelet was applied to evoked potentials (EPs) and Chapter 4 involved wavelet analysis of various EKG signals. The data used for the signals in Chapters 3 and 4 were simulated and not recorded from actual subject's as in Chapter 3.

CHAPTER 2

APPLICATION OF WAVELETS TO MOTOR EVOKED POTENTIALS INDUCED BY CORTICAL MAGNETIC STIMULATION

2.1 Introduction

It is known that stimulation of the brain's motor cortex will create contractions of a particular muscle group depending on the area of the brain that was excited. The motor cortex is usually stimulated by electrical pulses via electrodes placed on the scalp. A new method of cranial stimulation is achieved by applying a time-varying magnetic field to the brain. This method of stimulation is known as cortical magnetic stimulation. Cortical magnetic stimulation was performed on a subject where the quadricep muscles where forced to contract. The electrical potentials resulting from the muscle contractions, known as motor evoked potentials (MEP's), were recorded. The wavelet transform was then performed on the recorded MEP signals and an interpretation was made.

2.2 Introduction to Cortical Magnetic Stimulation

Clinical neurophysiology has made significant progress in recent years. Considerable interest has recently been given to the techniques of stimulation of the human brain. This has occurred since scientists found that transcranial stimulation can be achieved by placing electrodes on the scalp, resulting in stimulation of the motor cortex. The motor cortex controls the movement of the body. Therefore by stimulating the brain a particular body part will move depending on the area of the brain that is stimulated. Since this discovery, electrical brain stimulation has been used in several clinical and neurological studies. The main disadvantage of this technique is that the subject experiences pain from the current flowing through the electrodes. [8] Recent experimentation has shown that the electrical

activation of the motor cortex can be stimulated by an external magnetic field. This new technique of cranial stimulation is known as cortical magnetic stimulation. [6]

The stimulator for cortical magnetic stimulation creates a potential that travels through a coil that is placed on the scalp. The coil creates a time-varying magnetic field inducing a current in the motor cortex. [7] One advantage of this technique is that the subject under test experiences no pain. The patient may experience some fatigue and occasional discomfort if the muscles in the neck or face are accidentally stimulated. [8] Another very important advantage of magnetic verses electrical stimulation, is the ability to reach regions of the cortex below the skull with little or no attenuation. In fact, the resistance of the skull is one to two orders of magnitude greater than the resistance of soft tissues. The stimuli generated by electrical pulses through electrodes are attenuated by the skull. [7] Magnetic stimulation can also be applied to the nerves throughout the body (the peripheral nervous system) as well.

2.3 Basic Principles of Cortical Magnetic Stimulation

Cranial nerves can be stimulated by an applied electrical current. Stimulating the brain with either needle or surface electrodes is commonly performed. As mentioned previously, electrical stimulation can also be induced by applying a magnetic field to the region of interest. Energy is released from the stimulator and released through the coil which is circular in shape and placed on the scalp. The basic laws of electromagnetism state that a time-varying field will induce an electrical field in any specified loop within its vicinity, where the original loop would be the stimulating coil and the induced loop is in the brain. [8] According to Faraday's law, whenever a magnetic field changes there is an induced electrical field. [9] A stationary magnetic field does not induce an electrical field. Therefore, a time-varying field is required.

The stimulator that creates the energy required for the magnetic field is the Cadwell MES-10 Magnetic Stimulator. The stimulating coil is attached to the Cadwell

which is responsible for creating the field. The coil creates a magnetic field with a focal point so only a particular area of the brain will be stimulated while not stimulating other areas. For peripheral stimulation, in the forearm for example, the induced current would be in the forearm as shown in figure 2.3.1.

In order to create the required time varying field, the stimulator must contain a network including a capacitor and an inductor. If the inductor and capacitor are connected through a switch, the energy moves from the capacitor to the inductor creating a large magnetic field. If the switch remains closed the energy is transferred between the inductor and the capacitor until the energy is lost. Most of the energy is transferred between components without any relative loss in the magnetic stimulator. [7] The oscillation frequency of the *L-C* network is

$$f = 1/\sqrt{LC} \tag{2.1}$$

The basic circuitry for the Cadwell MES-10 magnetic stimulator is shown in figure 2.3.2. The frequency for the Caldwell MES-10 is 3560 Hz with a period of 280 uS, and 3-4 oscillations occur before the switch is opened. [6] The power that the Cadwell MES-10 distributes to stimulate has a maximum value of 2.2 tesla when stimulating at 100% of

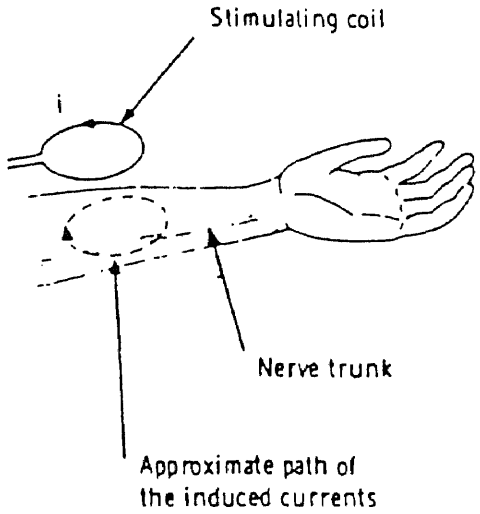

Figure 2.3.1 Induced current resulting from peripheral magnetic stimulation

its capacity. [6] Of course one can adjust the amount of stimulation by controlling the percentage of the stimulator's output current. To create a difference in the electrical potential in the nerve to generate muscle movement, the stimulus length must be 100-300 *m*S and the current density in the nerve must be 1-2 *u*C/cm^2. [7] The Cadwell MES-10 meets these required specifications.

The 2.2 tesla, 450 J of energy, is necessary since the brain is almost transparent to the magnetic field. [6] The induced cranial current is 1/100,000 the size of the inducing current in the coil. Also, the total energy delivered to the brain is approximately 0.1% of the brain's metabolic rate. [6] Magnetic stimulation is performed world-wide and is recognized and funded by organizations such as National Institutes of Health (NIH).

2.4 Results of Wavelet Analysis

Cortical magnetic stimulation was performed on two subjects where data containing motor evoked potentials (MEPs) were recorded from the quadricep muscles on the subject's legs.

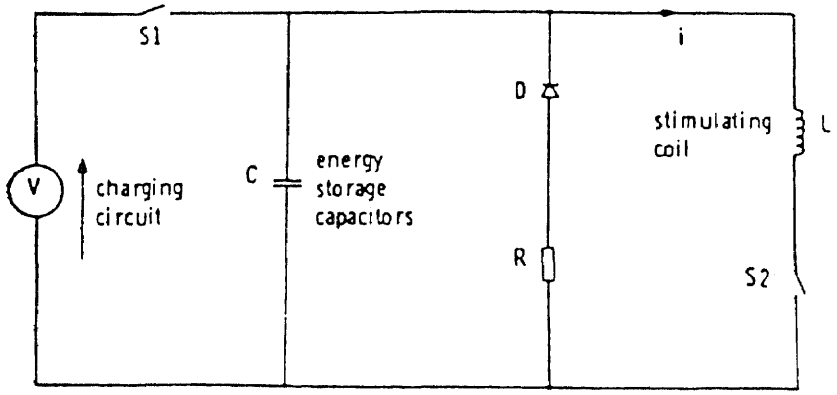

Figure 2.3.2 Stimluator circiut

MEPs represent the electrical potentials created when a muscle contracts. There were four channels and each was used to record a different region of the quadricep muscle. Each channel was recorded using a sampling rate of 5 kHz which is low for measuring MEPs. The usual sampling rate is 20 kHz, but 20 kHz is the maximum sampling rate available for the equipment used. [6] Therefore the sampling rate had to be equally distributed among the four separate channels. The original MEP waveforms are shown in figures 2.4.1 and 2.4.2.

The equipment used to record the data was the Dantec EMG Counterpoint. This device is able to detect the MEPs through surface electrodes connected to the Dantec's input. The surface electrodes were placed externally on the skin. A conduction jel was placed between the surface electrode and the subject's skin. The jel is used to ensure that a proper conduction of the MEPs is transferred to the electrode. [12] The data was then collected on a computer connected to the output of the Dantec.

The magnetic stimulation was performed using the Cadwell MES-10. A figure eight coil was used to trigger the stimulation of the MEPs. This coil was implemented due to its ability to localize the focal point of the magnetic field responsible for stimulation. [7] This ensures that the area of interest will be stimulated and other unrelated areas are not stimulated. Other coils that are circular in shape do not produce a focal point as narrow as the figure eight coil, sometimes resulting in stimulation of other muscles. [9]

The wavelet applied to the MEPs was an orthonormal wavelet with a filter length of six. The values used for the corresponding $h(n)$ and $g(n)$ wavelet filters are in table 2.4.1. A filter length of six was used since the wavelet coefficients at scales lower than 2^{-6} were basically redundant. No differences in the wavelet coefficients were found at scales lower than 2^{-6} except for expected changes in the scale. The original MEP signals are in figures 2.4.1a to 2.4.2b for channels 1 to 4, respectively. There are obvious differences among the four signals. First, it must be noted that channel 2 is inverted with respect to channels 1, 3 and 4 due to the electrode configuration used to record MEPs. Since the

Table 2.4.1 Wavelet filters applied to MEPs

h(n)	g(n)
0.2352	0.0249
0.5706	0.0604
0.3252	-0.0955
-0.0955	-0.3252
-0.0604	0.5706
0.0249	-0.2352

wavelet transform is displaying frequency components, the wavelet coefficients of channel 2 will not be inverted. Also, the basic shape and location of the peaks vary and the scale for channels 1 and 2 are twenty times greater in magnitude than for channels 3 and 4. Although channels 1 and 2 are not similar, channels 3 and 4 are obviously similar.

The first wavelet coefficients are shown in figures 2.4.3 and 2.4.4 (all wavelet coefficients of MEPs are displayed in Appendix E). Interestingly, channels 1 and 4 obtain very similar waveforms, though the scales and the original waveforms are different. One can then speculate that the contents of the two signals, for a particular frequency region, are the same. It is apparent that channel 3 contains some similarities to channel 4, such as the basic shape of the waveform. Also, channel 2 has no similarities to any of the three other channels. The lower levels of the wavelet represenatation must next be observed for a complete analysis of the MEP waveforms.

The second wavelet coefficients of the wavelet representations are shown in figures 2.4.5 and 2.4.6. It is obvious at this level that channels 3 and 4 are similar in structure but are not exactly the same. Channels 1 contained no similarities to any of the

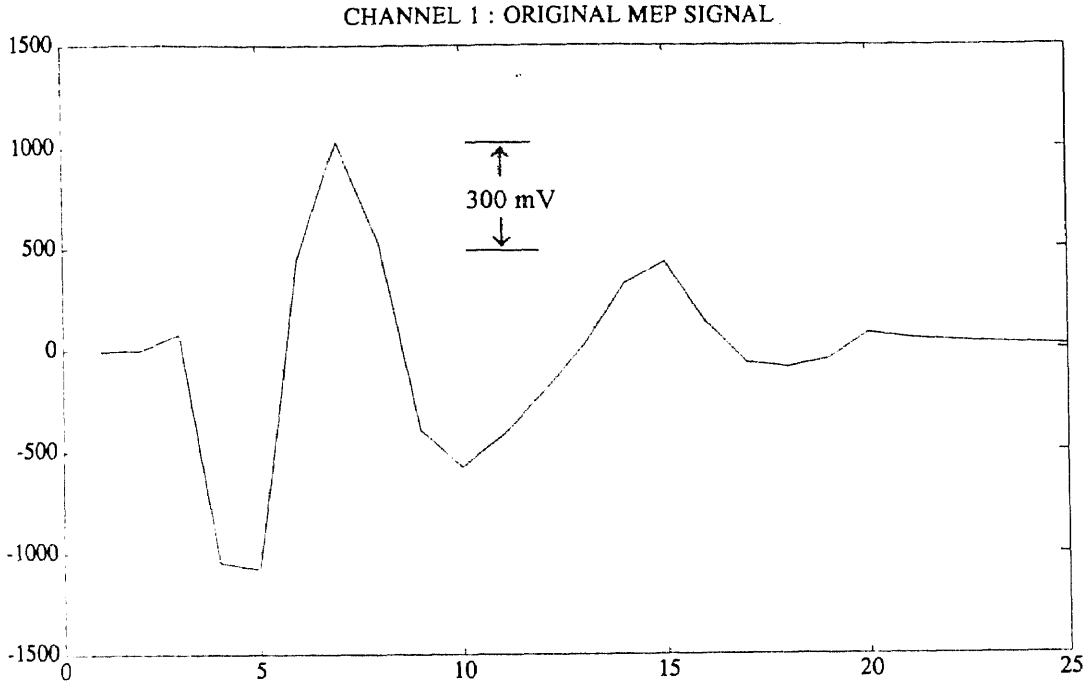

(a) Channel 1

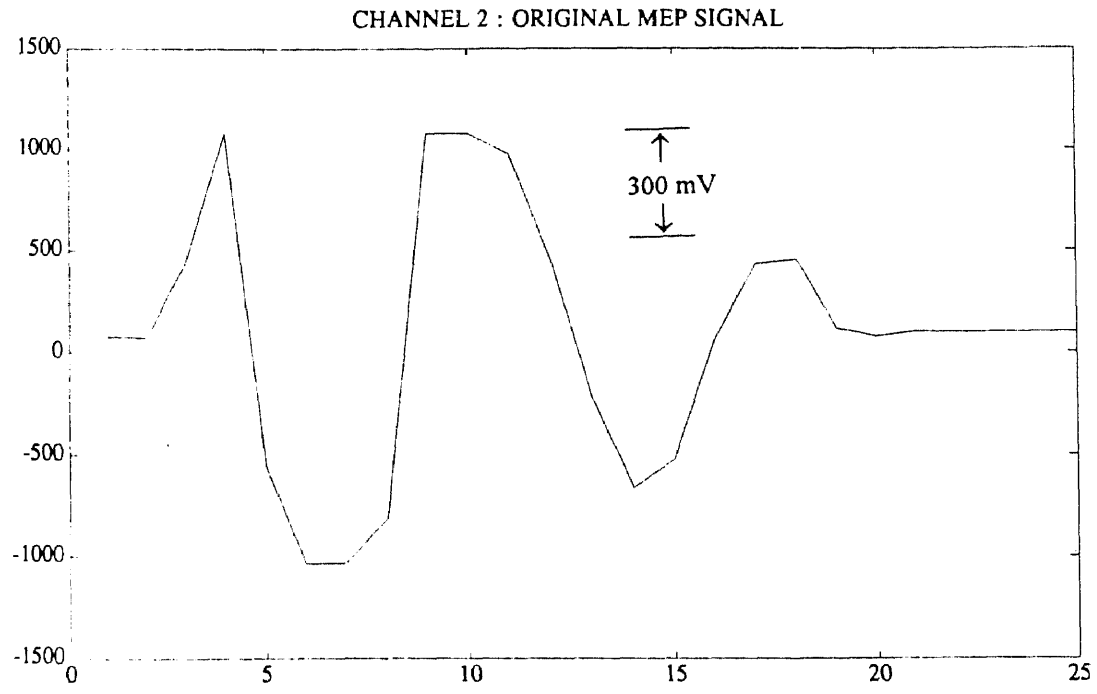

(b) Channel 2

Figure 2.4.1 Original MEP waveforms

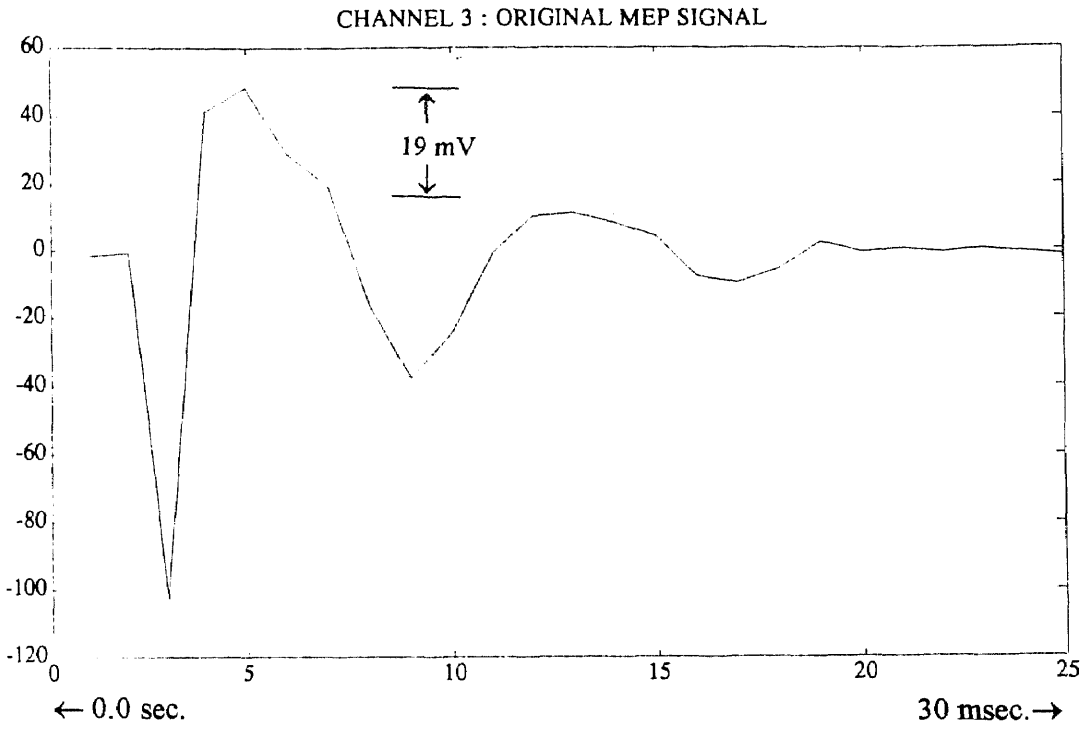

(a) Channel 3

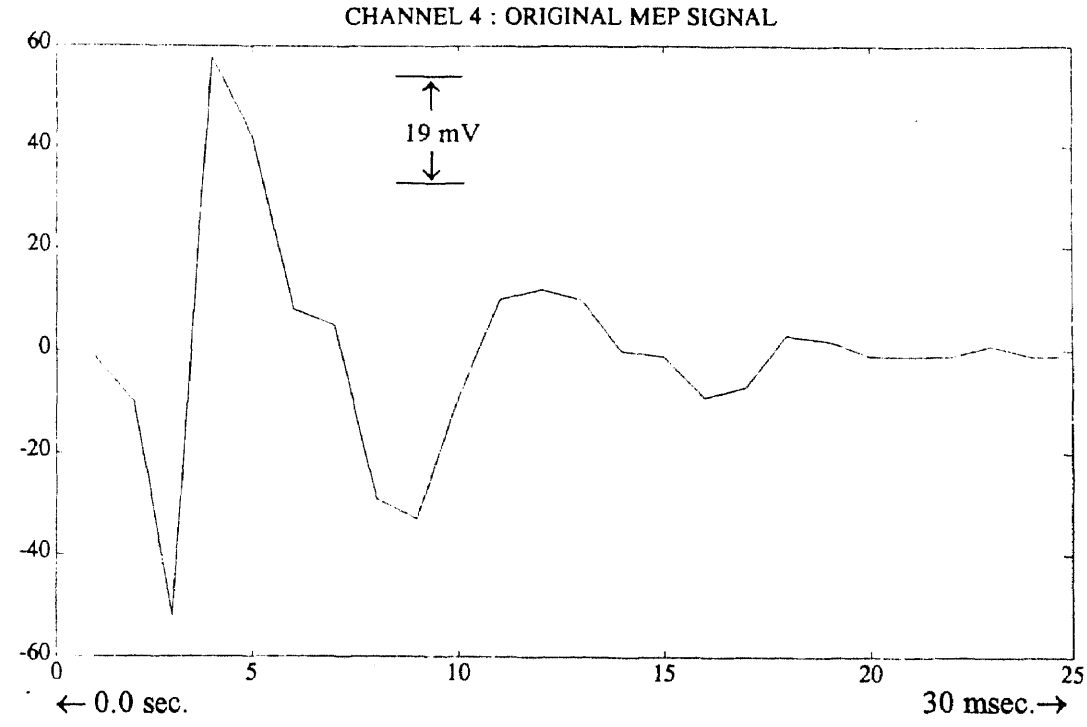

(b) Channel 4

Figure 2.4.2 Original MEP waveforms

three other channels. Similar results were observed for channel 2. The third level wavelet coefficients shown in figures 2.4.7 and 2.4.8 were similar to the second set of wavelet coefficients.

The fourth level wavelet coefficients are shown in figures 2.4.9 and 2.4.10. Channels 1 and 2 were different from all the channels. The only channels that were similar, and as a matter of fact were almost exactly the same, were channels 3 and 4. Wavelet coefficients 5 and 6, shown in figures 2.4.11 through 2.4.14, are exactly the same as the fourth level wavelet coefficients. From levels four through six there were no changes in the waveforms.

Initially, channels 3 and 4 were the only channels that had similarities in the original MEP waveforms with amplitude's 20 times lower than channels 1 and 2. The original waveforms in channels 3 and 4 contained some similar flow or structure to the peaks while there were differences in the amplitude and location of the various peaks throughout the signal. As the levels of the wavelet representation were observed, the lower scale wavelet coefficients for channels 3 and 4 were the same.

The wavelet representation brought out signal components not present in the original signals. The wavelet basically extracted the essence of the MEP signals from all four signals. This clearly shows the usefulness of the wavelet representation for bringing out details that were not at first apparent.

2.5 Discussion

The results obtained proved the wavelet to be a successful tool for extracting signal components throughout various level of the wavelet representation. The wavelet coefficients brought out details of the signals that were not apparent. The wavelet even brought out components that were the same as it did in channels 3 and 4. Although some important results were found, the results are not conclusive. The available sampling rate was 5 kHz per channel while 20 kHz was needed to meet the Nyquist sampling rate. The

wavelet was still successful but for an accurate interpretation of the results a higher sampling rate is definitely necessary.

All four recorded channels were above the threshold of the stimulation required to generate a muscle contraction. The term threshold refers to the amount of electrical stimulation present in the muscle required to generate a contraction. [6] In this case, the initial stimulation was in the brain and the muscle of interest was the quadriceps. Quite often, when the muscle of interest is stimulated the muscle does not contract. Even though the muscle does not contract an MEP is generated which is very low in amplitude. This MEP is said to be below threshold.

For future work it would be interesting to perform the wavelet transform to signals at various levels of threshold and see if there are any similarities to the various levels of the wavelet coefficients. This would then determine if MEPs generated by cortical magnetic stimulation below threshold contain the same pertinent information as the MEPs above threshold. Researchers do not include MEPs below threshold in their neurological studies when performing cortical magnetic stimulation. This results in unnecessary or wasted stimulations of the brain. If the wavelet analysis proves that there is similar information for various levels of threshold, the number of unnecessary stimulations would be greatly reduced. It would also be interesting to compare the wavelet coefficients of a peripheral electrical stimulation with cortical magentic stimulation.

2.6 Conclusion

The wavelet representation of the motor evoked potentials provided some insight into the contents of the signal components. It was shown that although the original signals differed in the general shape of the waveform and in scale, there were similar components that were brought out by the wavelet coefficients. The signals obtained were recorded at a sampling rate lower than the required sampling rate so a complete and thorough examination of the results could not be made. Although the sampling rate was inadequate,

the wavelet transform still performed better than expected. Equipment with higher available sampling rates is required to obtain improved results, especially if one wishes to pursue the work developed here.

CHAPTER 3

APPLICATION OF THE WAVELET TRANSFORM TO EVOKED POTENTIALS

3.1 Introduction

Evoked potentials (EPs) are recorded signals from the nervous system indicative of the nervous system's performance. [12] EP waveforms are recorded from the nerves by placing surface electrodes over the neurological site of interest. As thousands of EPs are generated a process known as signal averaging is performed and the EP waveform emerges. [17] Once the EPs are obtained an evaluation of the characteristics of the waveforms can be related to the performance of the nervous system. It will be shown that the wavelet transform brings out structures that are similar between a single EP and signal averaged EP.

3.2 Introduction to Evoked Potentials

Evoked potentials (EPs) provide a non-invasive way for obtaining information to evaluate the function of the nervous system. Non-invasive procedures and corresponding results are obtained externally verses internally and do not require the physician to enter the subject's body. [17] EPs are achieved by stimulating a nerve or a group of nerves, and recording the resultant waveforms at various points along the neurological pathways. The information needed for a clinical diagnosis is embedded in the recorded waveforms. These waveforms are due to the brain's reception of an applied external stimulus. [17]

EP testing is most commonly used for examining the somatic nervous system and the central nervous system. The somatic nervous system consists of the nerves throughout the body responsible for movement. The central nervous system (CNS) consists of the brain and the spine and is the center of all neurological activity throughout the body. EP

testing is performed to detect injuries, disorders and the development and maturation of the nervous system.

3.3 Basic Principles of Evoked Potentials

There are several types of EPs that are used for testing a specific section of the nervous system. The testing is performed to provide information on how the damaged or diseased area of the nervous system is functioning. For example, to test the visual neurological pathways, pattern-shift evoked potentials (PSEVPs) are recorded.

The stimulus for PSEVPs is a checkerboard or a strobe flashed in front of the subject's eyes, at which time the brain waves are recorded. The information provided in the resultant waveforms supply information on the nerves in the CNS responsible for sight. Other types of EPs are brain auditory evoked potentials (BAEPs) used for investigation of the cochlear nerve (hearing) and brain stem auditory pathways. Motor evoked potentials (MEPs) evaluate the functioning of the central motor pathways responsible for movement, and somatosensory evoked potentials (SEPs) for evaluation of the somatic nervous system and CNS. [17]

EPs are generated in response to an invoked stimulus, where the stimulus varies for the particular EP to be generated. BAEPs use a click for a stimulus since hearing is involved, and EPs and SEPs use electrical stimulation to stimulate nerves throughout the body. The stimulus, whether electrical, visual or audio, is controlled and created by an electrical square wave of 100 to 200 microseconds in duration to generate a proper response. The time span between stimulations is approximately 10 milliseconds to allow for proper data collection. [17]

The evoked stimulus response is recorded from the nerves of interest via surface electrodes placed externally on the scalp. A conduction jel is applied between the electrode and the surface of the skin to reduce the electrode impedance at the surface of the skin. An electrode impedance of 3,000 ohms is desired. [18] Some cases call for

needle electrodes but this is not commonly practiced. The electrodes are placed on the scalp according to the International 10-20 System of electrode placement. [17] This does not guarantee that the electrodes on the scalp lie on specific brain structures, but ensures different laboratories use the same sites for repeated testing. The 10-20 system is shown in figure 3.3.1.

EPs must be amplified since the amplitude of the resultant waveforms is in the range of 0.1 - 20 uV. Because of their low amplitudes and their mixture with normal background brain waves, activity varies from twenty to several hundred microvolts in amplitude. [12] The EPs waveforms must be amplified by approximately 100,000 to 500,000 times depending on the outcome for the particular type of testing performed. The amount of amplification used also depends on the amplitude of the signal of interest and the voltage handling capabilities of the analog to digital converters at the input of the data

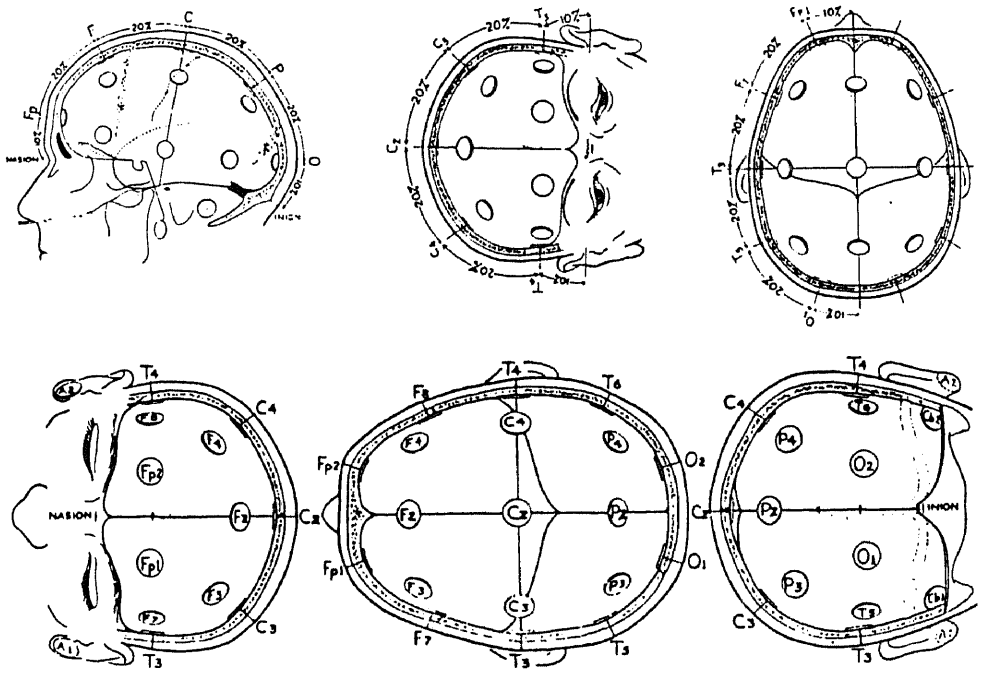

Figure 3.3.1 International 10-20 System for electrode placement

acquisition system. Once the data is obtained the EPs must be distinguishable from other brain waves present.

Separation of EP waveforms from the other cranial electrical activity is accomplished by a process known as signal averaging. [17] The brain's electrical response to the stimulus is always at the same time interval after the stimulus. Other present brain activity is not coupled to the stimulus and computers can extract the EP by searching for it in the waveform by using the location of the stimulus as a reference point. The stimulus is performed repetitively and the computer averages the new data for each successive stimulus with the previously averaged results. This process is continuously performed until the desired waveform becomes clear. Most EP testing requires 1000 signal averages to obtain an accurate waveform. [17] SEP waveforms recorded from various sections of the brain are shown in figure 3.3.2. The results were acquired using the 10-20 system and utilized approximately 1000 signal averages.

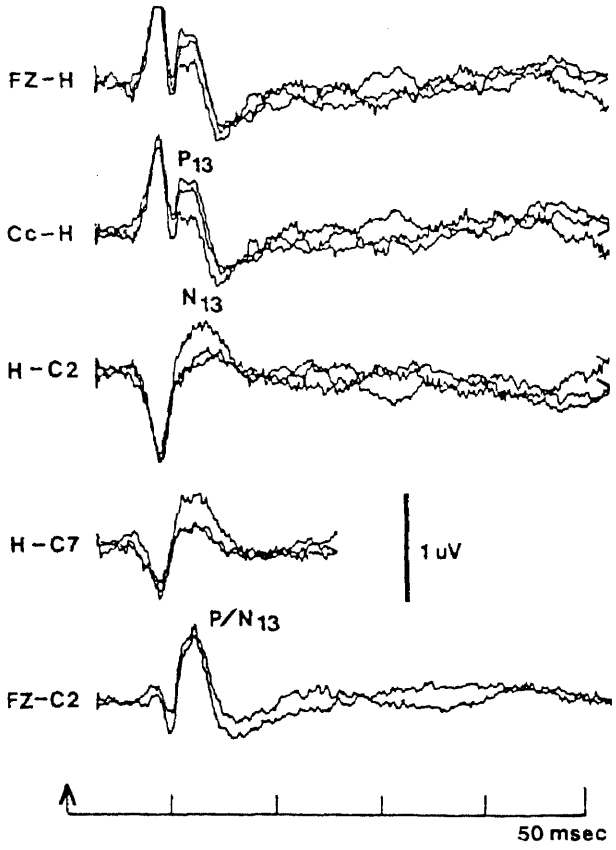

Figure 3.3.2 Various SEP waveforms

Signal averaging is an important aspect of EP testing and analysis since it allows the original undetectable EPs to be displayed and evaluated. Wavelet analysis of EPs has been given little attention by medical research since wavelets are relatively new. It will be shown that wavelets provide a means for obtaining and examining EP structures.

3.4 Results and Discussion of Wavelet Analysis to Evoked Potentials

A length 12 orthonormal wavelet was applied to a single EP and the same EP signal averaged 1000 times. A filter length of 12 was used since the wavelet coefficients did not bring out the structure for the single EP until scales at a level of 2^{-8} were reached. The Matlab programs to calculate the $h(n)$ and $g(n)$ wavelet filter coefficients are listed in Appendix C.

An EP was generated similar to the FZ-C2 SEP waveform in figure 3.3.2 using a program written in Matlab listed in Appendix C. The shape of the single EP without any background EEG is shown in figure 3.4.1. Notice that the EP is 0.06 units in amplitude. Next, the signal in figure 3.4.1 was embedded in EEG background which is shown in figure 3.4.2a. This signal represents an original EP waveform after amplification but prior to any signal averaging. The EP was signal averaged 1000 times and is shown in figure 3.4.2b. Observe how the shape of the EP is brought out while the background brain activity is reduced. All programs for EP simulation are in Appendix C. The wavelet transform was then applied to both EPs once the EPs were generated.

The first level wavelet coefficients for both the single and signal averaged EP waveforms are shown in figure 3.4.3. The wavelet coefficient of the single EP shown in figure 3.4.3a does not bring out any structure of the EP waveform. However, the structure of the EP is brought out in the first wavelet coefficient of the signal averaged EP shown in figure 3.4.3b. The single EP only displays the background activity while the signal averaged EP has a large hump. Similar results were obtained throughout the lower levels of thewavelet representation, as shown in figure 3.4.4 for the second set of wavelet

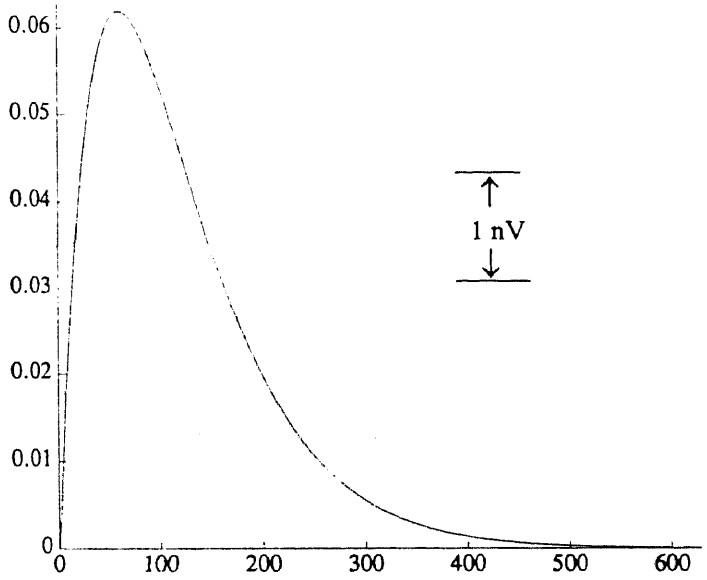

Figure 3.4.1 EP without EEG background

coefficients. The structure of the EP is not displayed in the single EP waveform until the lower levels of the wavelet representation are reached

This is clearly shown in the ninth level wavelet coefficients shown in figure 3.4.5. The single EP signal (figure 3.4.5a) does not contain the waveform of the signal averaged EP (figure 3.4.5b) but there is a definite relation of the structure brought out by the wavelet. The single EP contains structure similar to the signal averaged EP. Following the waveform of the signal averaged EP, there are smooth sections where the amplitude increases and decreases. The peaks and valleys of the waves contain signal components that are erratic and are obviously obtained from the background EEG. Following the single EP in the same manner, there are sections of the waveform that are smooth and erratic that line up with the components of the signal averaged EP. The different sections of structures are due to the wavelet and not the EP.

The peak between data points 450 and 550 of figure 3.4.8 contains the information of the EP. This EP is shifted and compressed due to the wavelet's decrease in time resolution. The side lobes which are on both sides of the peak containing the EP information are created by the wavelet. After closely examining the lowest wavelet coefficients, there may be similar structures of the single EP related to the signal

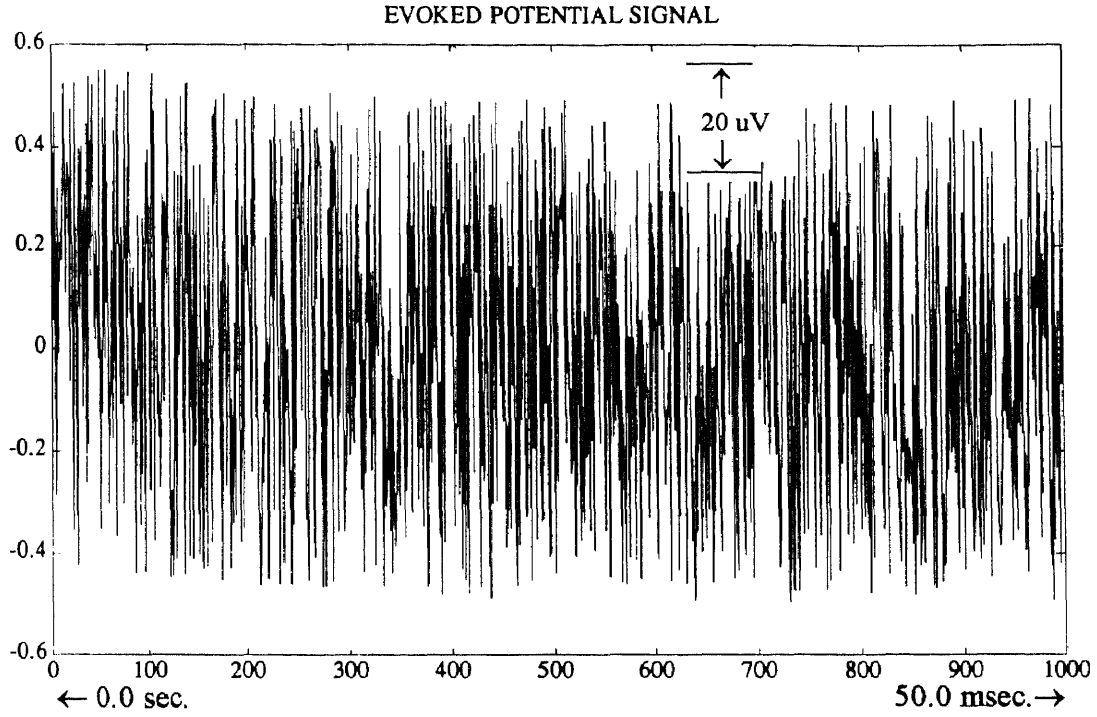

(a) Single EP

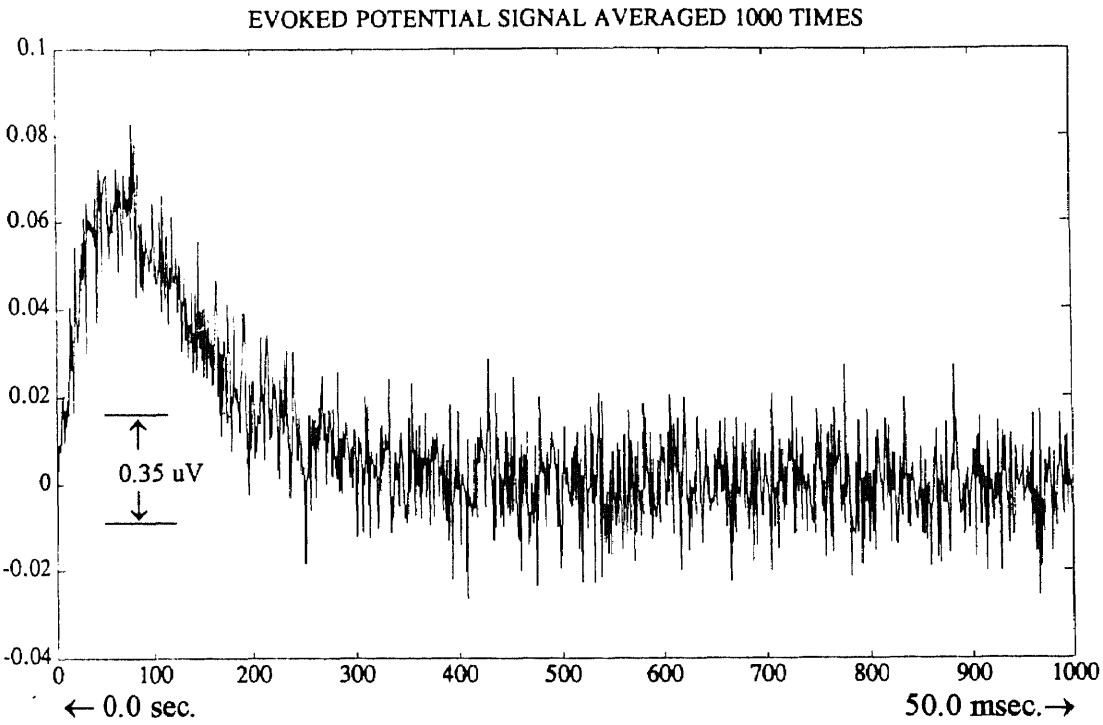

(b) Signal averaged EP

Figure 3.4.2 Original EP waveforms

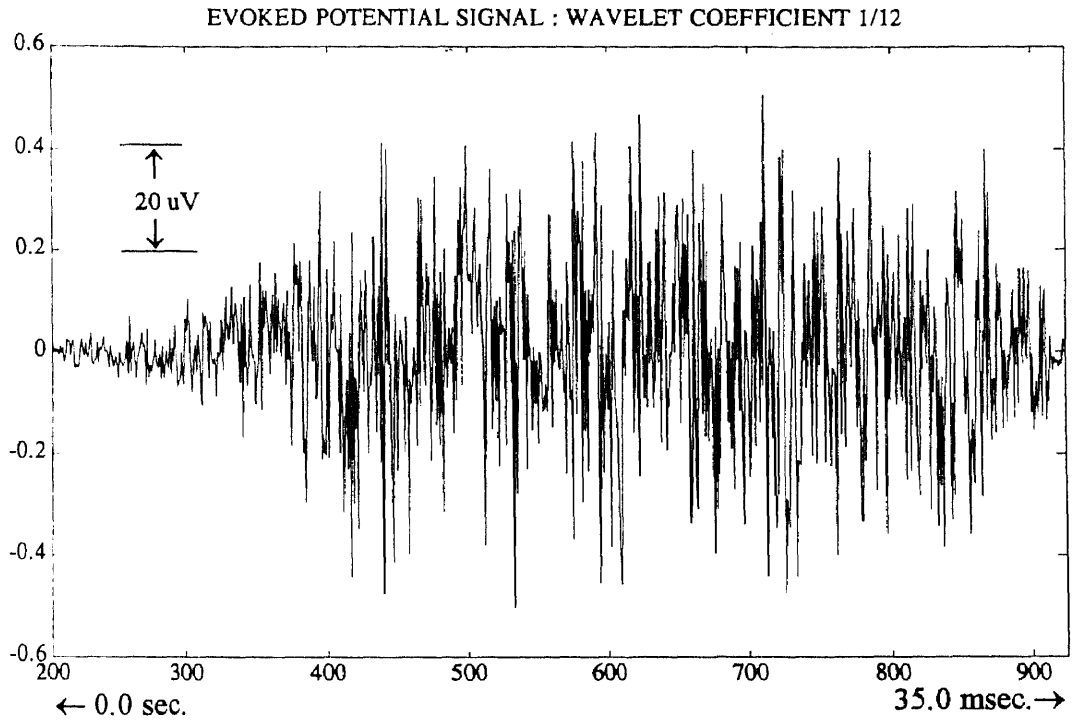

(a) Single EP

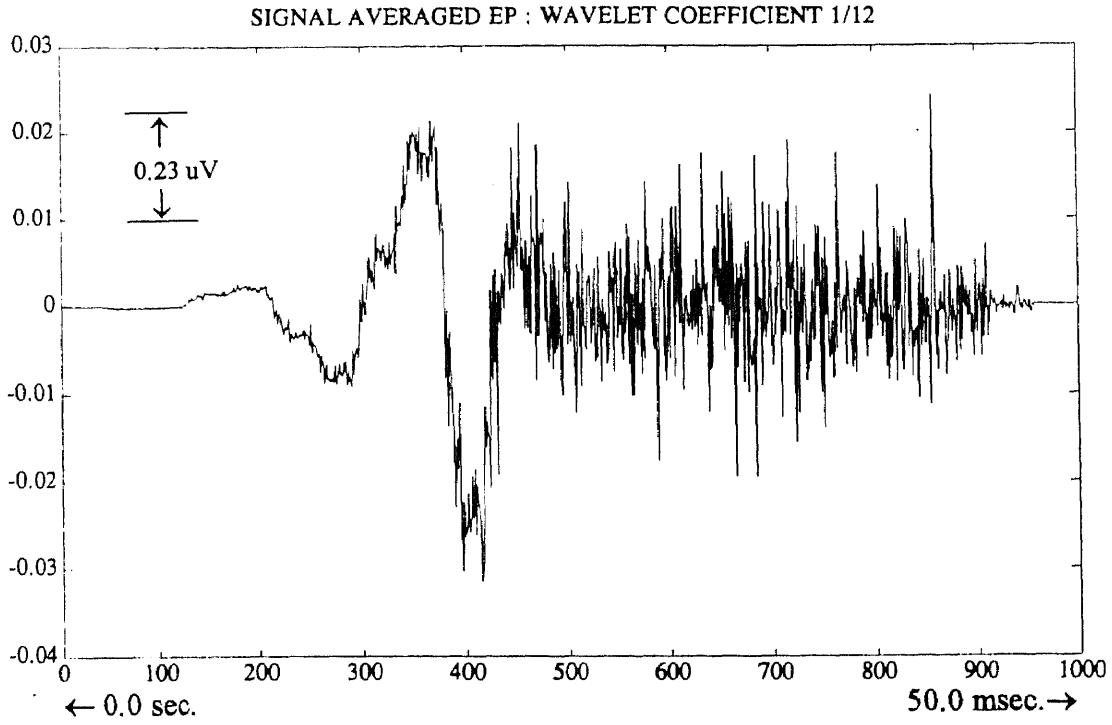

(b) Signal averaged EP

Figure 3.4.3 First level of EP wavelet coefficients

averaged EP by the amplitude of the peaks of the random structure in the single EP wavelet coefficient. The random structures are obtained from the background EEG.

The information of the EP (the single pulse without the background EEG) envelopes the structures of the background EEG. The envelope is the EP pulse components brought out by the wavelet with the background EEG contained within the envelope. Figure 3.4.9a shows the twelfth wavelet coefficient of the EP pulse. Figure 3.4.9b contains the twelfth wavelet coefficient of the background EEG enveloped by the EP pulse and figure 3.4.9c shows the twelfth wavelet coefficient of the background EEG without the EP pulse. These figures display how the EP pulse structure is brought out by enveloping the background EEG.

This can be compared to a radio signal where the envelope of the signal carries the desired signal information within the envelope. In this case of EPs, the envelope is the information, not what is contained within it. That is, the background EEG which does not contain EP information, is contained in the envelope of the EP details brought out by the wavelet.

3.5 Conclusion

The wavelet representation of EP waveforms provided a new tool for observing EP structures. The EP structure of both the single and signal averaged EP waveform were similar and were made apparent in the lower scales of the wavelet coefficients. The wavelet brought out the structure of the single EP waveform even though the amplitude of the EP was small and embedded in the background brain waves. Although the EP pulse details were brought out by the wavelet, there is still no clear relation between the wavelet coefficients of the single EP and the signal averaged EP. There must be a more detailed analysis of wavelets applied to signal averaged EPs for any evidence relating the wavelet coefficients of single and signal averaged EPs.

CHAPTER 4

APPLICATION OF THE WAVELET TRANSFORM TO THE ELECTROCARDIOGRAM

4.1 Introduction

The electrocardiogram (EKG) is a recording of the bioelectric potentials of the heart's activity. EKG signals are easily recorded by placing electrodes on the surface of the skin near the heart. Once the EKG is obtained, an interpretation of the waveforms can be made by observing the location and amplitude of the peaks. An alternative method for observing EKG signals can be achieved by applying the wavelet transform to the signal. The wavelet coefficients are obtained and an evaluation of the different scales of the wavelet representation can be made.

4.2 Introduction to the EKG

The EKG is a fascinating combination of biology, physics and electricity. The EKG is an extremely important and informative measurement of the bioelectric potentials of the function of the heart. The EKG is mostly used in diagnosis for the detection of disease and damage done to the heart. The EKG is obtained by using an instrument known as the electrocardiograph.

The electrocardiograph is the major diagnostic instrument of cardiac electrophysiology. It is estimated that approximately 150 million standard 12-lead EKGs are recorded annually. [11] The EKG is clearly a primary part of evaluation and prevention of heart disease. This clearly shows the important role the EKG plays in clinical diagnosis and any research performed to improve or create new ways of evaluating bioelectric information.

4.3 Basic Theory of the EKG

The heart is made up of cells just as any other organ in the body. The tissue of the heart is composed of cells immersed in fluid. The cells are surrounded by a membrane through which fluid that contains ions and molecules may pass in either direction. [12] The interior of the cell has a negative potential with respect to the exterior. The potential difference created is typically 70 mV. [12] Therefore cells in the resting state are electrically polarized. [11] Muscle and nerve cells are unlike other cells since the transmembrane potential depolarizes abruptly and then returns to its original resting value. [12] This change in potential is produced by a movement of sodium and potassium ions across the membrane, commonly referred to as the sodium-potassium pump. The return path for the ions often involves the entire body which is the case for the cells in the heart. [11] The electrical activity of the cells results in electric currents and electric fields throughout the whole body. The skin has a natural resistance and therefore,
potential differences are formed on the skin due to the electric currents that the heart creates. The resulting currents flowing through the skin can be readily measured, and gives rise to the EKG.

The heart's activity is transmitted throughout the heart by specialized nerve fibers which carry the electrical potentials that travel and create cardiac muscle movement. [11] If there is any damage or disease of the heart's conduction system there will be disturbances in the current pathways of the heart which will be displayed in the EKG. These disturbances are usually quite large.

The EKG is essentially a record of the potential difference developed at the leads that are placed on the skin, where the term "lead" refers to a particular arrangement of the electrodes. Figure 4.3.1 shows a standard 3-lead configuration for an EKG recording. Other EKG configuration's require a total of 12 electrodes, where six of the electrodes are placed across the subject's chest. [20]

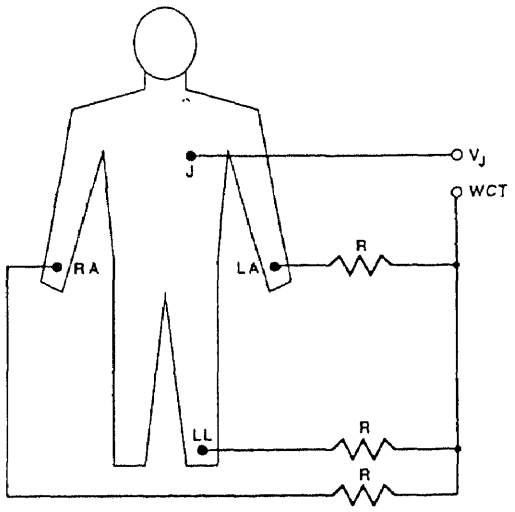

Figure 4.3.1 Standard EKG lead configuration

Other EKG configuration's require a total of 12 electrodes, where six of the electrodes are placed across the subject's chest. [20]

An EKG of a normal heart beat is shown in figure 4.3.2. The corresponding peaks and waves of the EKG are related to the function of the particular areas of the heart. The relation between the heart and the EKG are as follows

P-wave: Results from the spread of excitation through the atria. The atria is the chamber of the heart that receives blood from the veins and passes the blood on to the ventricles.

QRS Complex: Results from the excitation of the ventricles. The ventricles are responsible for pumping the blood to the arteries carrying the blood away to the body.

T-wave: Results from the recovery of the cells in the ventricles.

Identifying the P, QRS and T waves is not always straight forward and obvious. EKG diagnosis and evaluation rely solely on the identification of these waves, which is sometimes difficult for a human as well as a computer. The observer usually searches for changes in the size and shape of the waves and changes in the rhythm that can be periodic

or non-periodic. When the source of the problem is detected the physician can then properly treat the patient's illness.

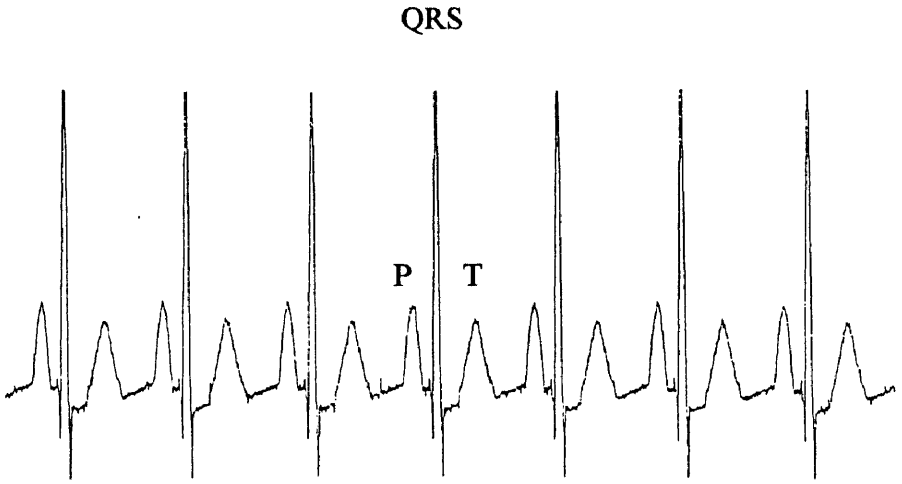

Figure 4.3.2 Normal EKG pattern

Recent developments have been made in the science of EKG signal analysis. For years researchers have observed the effects of heart disease in the time EKG waveform and paid little or no attention to the frequency aspects of the EKG. But one must understand that the properties that configure the EKG signal are created by the frequency properties of the signal. Wavelets provide a tool for examining the EKG in the time domain while separating the signal into its separate frequency components.

4.4 Results and Discussion of EKG Wavelet Analysis

An orthonormal wavelet of length 4 was applied to several EKG signals. The corresponding h(n) and g(n) filters used for the wavelet representation are listed in table 4.4.1. A length 4 filter was used since the wavelet coefficients at scales lower than 2^{-4}

were basically redundant and at this time a proper evaluation of the signal contents could not be made. The matlab programs for obtaining the filter coefficients are listed in Appendix C.

The EKG signals were created using the Laerdal Medical Heartsim 2000. This allowed the creation of different disorders and diseases of the heart without having to use real subject's. The heart simulator was utilized since it was necessary to maintain a regular pattern of heart beats for consistant wavelet results that can be easily detected. Real EKG data is not consistant and was therefore not used. The sampling rate of all EKG signals generated is 200 samples per second. This meets the Nyquist criterion since the highest frequency component of the EKG is 100 Hz. [12]

Table 4.4.1 Wavelet filter coefficients

h(n)	g(n)
0.3415	-0.0915
0.5915	-0.1585
0.1585	0.5915
-0.0915	-0.3415

The wavelet was first applied to a normal EKG signal shown in figure 4.4.1a. The first four wavelet coefficient decompositions are shown in figures 4.4.1b to 4.4.4. The first wavelet coefficient, figure 4.4.1b, is obviously obtained from an EKG signal and has the basic shape of the EKG. This first decomposition level is similar to the original signal

and one can easily see that this wavelet coefficient was obtained from an EKG signal. The results were similar for the second wavelet coefficient shown in figure 4.4.2. This is not the case with the remainder of the wavelet coefficients.

The next lower wavelet coefficients are not as distinctive as the first and second wavelet coefficients. At first, the decomposition levels of the EKG signal seem to be distorted, overlapping and repetitive. This distortion and overlapping of the EKG components occurred primarily due to the nature of the wavelet itself resulting from the time translations and dilations of the wavelet being applied to the signal. After looking more closely at a particular region of the wavelet coefficients, the properties of the signal become apparent. This is shown in figure 4.4.3b.

The largest spike of the normal EKG, the R wave peak, is predominant in the original signal and is carried through the entire set of wavelet coefficients. This spike appears in any level of the wavelet representation without having to zoom in on a particular region of the signal. For example, the third wavelet coefficient in figure 4.4.3a seems chaotic and unrelated to the original EKG signal. One can easily see the R peaks, but the rest of the signal components are not as obvious. Figure 4.4.3b concentrates on the middle of the third wavelet coefficient and the R wave peak is observed along with additional components that resemble the P, Q, S and T waves. Similar results were observed for the fourth wavelet coefficient shown in figure 4.4.4.

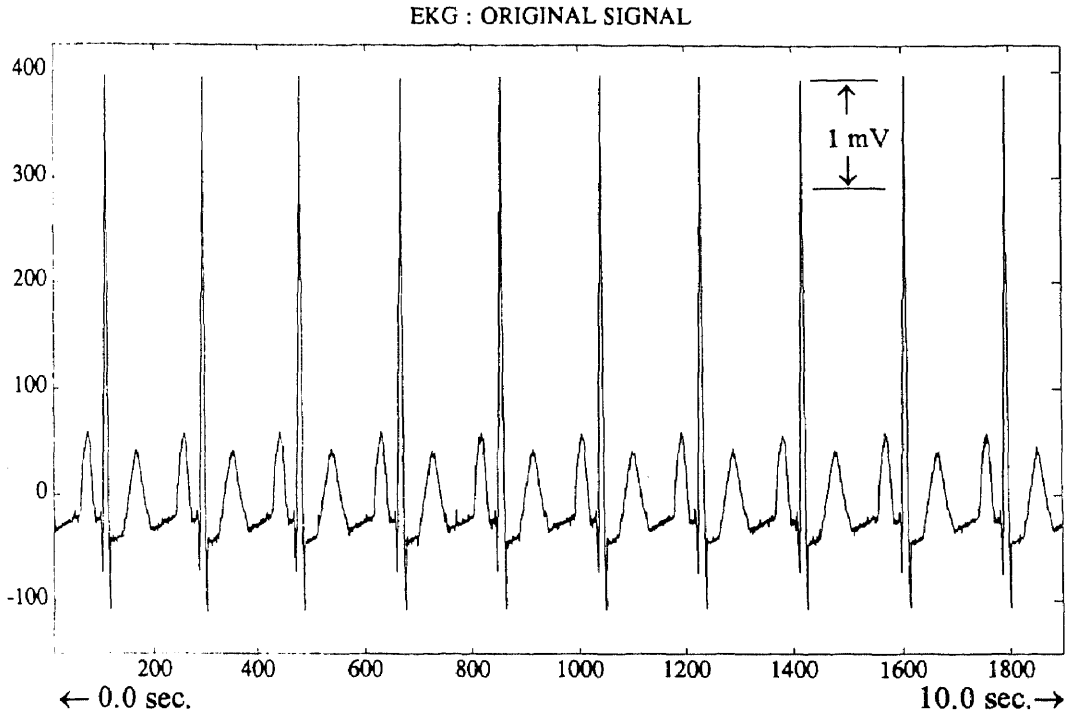

(a)

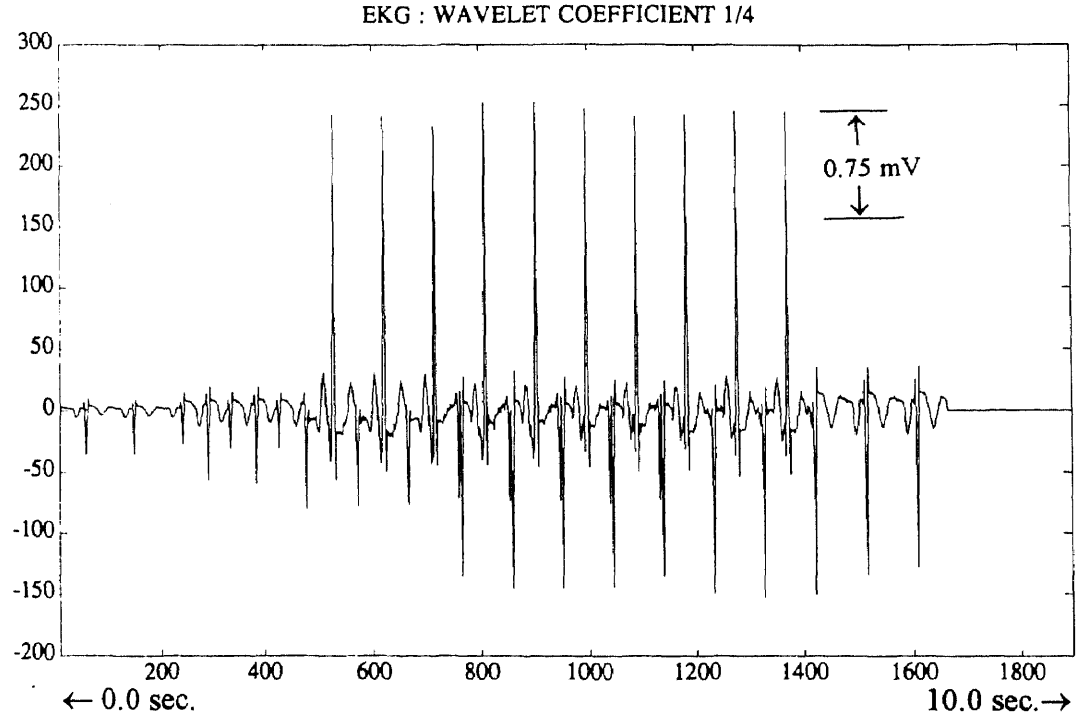

(b)

Figure 4.4.1 Normal EKG

60 Hz noise is usually embedded in the EKG recoridngs. Noise is created by bioinstruments and fluorescent lighting present in labs. [11] Even though noise can be filtered it is interesting to see the effects the wavelet representation has on an EKG signal with noise. 60 Hz noise was added to the normal EKG signal in figure 4.4.1a and is shown in figure 4.4.5a. The wavelet transform was then applied to the EKG signal with noise and is displayed in figure 4.4.5a.

The first wavelet coefficient is displayed in figure 4.4.5b. It is obvious that this signal is derived from an EKG signal. The EKG P, QRS and T waveforms are present along with some signal components that are apparently noise. The second wavelet coefficient is displayed in figure 4.4.6, with a zoomed in section of the second wavelet coefficient in figure 4.4.6b. The EKG waveforms are present and the 60 Hz noise has been filtered.

The sampling rate of the EKG is 200 Hz and the highest frequency component is 100 Hz. The first wavelet coefficient contained the frequency components in the range of 50 to 100 Hz. The second wavelet coefficient contains frequency components in the range of 25 to 50 Hz. (This is a result of the wavelet's bandpass filtering feature applied to the EKG signal.) Therefore, the noise was passed into the first wavelet coefficient and will not be present in any lower wavelet coefficients. This is shown in figures 4.4.6 and 4.4.7 where there is no noise present but the EKG waveforms are present. There are also changes in amplitude of the wavelet coefficients with noise when compared to the amplitudes of the wavelet coefficients of the EKG without noise. Even though the scales are slightly changed, the separate P, QRS and T waveforms can still be distinguished from one another.

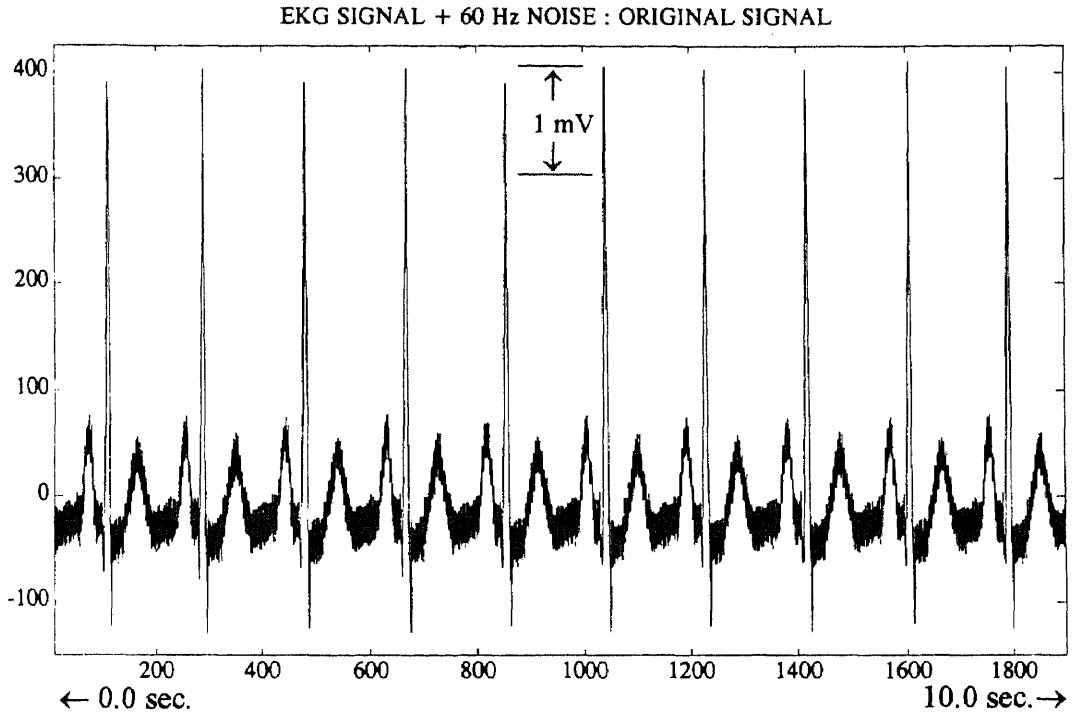

(a)

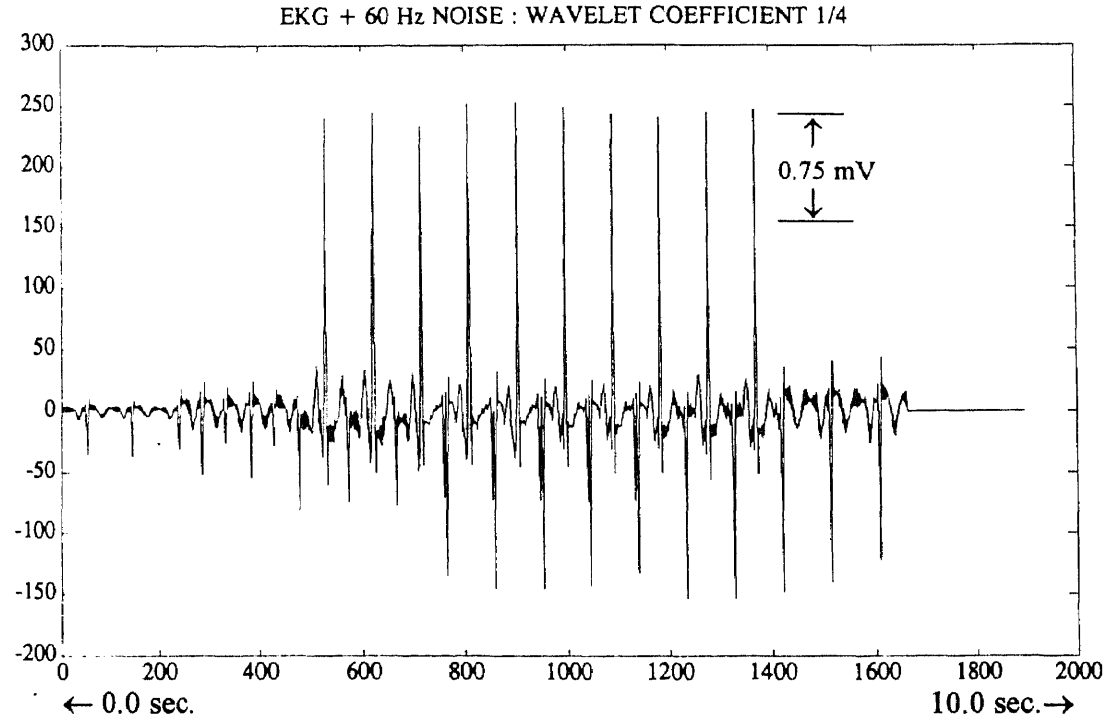

(b)

Figure 4.4.5 Normal EKG with 60 Hz noise added

The wavelet representation was also applied to irregular EKG signals. The first irregularity is known as a multifocal premature ventricular contraction (PVC). PVCs are created when the ventricles discharge independently from the rest of the heart. [12] This is shown by the large broad spikes which are larger in amplitude and duration than the R wave peaks.

This signal is displayed in figure 4.4.9a. The first wavelet and second wavelet coefficients are in figures 4.4.9b and 4.4.10, respectively. The first and second wavelet coefficients of this signal are apparently similar and contain the basic properties of the original signal, such as where the R peaks and the PVCs occur. However, the lower wavelet levels, 3 and 4, do not initially exhibit properties of the original EKG signal.

After zooming in on a section of the wavelet, the P,QRS, T and PVC waves of the signal become apparent. This is shown in figure 4.4.10 for the third wavelet coefficient and figure 4.4.11 for the fourth wavelet coefficient. The PVCs are still predominant throughout the wavelet representation. This was expected since the PVCs are very large in the original EKG signal.

The wavelet was also applied to an EKG signal containing an atrial fibrillation (AFIB). Atrial fibrillation occurs due to rapid unsynchronized contractions of the atria that prevent effective pumping of the blood to the ventricles. [12] This result is several outstanding P waves throughout the EKG sequence. An EKG with AFIBs is shown in figure 4.4.13a. The wavelet transform was applied and the resulting wavelet coefficients are displayed in figures 4.4.13b through 4.4.16.

The R wave is still predominant throughout the various levels of the wavelet representation. The EKG signal and added P wave components are apparent in the first wavelet coefficient. The lower wavelet coefficients, 2 through 4 (figures 4.4.14-4.4.16), also display the EKG and the additional P wave components in the closely examined sections of the wavelet levels.

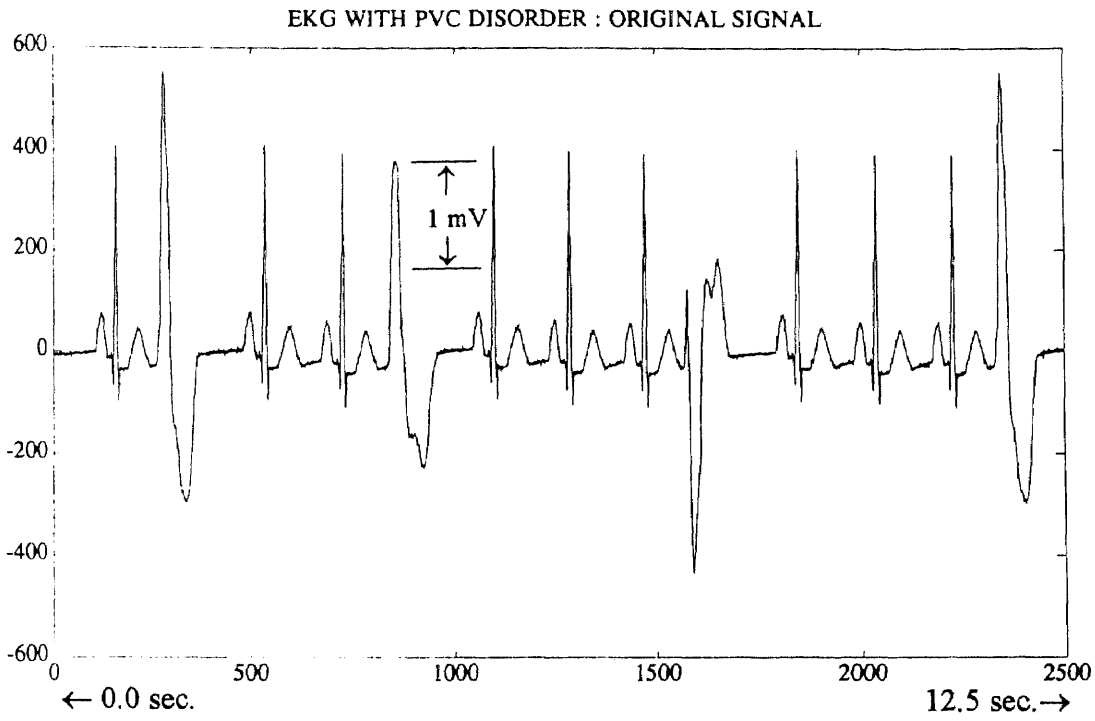

(a)

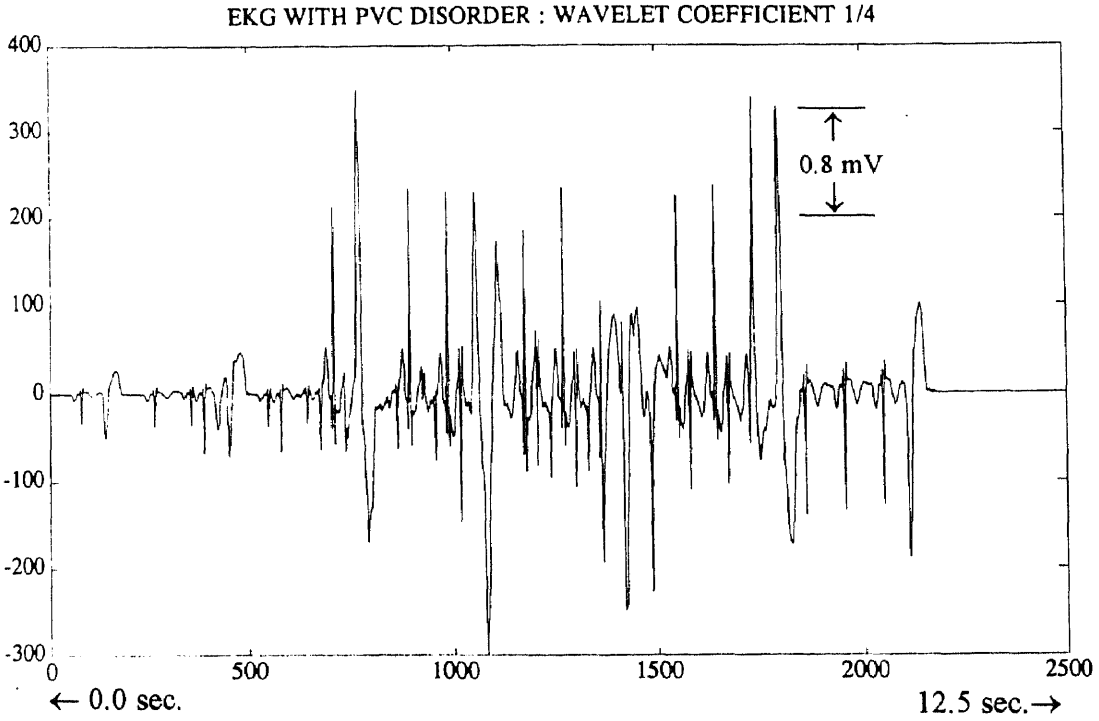

(b)

Figure 4.4.9 EKG with PVCs

4.5 Conclusion

The wavelet representation of EKG signals provided a new means for observing EKG waveforms. All signal components were carried through the various levels of the wavelet coefficients. Differences in the rhythm and pattern of the EKG can be detected for various disorders of the heart which were apparently brought out in the wavelet coefficients. The wavelet also successfully filtered out noise present in the EKG without distorting the resulting wavelet coefficients. Although the wavelet performed its task well, this direct application of the wavelet is not ideal for diagnosis since irregularities of the heart are very noticeable in the original signal without having to apply wavelets. Perhaps the wavelet would best be applied to time-frequency analysis of the EKG such as EKG spectrograms.

CHAPTER 5

CONCLUSION AND DISCUSSION

5.1 Discussion of Wavelet Transform Results

The wavelet transform proved to be a successful tool for interpreting MEP, EP and EKG biomedical signals. Structures of these signals that were not at first apparent in the original signal were exposed throughout the levels of the wavelet representation. This was shown in the previous chapters of this paper.

The MEPs are a perfect example of how details not initially present are displayed. The original MEP waveforms in channels 3 and 4, which were smaller in amplitude than channels 1 and 2, contained similar waveforms but were obviously different in peak location and amplitude. The similarities of channels 3 and 4 were shown in the very first set of wavelet coefficients. As the levels of the wavelet coefficients decreased the fine scale components of the signal were essentially the same. The MEP signals were recorded at sampling rates lower than the Nyquist rate. Therefore a completely accurate interpretation could not be made. The lower sampling rate did not affect the resulting wavelet coefficients as would be expected. Wavelet coefficients 3 through 6 were the same and differed only in amplitude. The reason for no variation in the wavelet coefficients is assumed to be due to the low sampling rate.

The EKG was recorded at a proper sampling rate and the resultant wavelet coefficients obviously differed from the MEP wavelet coefficients. The EKG clearly exhibited the properties of wavelets such as time dilation and translation. This is clearly shown by the "compressed" wavelet coefficients and the side lobes present at the ends of the coefficients.

The lower wavelet coefficients still contained structures that were identified as EKG waves (P, QRS and P waves) since the sampling rate was adequate. In other words,

since there were enough data points in the original signal the details of the lower coefficients contained enough data points to display the exposed components of the waveforms. As the EKG wavelet coefficients decreased in level, the time resolution decreased as there was an increase in frequency resolution. The MEP did not exhibit these properties, such as the side lobes of the EKG, but still decreased in scale as expected.

Wavelets also brought out irregularities present in EKGs with disorders such as the PVCs and AFIBs. The decomposition of these signal showed that the wavelet transfers all waveform structures whether large or small in amplitude, relative to the original signal. This is clearly demonstrated by the R waves which are obvious throughout the entire decomposition. Even when the time axis is compressed, the R waves are still predominant. The PVCs and AFIBs were also predominant in scale and repetition which were also exhibited at all levels. However, when concentrating on a particular region of the wavelet coefficients the other signal components which were not as large or predominant were still present and not outweighed, as one might speculate.

The wavelet analysis of the MEPs and EKGs were similar yet different. They were similar due to the fact that structures not originally present were exposed, but were different since the EKGs contained many waveforms and the MEPs contained only a few peaks. The MEPs finer frequency components were not displayed as in the EKG. The wavelet representation of the EP could be considered a combination of these two properties.

The wavelet analysis of the single EP and signal averaged EP showed that there was structure similar to both waveforms. The structures were defined by the background brain waves (EEG waves) separated by smooth sections of the signals. The rises and declines of the peaks in the signal averaged EP matched up with the sections of the single EP that leveled off. These sections of structure is a result of the wavelet. After examining the wavelet coefficients more closely, it was shown that the details of the EP pulse exposed by the wavelet enveloped the background brain waves.

The larger number of components were obviously the background brain waves which were predominant in the single EP while the pulse was the predominant feature of the signal averaged EP. Although the EP pulse was very small in amplitude in the single EP, its structure was displayed throughout the lowest levels of the wavelet coefficients. This correlates with the theory of wavelets presented. Recall that, the wavelet is essentially a bandpass filter passing the lower frequency components to the next wavelet level.

Noise (that is 60 Hz noise) was introduced into a normal EKG signal. The first wavelet coefficient contained noise which was present but not as great in amplitude and duration as in the original signal. The lower wavelet coefficients did not contain the noise. This occurred since the highest frequency component of the EKG was 100 Hz. The first wavelet coefficient contained the frequency components in the range of 50 to 100 Hz were noise is present. The components in the frequency range of 0 to 50 Hz was lowpass filtered to obtain the next lower levels of coefficients.

Since the wavelet is a bandpass filter passing only the lower end frequency components into the next wavelet level, the noise is not present in any levels except for the first wavelet coefficient. Noise was not present in the lower wavelet coefficients, but the amplitude of some components were slightly altered when compared to the EKG without noise.

5.3 Future Prospects

The results and observations made provide an excellent background for future work in the area of the application of wavelets to biomedical signal analysis. The biomedical signals presented in this work gave new insight into the usefulness of wavelets.

The MEPs were recorded below the Nyquist sampling rate and wavelet coefficients were still produced. In order to obtain accurate results, wavelet analysis of MEPs must be performed with signals recorded at appropriate sampling rates. Also, the

MEPs were recorded above threshold, where threshold is the minimum response of muscle movement to generate an MEP. A promising study would be to determine if the wavelet will bring out similar details for various levels of threshold. This would be beneficial since researchers often ignore MEP waveforms which are below a set threshold. Perhaps there is relevant information embedded in the wavelet coefficients throughout the different levels of threshold.

Wavelet EP studies have been performed and there is proof that details in the wavelet levels contain information that can be compared to injury-related changes in EP results. [24] Wavelets are also implemented in filtering techniques of BAEPs. [23] EP studies of wavelets could include developing a correlation between the structure of a single EP with a signal averaged EP. This correlation could relate various EP waveforms to one another which in turn would lead to using wavelets for clinical evaluation. There has not been any major findings in using wavelets for a direct approach in clinical diagnosis.

Direct application of wavelets can be used to detect QRS complexes embedded in abnormal events such as ischemia [21] and in the prediction of ventricular tachycardia. [22] In some cases it may be beneficial to incorporate wavelet analysis with other signal processing methods. For example, wavelets can be applied to EKGs for detecting ventricular late potentials. Ventricular late potentials are considered markers for life-threatening arrhythmias. In this case, time frequency plots of the wavelet coefficients of a single EKG heartbeat were used for detection of late potentials. [20] Perhaps, wavelet analysis of single EKG pulses along with trains of EKG pulses can be incorporated using the details of both for interpretation of abnormal events. Also, most of the observations made are with the wavelet coefficients. Perhaps there is important information lying in the scaling coefficients as well as in the wavelet coefficients.

5.3 Conclusion

The wavelet proved to be a beneficial tool in biomedical signal analysis. The wavelet representation of biomedical signals provided insight to the properties and structures of signals not initially displayed. The levels of the wavelet coefficients brought out these signal components and structures that were present in the original signals. The wavelet transform also proved to perform adequately even if the sampling rate was lower than required Nyquist sampling rate.

Dominant structures were carried through the levels of the wavelet coefficients. The wavelet not only displayed the larger signal components but also displayed the signal components that are less predominant. Although the smaller waveform components were not present in the resulting wavelet coefficients, the components appeared in general structures which were distinguishable.

Wavelet analysis of biomedical signals must eventually lead to a clinical correlation of the actual waveforms now used in clinical evaluations. Though there has been some work done with wavelets, wavelets are a new aspect of signal analysis and are not as commonly known as the Fourier transform. New methods of evaluating biomedical signals must constantly be developed. Any work performed and results achieved in the area of biomedical signal analysis will greatly benefit all.

APPENDIX A

ESSENTIALS OF ORTHONORMAL WAVELET FILTERS

An FIR filter with impulse response [$h(0)$, $h(1)$, ·····, $h(N\text{-}1)$] is given. The convolution of this filter with an infinite signal $s(n)$ followed by decimation (subsampling the result by 2 or taking every other term) corresponds to the matrix multiplication of the signal $s(n)$ by

$$\mathrm{H} = \begin{matrix} \vdots & \vdots & \vdots & \vdots & \vdots & \vdots & \vdots \\ \cdots h(N-1) & h(N-2) & \cdots\cdots & \cdots\cdots & h(0) & 0 & 0 \cdots \\ \cdots\ 0 & 0 & h(N-1) & \cdots\cdots & h(2) & h(1) & h(0) \cdots \\ \vdots & \vdots & \vdots & \vdots & \vdots & \vdots & \vdots \end{matrix} \tag{A.1}$$

Let us now assume that the impulse response and its shifted versions by even shifts form an orthonormal set given by

$$\langle h(N-2l), h(N-2k) \rangle = \delta_{k,l} \quad k, l \in Z \tag{A.2}$$

where Z is an integer vector field.

The equivalent of A.2 in matrix notation is

$$\mathrm{H} \cdot \mathrm{H}^* = \mathrm{I} \tag{A.3}$$

where I is a unity matrix.

The projection of the original signal sequence $s(n)$ onto the subspace spanned by the rows of H is given by

$$H^* H \cdot S. \tag{A.4}$$

The multiplication by H* corresponds to upsampling by two followed by convolution with a filter having impulse response [$h(N-1), h(N-2), \cdots, h(1), h(0)$] which is the time reversed impulse response of $h(n)$.

N must be even in order for the set of $\{h(n-2k),\ k \in Z\}$ to form an orthonormal basis. If N were odd then $\langle h(n), h(n-L-1)\rangle = h(0)h(L-1) \neq 0$ unless either $h(0)$ or $h(L-1)$ were 0. Let V_{-1} be the space of $l^2(Z)$ and V_0 the supspace of V_{-1} spanned by the rows of H. Now let W_0 equal the orthogonal complement of V_0 in V_{-1} represented by

$$V_{-1} = V_0 \oplus W_0. \tag{A.5}$$

Now the filter

$$g(n) = (-1)^n h(L-1-n) \tag{A.6}$$

and its even shifted versions form an orthonormal basis for W_0. This is shown by the relation

$$\langle h(N-2l), g(N-2k)\rangle = \delta_{k,l} \quad k, l \in Z. \tag{A.7}$$

In matrix notation the filter $g(n)$ is represented by G. Due to the orthogonal relationship between W_0 and V_0 we have

$$H \cdot G^* = 0. \tag{A.8}$$

Based on the orthonormalilty of $h(n)$, $g(n)$ also forms an orthonormal set denoted by

$$\langle g(N-2l), g(N-2k)\rangle = \delta_{k,l} \quad k, l \in Z \tag{A.9}$$

and

$$G \cdot G^* = I. \tag{A.10}$$

The projection of the original sequence onto W_0 is given by

$$G^* G \cdot S. \tag{A.11}$$

A complete projection of the orthonormal subspaces is obtained and results in

$$H^* H + G^* G = I. \tag{A.12}$$

Finally we can say that $g(n)$ and $h(n)$ form an orthonormal basis for the space spanned in $l^2(Z)$.

APPENDIX B

LINEAR VECTOR SPACES AND ORTHONORMAL PROPERTIES OF VECTORS

B1: Vector Subspaces [13], [14]

Let a set of vectors X be a subset of a vector space V over a field K, where K is the field of scalars and the elements of K form an arbitrary vector field. If X is a subset of V the following identities for the subspace X are:

(i) $0 \in X$ (or $X \neq 0$)

(ii) X is closed under vector addition, or for every u, $v \in X$, the sum $u + v \in X$.

(iii) X is closed under scalar multiplication. For every $u \in X$, $k \in K$, the multiple

$k \bullet u \in X$

where $\in$ represents that the product $k \bullet u$ is contained in the vector space X. For the vector space S to be a subset of the vector space V, the following conditions must be met:

(i) The span S is a subspace of V which contains S.

(ii) If X is a subspace of V containing S, then $S \subset X$.

B2: Linear Spans and Vector Bases [13], [14]

Let a given set of vectors in a field V be represented by $v_1, v_2, \cdots\cdots, v_n \in V$. Then any vector in the form

$$a_1 v_1 + a_2 v_2 + \cdots\cdots + a_n v_n. \tag{B.1}$$

is a linear combination of $v_1, v_2, \cdots\cdots, v_n$.. The elements a_i are contained in the vector field K. The set of all linear combinations given by

$$\text{span}\,(\,v_1, v_2, \cdots\cdots, v_n\,) \tag{B.2}$$

is called the linear span of the vector space $V\,(\,v_1, v_2, \cdots\cdots, v_n,)$. Also, for a given vector space V, vectors $u_1, u_2, \cdots\cdots, u_n$ are said to span the vector space V if

$$V = \text{span}(\,u_1, u_2, \cdots\cdots, u_n\,) \tag{B.3}$$

For this to be true, there must exist scalars $a_1, a_2, \cdots\cdots, a_n$ such that

$$v = a_1 u_1 + a_2 u_2 + \cdots\cdots + a_n u_n \tag{B.4}$$

The vector V is then a linear combination of $u_1, u_2, \cdots\cdots, u_n$.

In other words, for a given set $S = \{u_1, u_2 \cdots\cdots, u_n\}$ of vectors is a basis if every vector $v \in V$ can be written as a linear combination of the basis vectors. A set S is a basis of V if the following conditions hold:

(i) $u_1, u_2 \cdots\cdots, u_n$ are linearly independent.

(ii) $u_1, u_2 \cdots\cdots, u_n$ span the space of V.

The vectors of V are linearly dependent over K if there exists $a_1, \cdots\cdots, a_n \in K$, with not all of the elements in $K = 0$, so that

$$a_1 v_1 + a_2 v_2 + \cdots\cdots a_n v_n = 0. \tag{B.5}$$

If the vectors are not linearly dependent then they are linearly independent.

B3: Orthogonal and Orthonormal Bases [13], [14]

To begin creating an orthonormal vector space let vector space V be an inner product space denoted by $\langle u, v \rangle$, where the inner product $\langle u, v \rangle$ is equivalent to $\int u(t)v(t)\,dt$. The vectors $u, v \in V$ are said to be orthogonal and u is said to be orthogonal to v if

$$\langle u, v \rangle = 0 \tag{B.6}$$

The orthogonal relationship is symmetrical so that if u is orthogonal to v then, $\langle v, u \rangle = 0$ and then v is orthogonal to u. This orthogonal relationship can also be expanded to the entire set of vectors contained in a designated space. To create an orthogonal set of vectors one can implement a procedure known as the Gram-Schmidt orthogonalization process. Once an orthogonal set of vectors is obtained, an orthonormal set of vectors can then be derived.

A set of vectors S, which is a subspace of V, is called orthogonal if each pair of vectors in S are orthogonal, and S is called orthonormal if each vector in S has unit length. In other words, $S = \{u_1, u_2 \cdots, u_n\}$ is orthogonal if

$$\langle u_i, v_j \rangle = 0 \quad \text{for } i \neq j \tag{B.7}$$

and orthonormal if

$$\langle u_i, v_j \rangle = 0 \quad \text{for } i \neq j \tag{B.8}$$

and

$$\langle u_i, v_j \rangle = 1 \quad \text{for } i = j. \tag{B.9}$$

To normalize an orthogonal set of vectors one must go through the process of multiplying each vector in the vector set by the reciprocal of its length in order to transform the set into an orthonormal set of vectors. A basis S of a vector space V is called an orthonormal basis if S is an orthogonal or an orthonormal set of vectors.

B4: Orthogonal Complements [13], [14]

Let S be a subset of an inner product space V. The orthogonal complement of S, given by $S^{\perp}$, consists of the vectors in V which are orthogonal to every vector contained in S. The vector $u \in S$ results in

$$S^{\perp} = \{\ v \in V : \langle v, u \rangle = 0 \ \text{ for every } u \in S\ \} \tag{B.10}$$

For a given vector u in V, we have

$$u^{\perp} = \{\ v \in V : \langle v, u \rangle = 0\ \} \tag{B.11}$$

where $u^{\perp}$ is all the vectors in V that are orthogonal to the given vector u.

APPENDIX C

MATLAB PROGRAMS

C1: Calculation of Wavelet Filter Coefficients [5]

filters.m

```
N = L/2;                                % L is the length of the wavelet filter sequence
a = 1; b = 1; c = 1;                    % initialize the variables
h = [1 1];                              % initialize factors of zeroes at -1
for j = 1:N-1;
   h = conv(h,[1 1]);                   % generate polynomials for zeroes at -1
   a = -a*0.25*(j + N-1)/j;             % generate the binomial coefficient of L
   b = conv(b,[1 -2 1]);                % generate variable values for L
   c = [0 c 0] + a*b;                   % generate variable value for L
end
q = sorts(roots(q));                    % factor L
h = conv(h, real(poly(c(1:N-1))));      % combine zeros at -1 and L for wavelet
h = h/sum(h);                           % normailze the filter sequence
h = [h];
LE = length(h);                         % LE equals the length of filter h
g = h(LE:-1:1).*cos(pi*[0:LE-1]);       % calculate filters for scaling function
```

C2: Calculation of Wavelet Coefficients

wavecoef.m

```
k = data;                               % enter signal to be seperated into
                                        % wavelet coefficiients
h = upsample(h, length(data)/length(h));  % insert zeroes between filter coefficients of h
g = upsample(g, length(data)/length(h));  % insert zeroes between filter coefficients of g
```

```
for T = 1:length(h)
    w = dnasmple(conv(g,k));          % obtain wavelet coefficients
    s = dnasmple(conv(h,k));          % obtain scaling coefficients
    W(:,T) = w';                      % store resulting wavelet coefficients
end
W(:,T + 1) = k';                      % store final scaling coefficient to achieve
                                      % signal reconstruction
```

C3: Upsampling and Downsampling Subroutines [5]

upsample.m

```
function y = upsample(x,Z);
% inserts Z-1 zeros between each term in the row vector x
L = length(x);
y(:) = [x,zeros(1,L)];
y = y.';
y = y(1:2*L-1);
```

dnsample.m

```
function y = dnsample(x)
% removes every other term in row vector x
L = length(x);
y = x(1:2:L);
```

C4: Evoked Potentials Simulation Program

evoked.m

```
% creates EPs and performs signal averaging
i = [0:1:999];                        % initialize 1000 data points
```

```
k = 10 * (exp(-i/60) - exp(i/59));          % create original EP pulse
r = rangen(1000);                           % add random background brain waves
H = [0];                                    % initialize counter for signal averaging
for T = 1:1:1000;                           % signal average 1000 times
    H = r + H + k';                         % perform signal averaging by adding EP
                                            % plus background brain waves
    r = rangen(1000);                       % create new background to be added
end
H = H/1000;                                 % normalize signal averaged results
```

rangen.m

```
function r = rangen(x)
% creates random background EEG for EPs
r = rand(x,1000);                           % create new background EEG
r = r - mean(r);                            % normalize background EEG
```

APPENDIX D

FIGURES

Figure **Page**

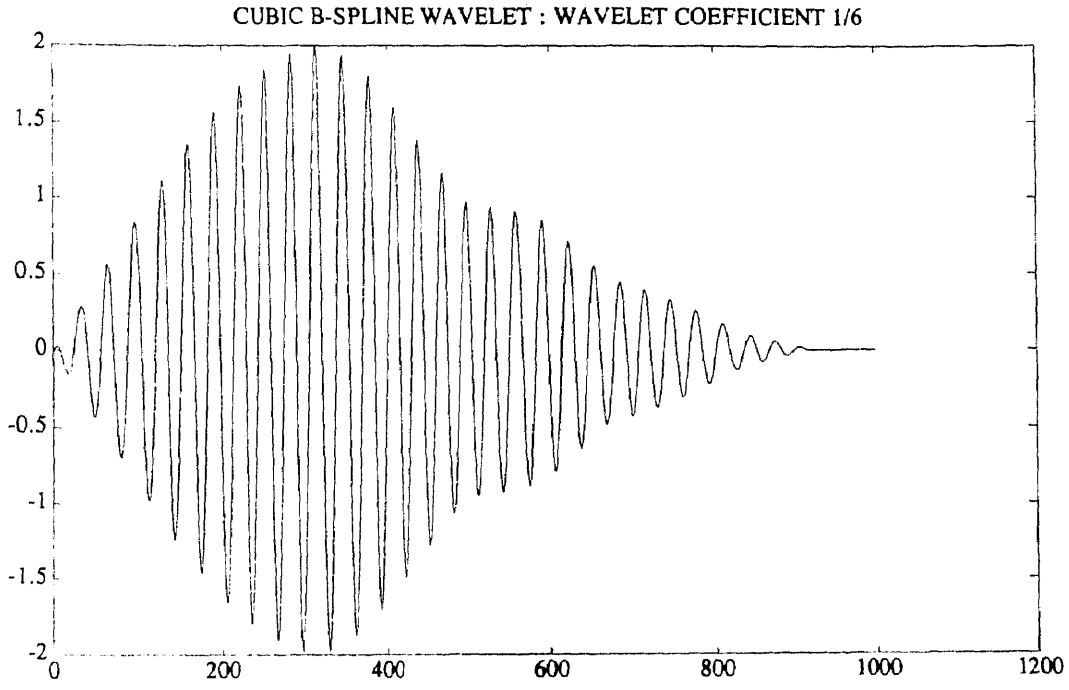
CUBIC B-SPLINE WAVELET : WAVELET COEFFICIENT 1/6
2
1.5
1
0.5
0
-0.5
-1
-1.5
-2
0
200
400
600
800
1000
1200

(c)

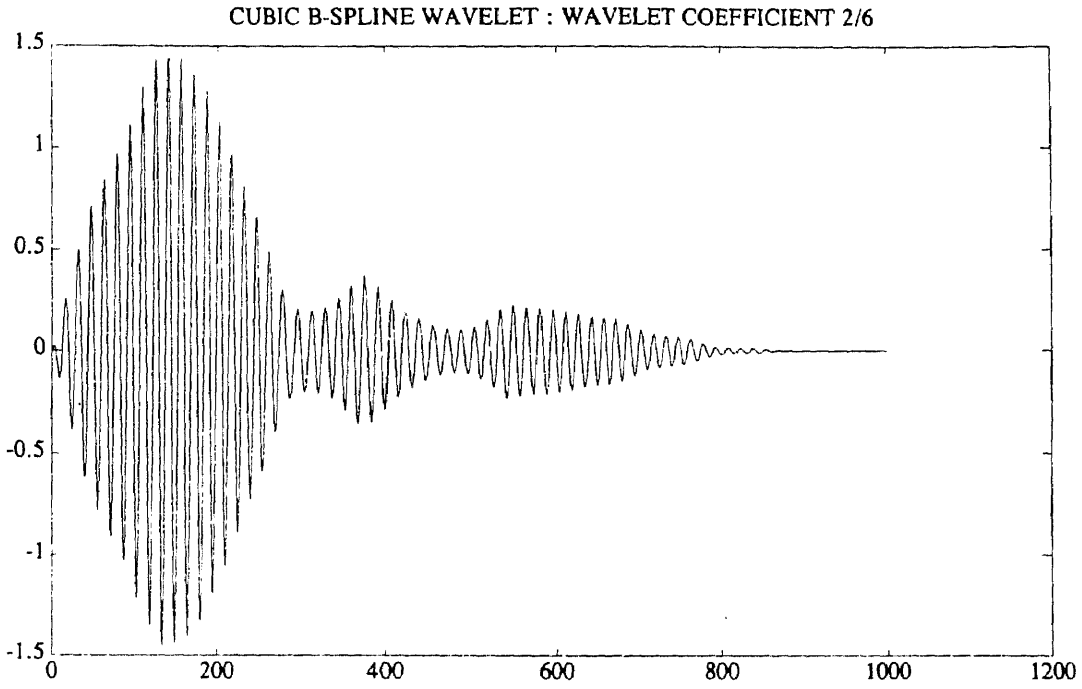
CUBIC B-SPLINE WAVELET : WAVELET COEFFICIENT 2/6
1.5
1
0.5
0
-0.5
-1
-1.5
0
200
400
600
800
1000
1200

(c)

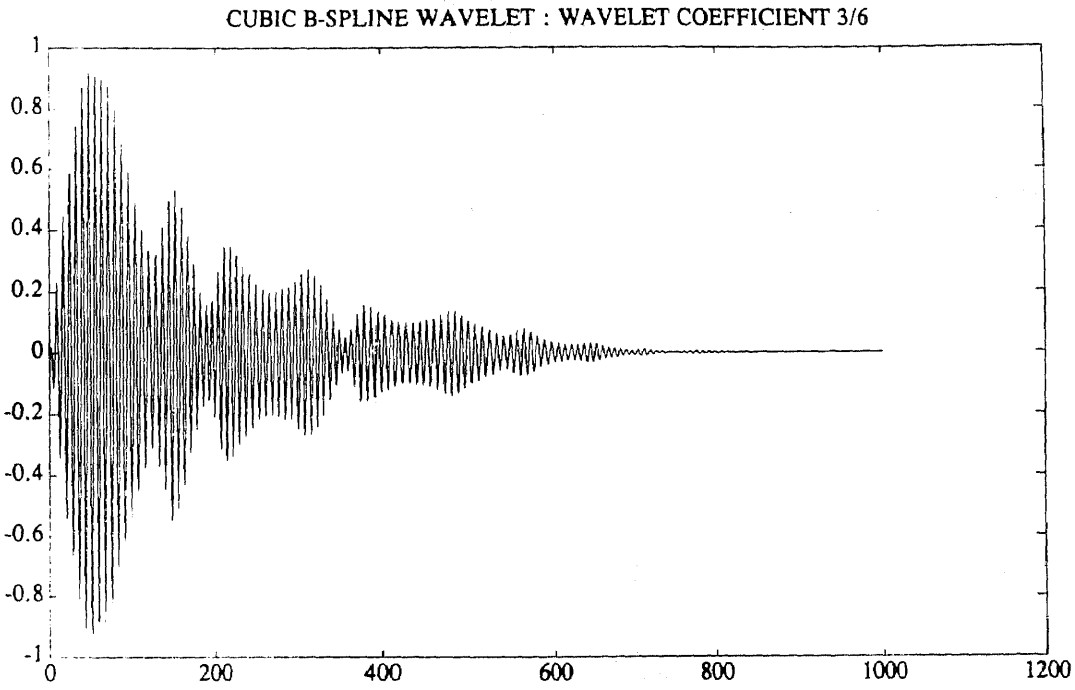
CUBIC B-SPLINE WAVELET : WAVELET COEFFICIENT 3/6
1
0.8
0.6
0.4
0.2
0
-0.2
-0.4
-0.6
-0.8
-1
0
200
400
600
800
1000
1200

(c)

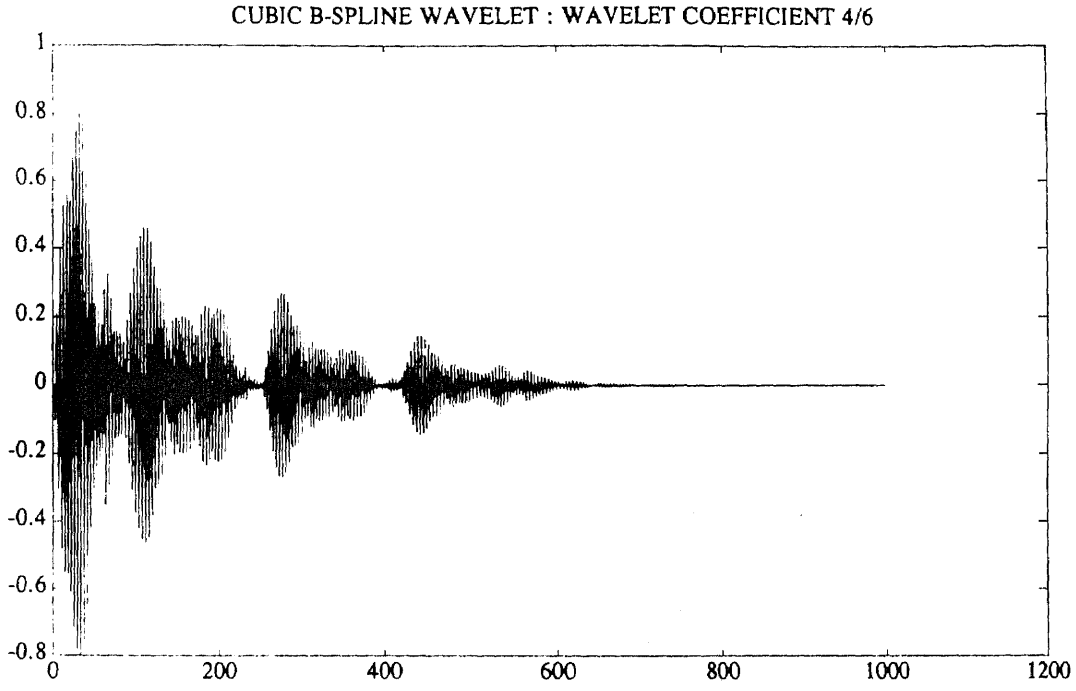
CUBIC B-SPLINE WAVELET : WAVELET COEFFICIENT 4/6
1
0.8
0.6
0.4
0.2
0
-0.2
-0.4
-0.6
-0.8
0
200
400
600
800
1000
1200

(c)

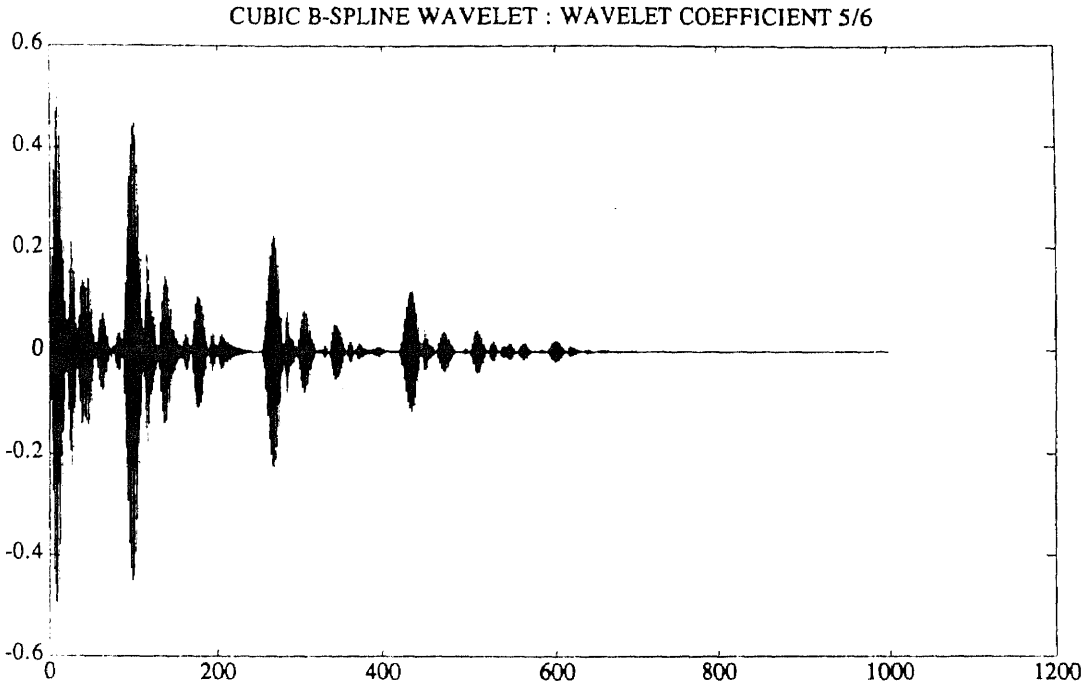
CUBIC B-SPLINE WAVELET : WAVELET COEFFICIENT 5/6
0.6
0.4
0.2
0
-0.2
-0.4
-0.6
0
200
400
600
800
1000
1200

(c)

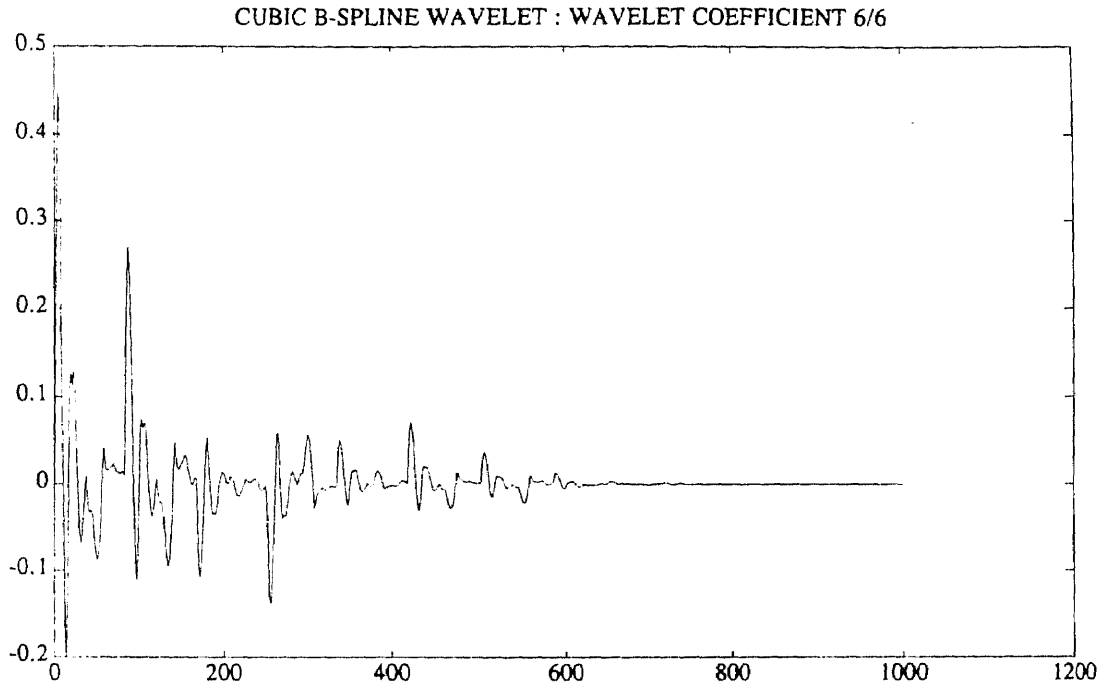
CUBIC B-SPLINE WAVELET : WAVELET COEFFICIENT 6/6
0.5
0.4
0.3
0.2
0.1
0
-0.1
-0.2
0
200
400
600
800
1000
1200

(c)

APPENDIX E

FIGURES

Figure **Page**

Figure **Page**

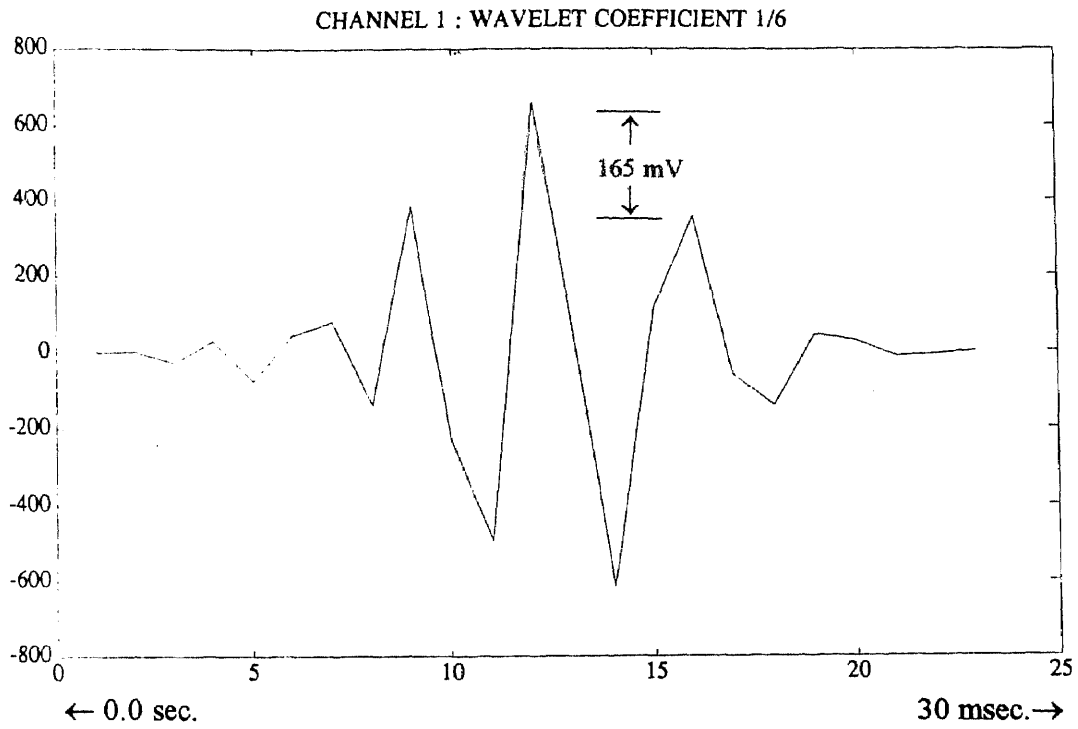

(a) Channel 1

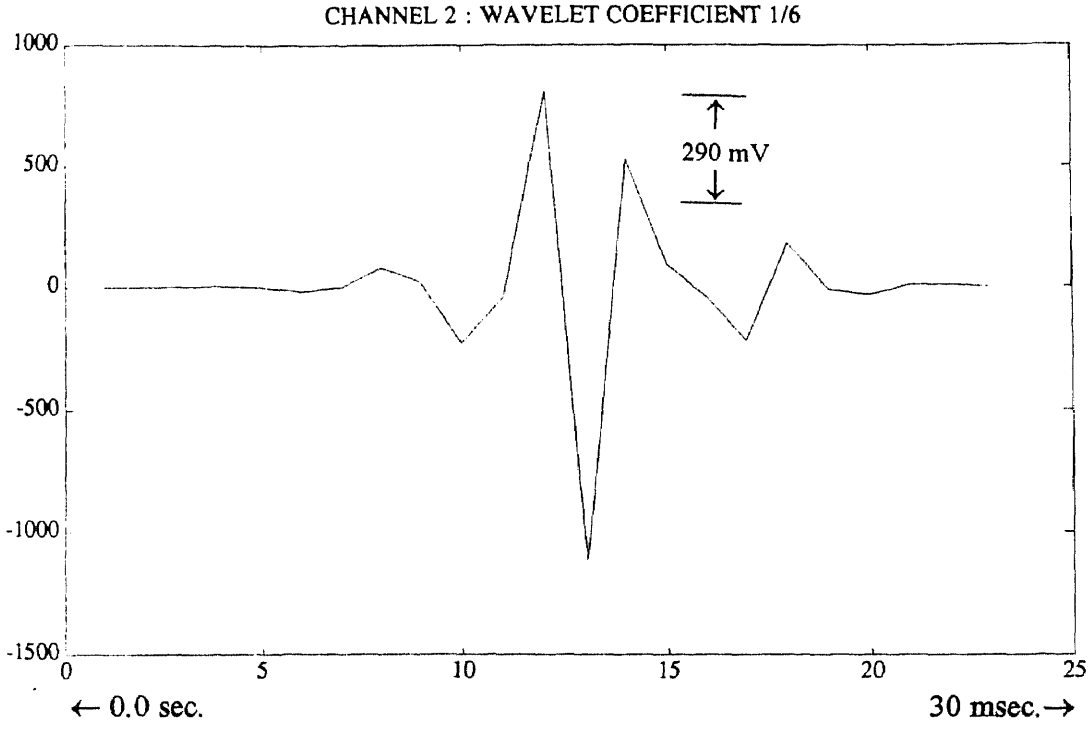

(b) Channel 2

Figure 2.4.3 First level of MEP wavelet coefficients

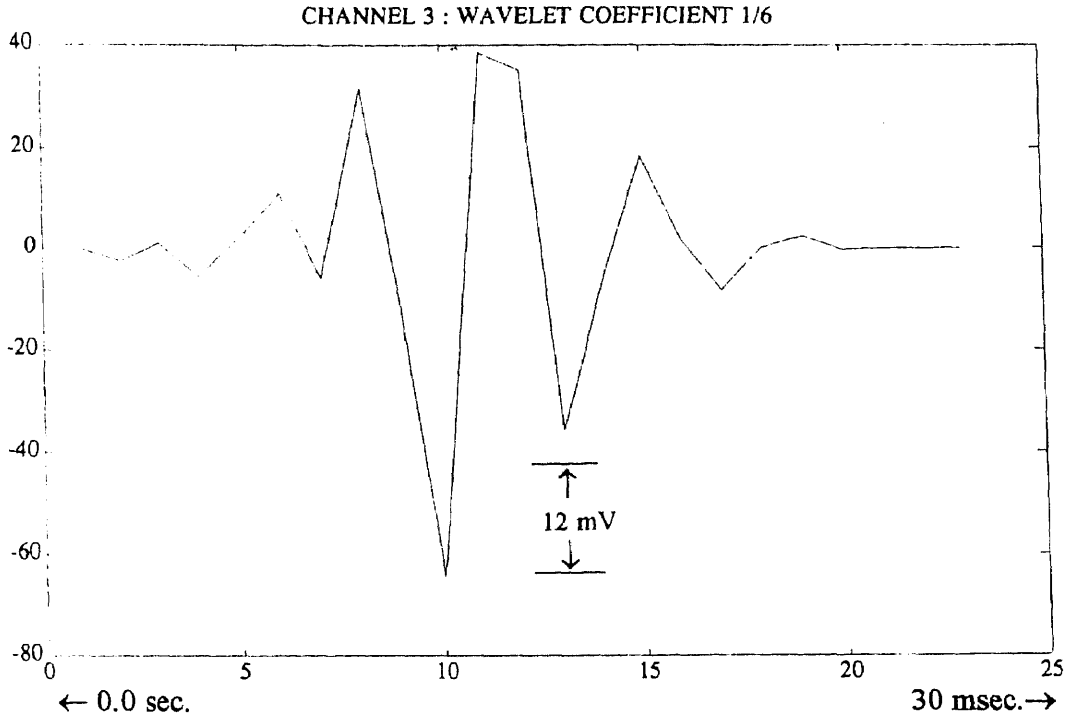

(a) Channel 3

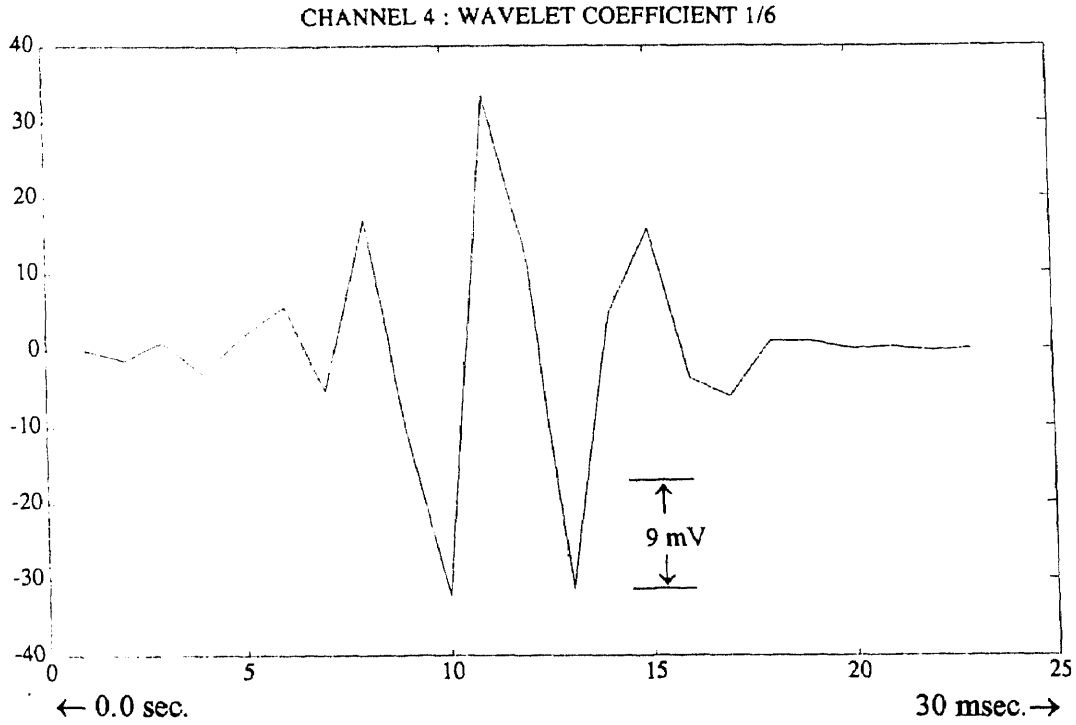

(b) Channel 4

Figure 2.4.4 First level of MEP wavelet coefficients

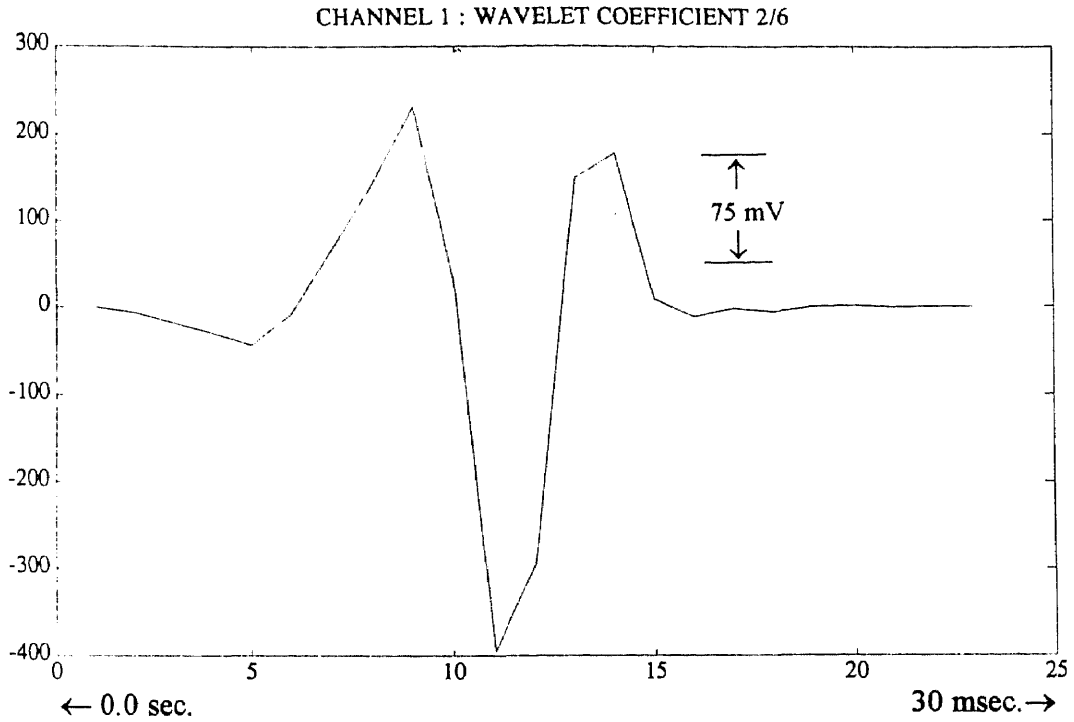

(a) Channel 1

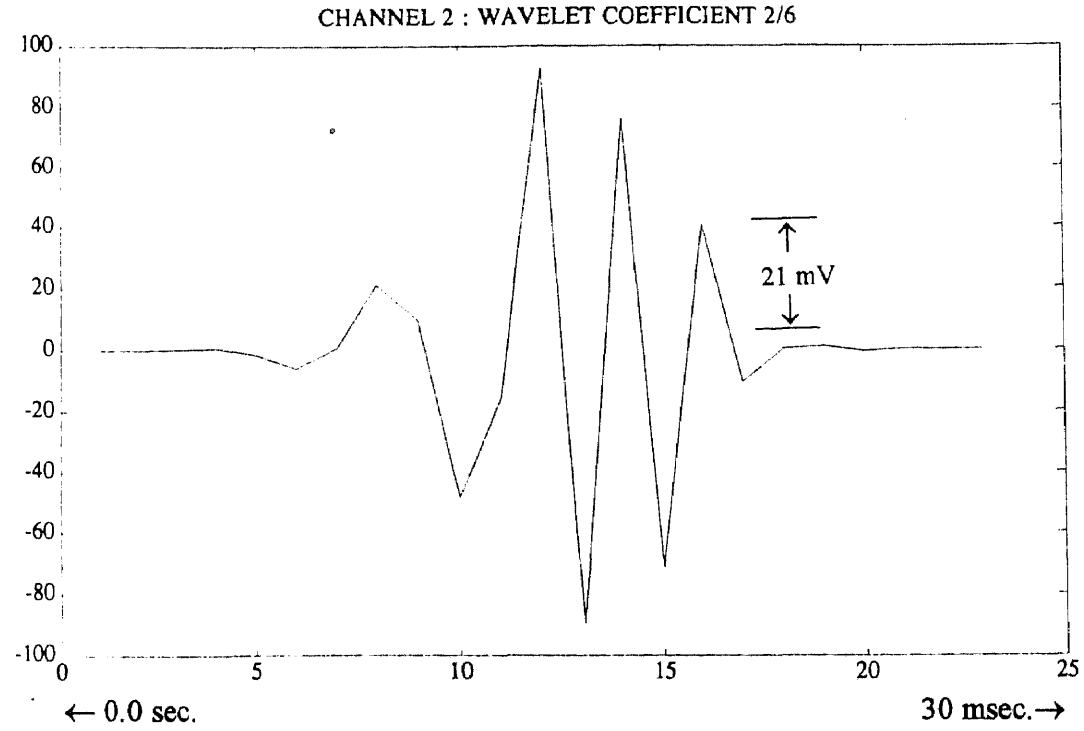

(b) Channel 2

Figure 2.4.5 Second level of MEP wavelet coefficients

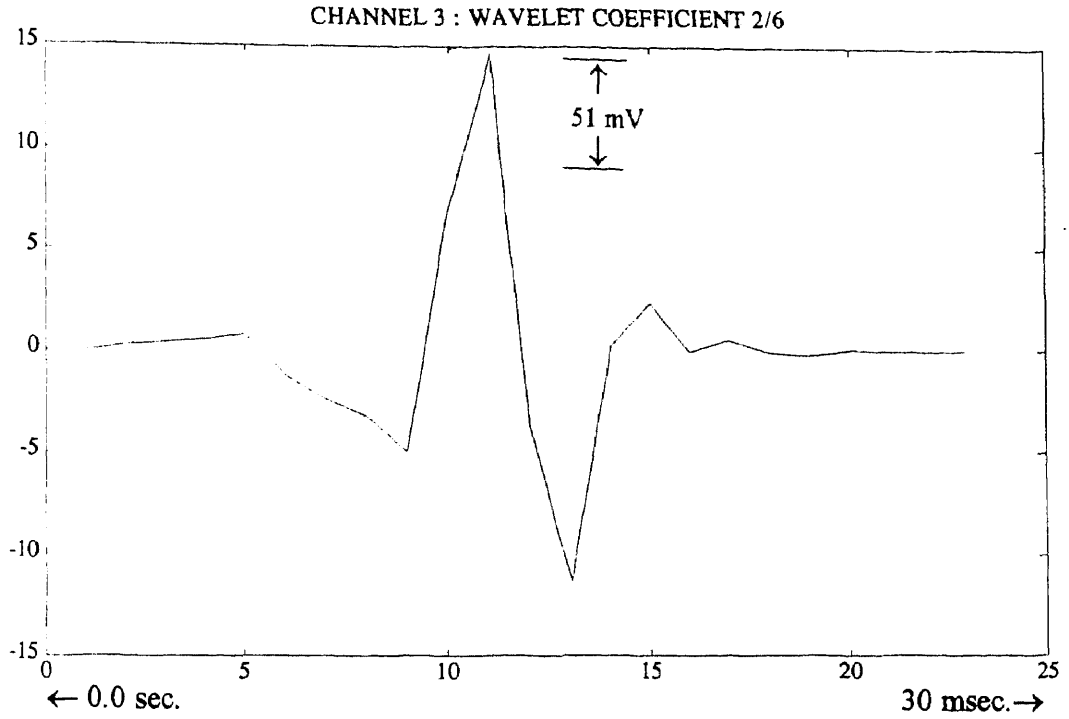

(a) Channel 3

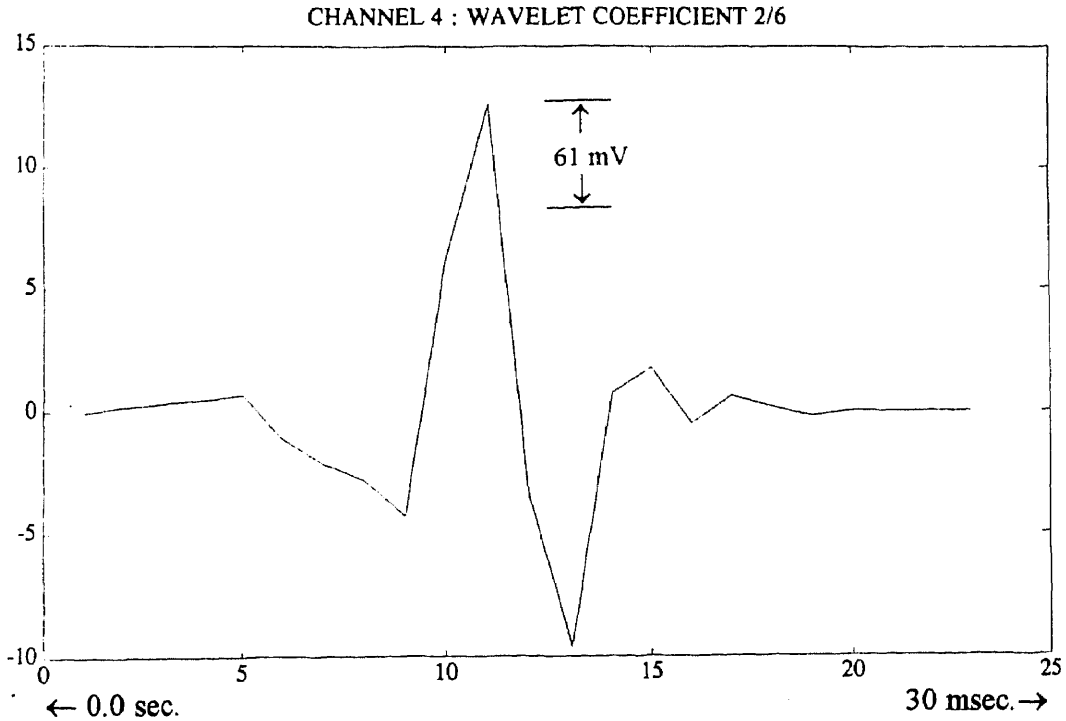

(b) Channel 4

Figure 2.4.6 Second level of MEP wavelet coefficients

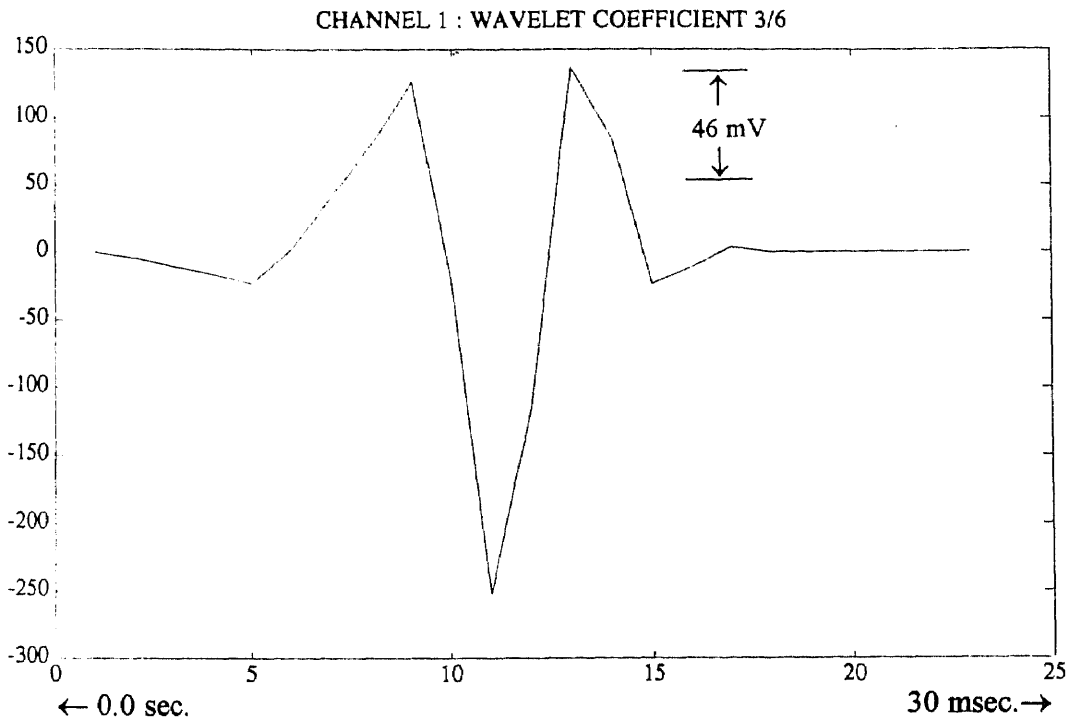

(a) Channel 1

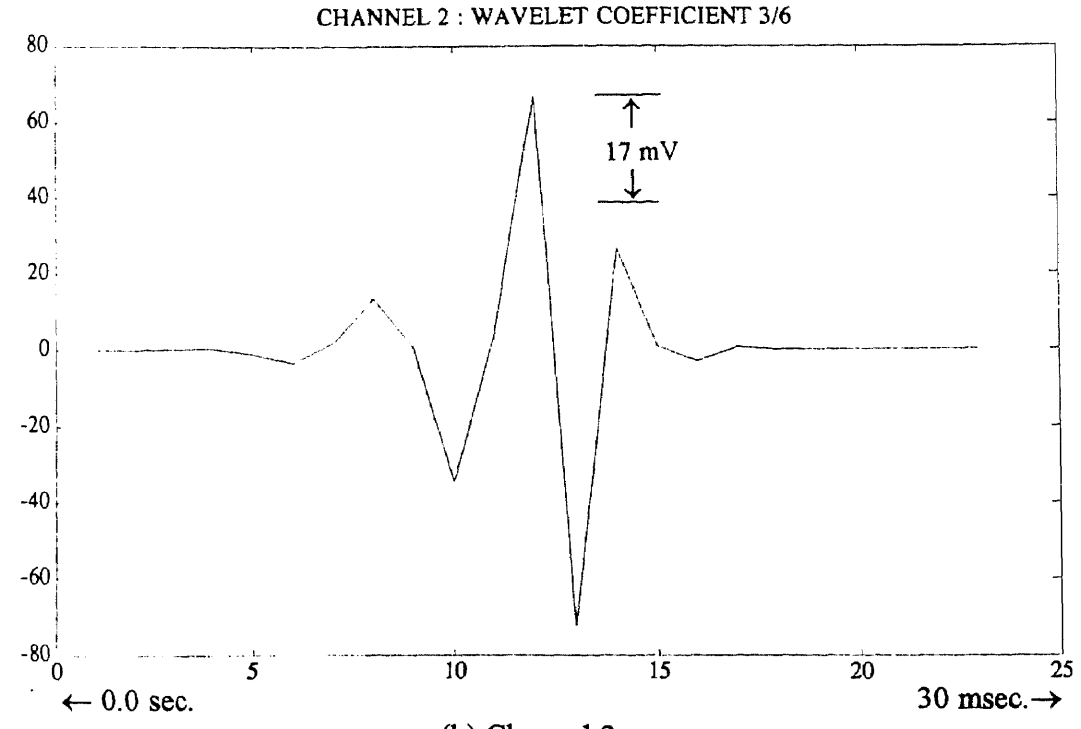

(b) Channel 2

Figure 2.4.7 Third level of MEP wavelet coefficients

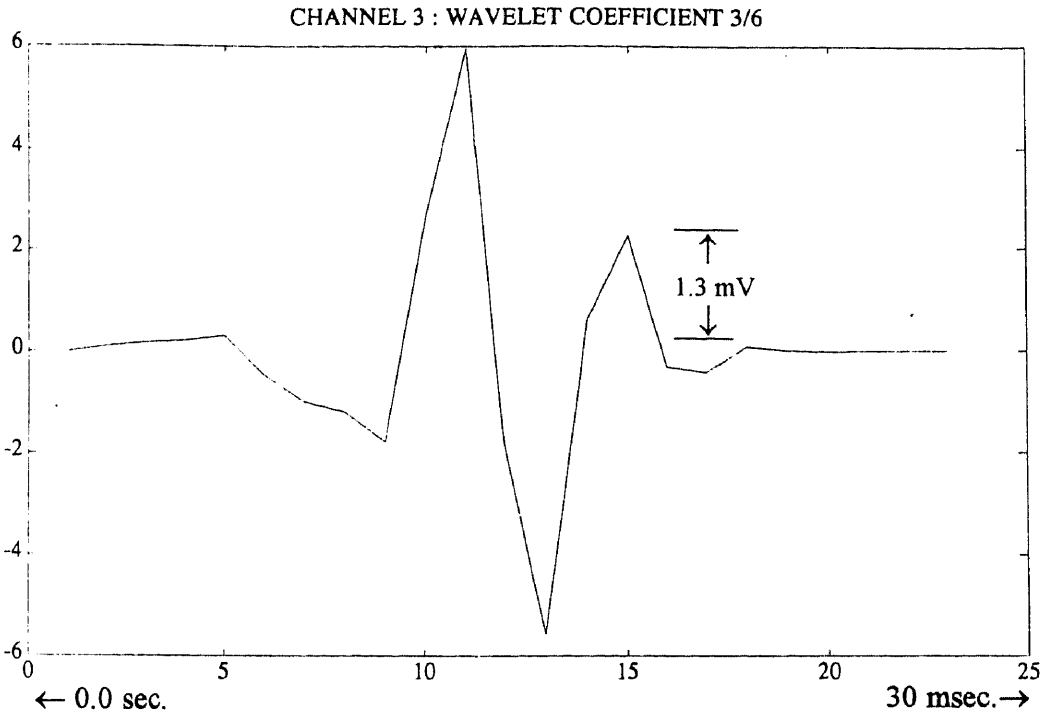

(a) Channel 3

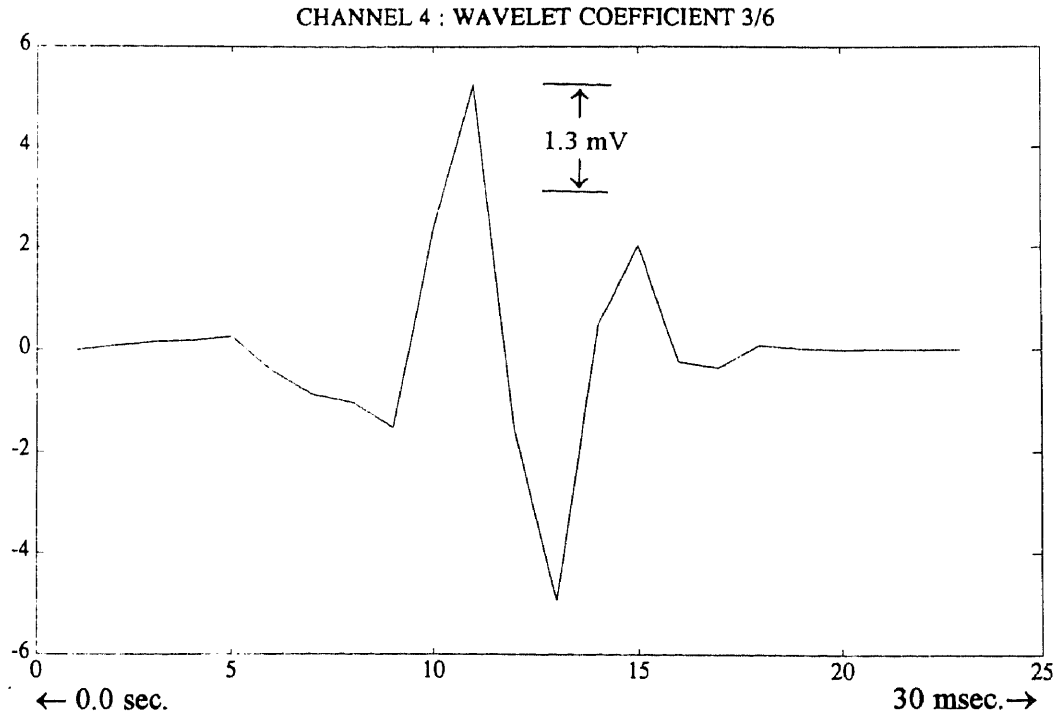

(b) Channel 4

Figure 2.4.8 Third level of MEP wavelet coefficients

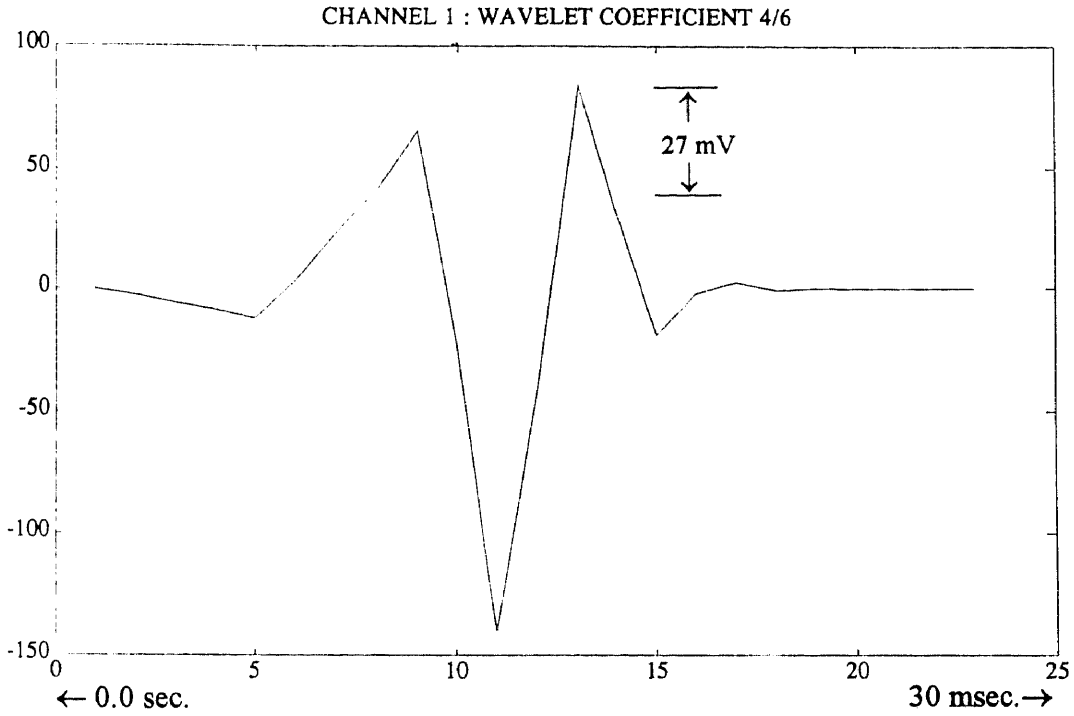

(a) Channel 1

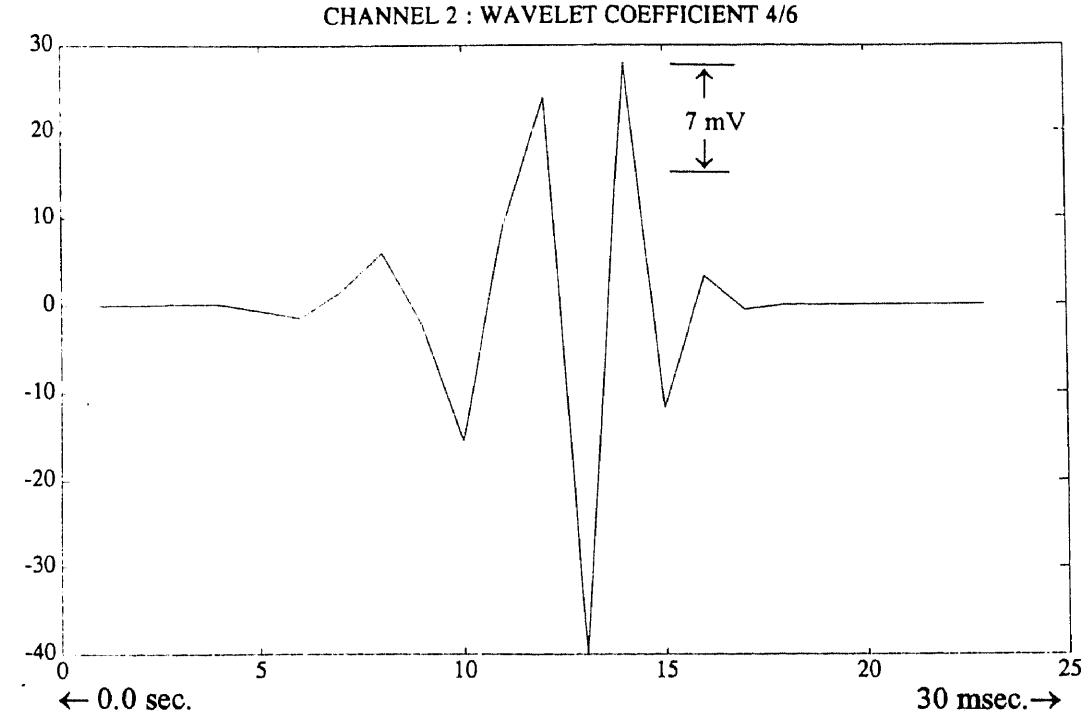

(b) Channel 2

Figure 2.4.9 Fourth level of MEP wavelet coefficients

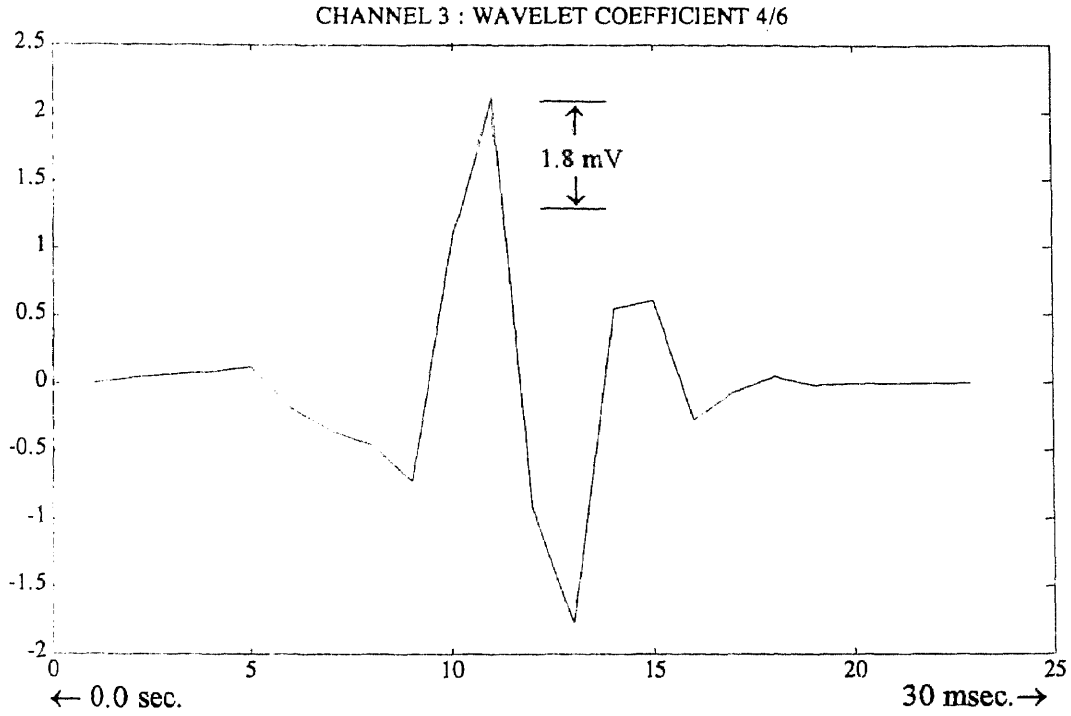

(a) Channel 3

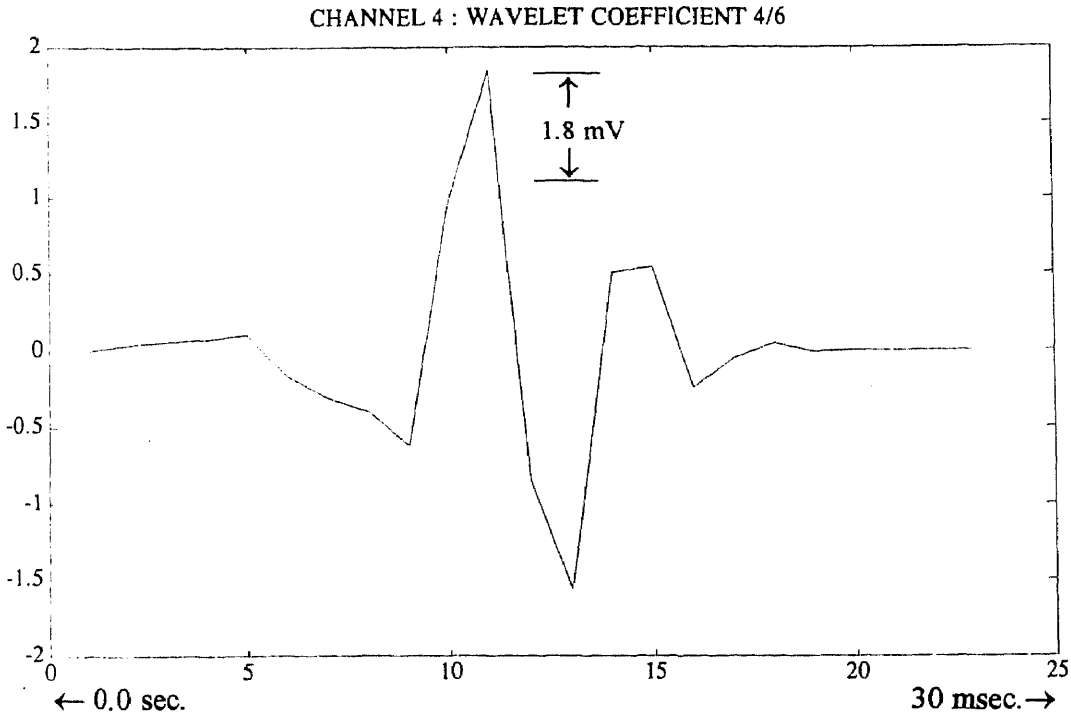

(b) Channel 4

Figure 2.4.10 Fourth level of MEP wavelet coefficients

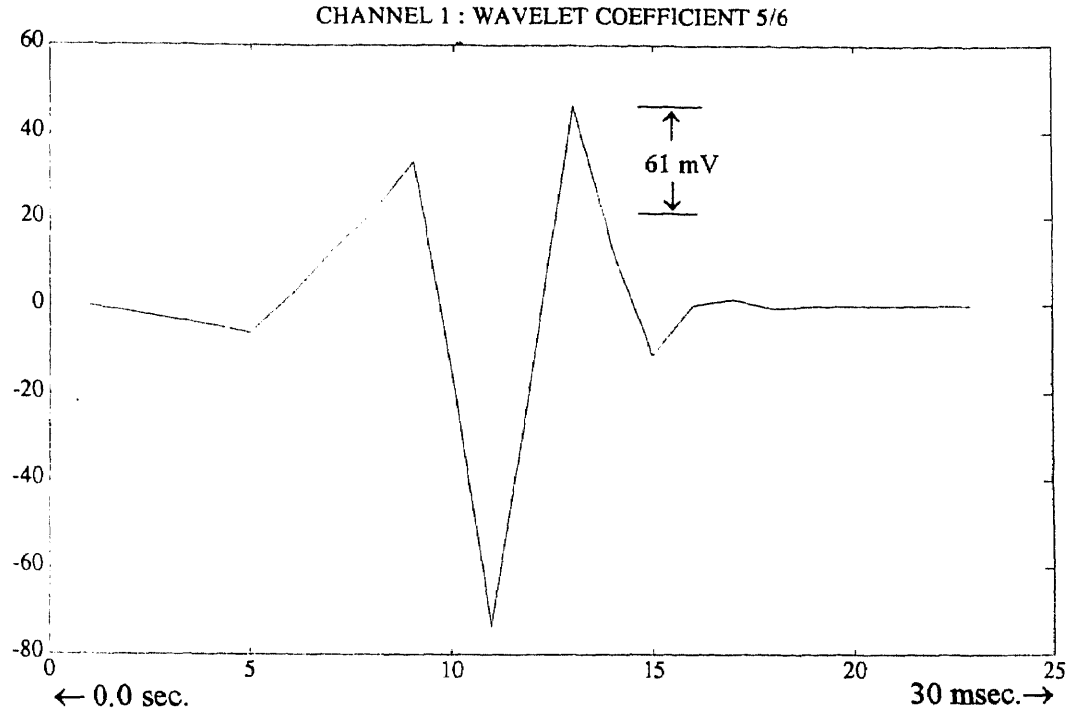

(a) Channel 1

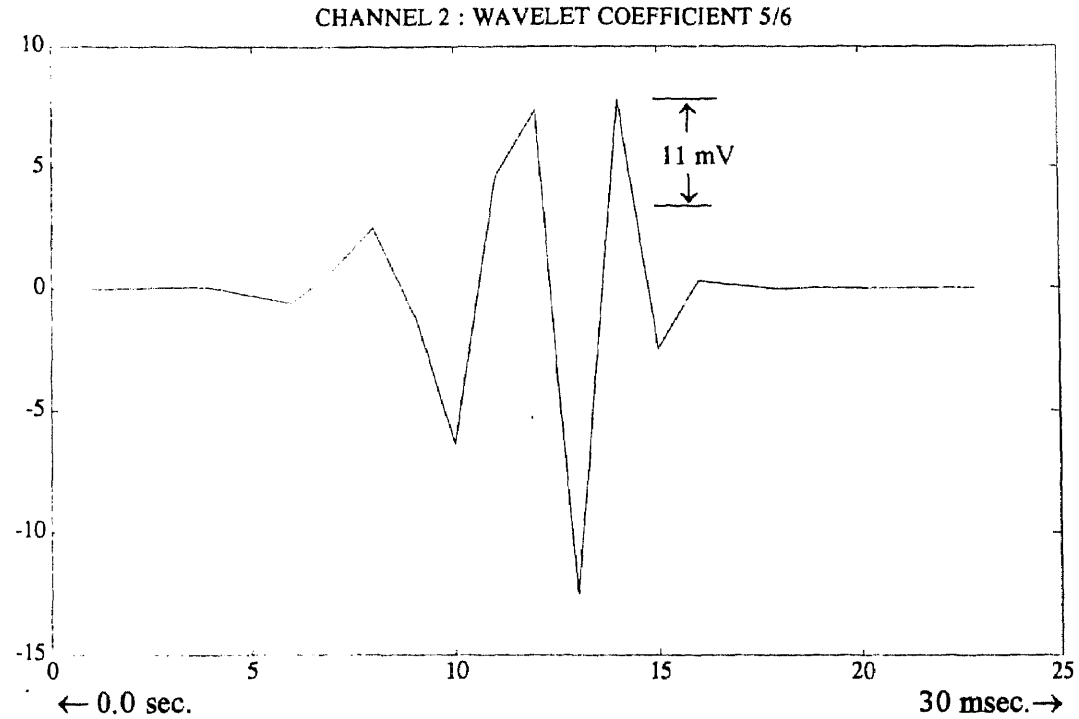

(b) Channel 2

Figure 2.4.11 Fifth level of MEP wavelet coefficients

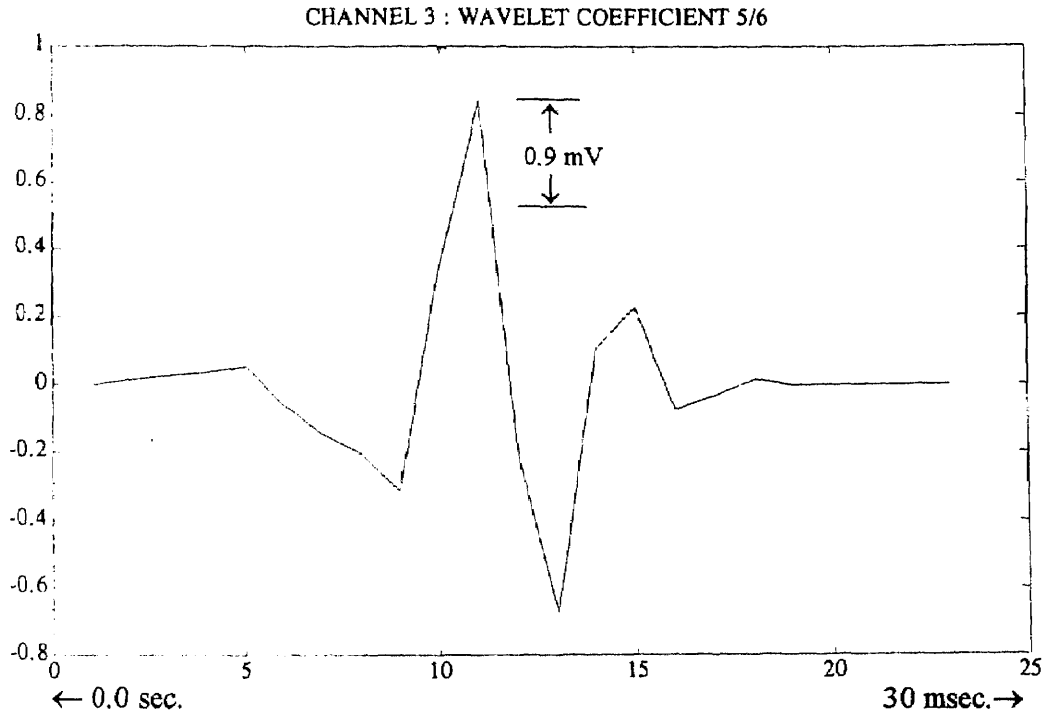

(a) Channel 3

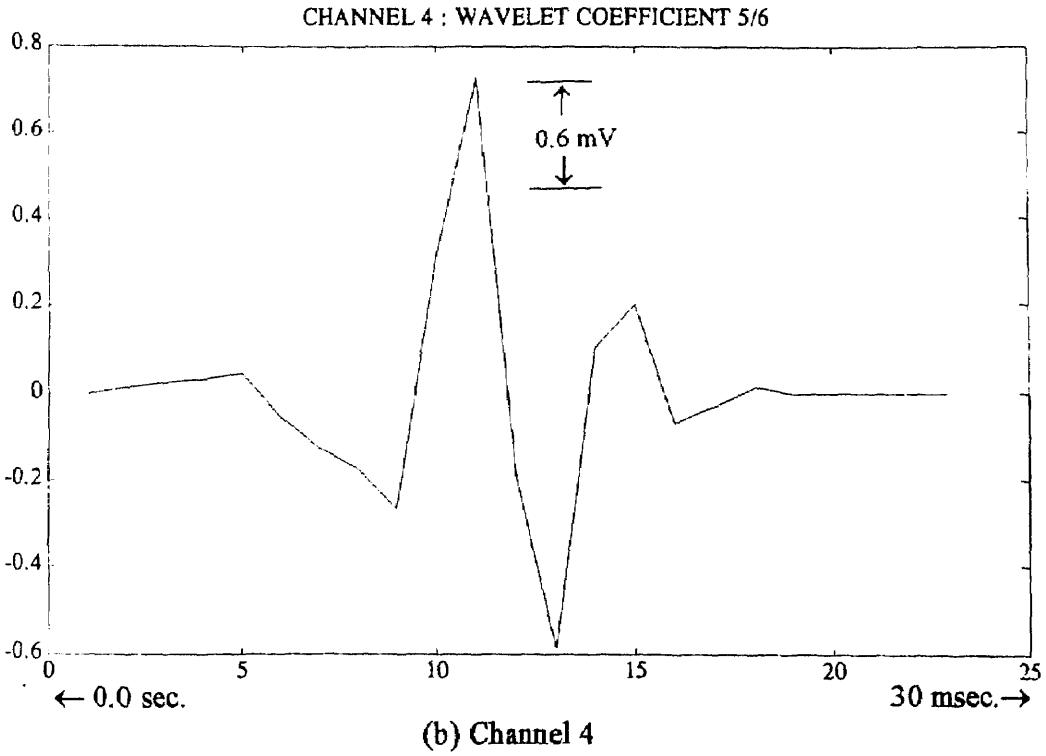

(b) Channel 4

Figure 2.4.12 Fifth level of MEP wavelet coefficients

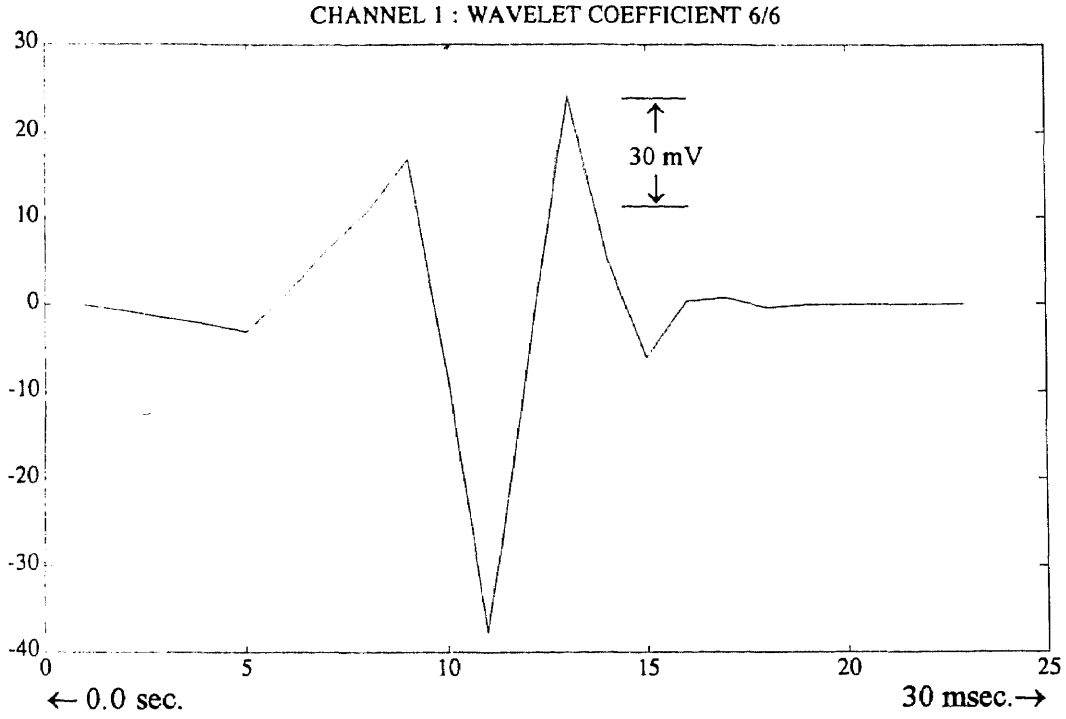

(a) Channel 1

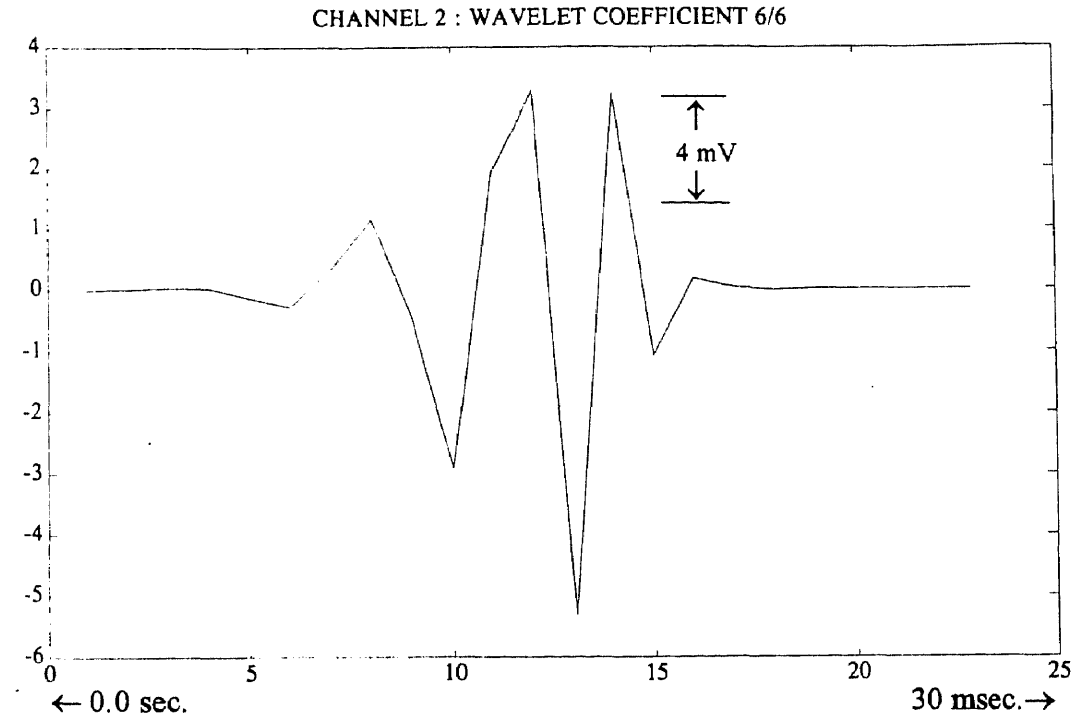

(b) Channel 2

Figure 2.4.13 Sixth level of MEP wavelet coefficients

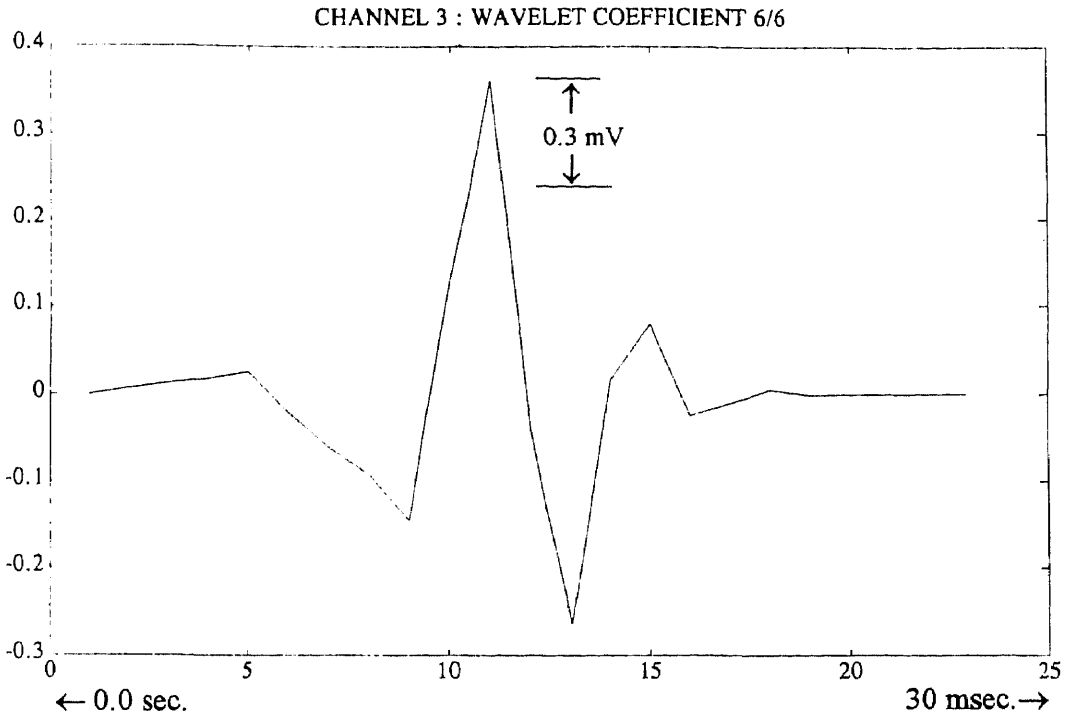

(a) Channel 3

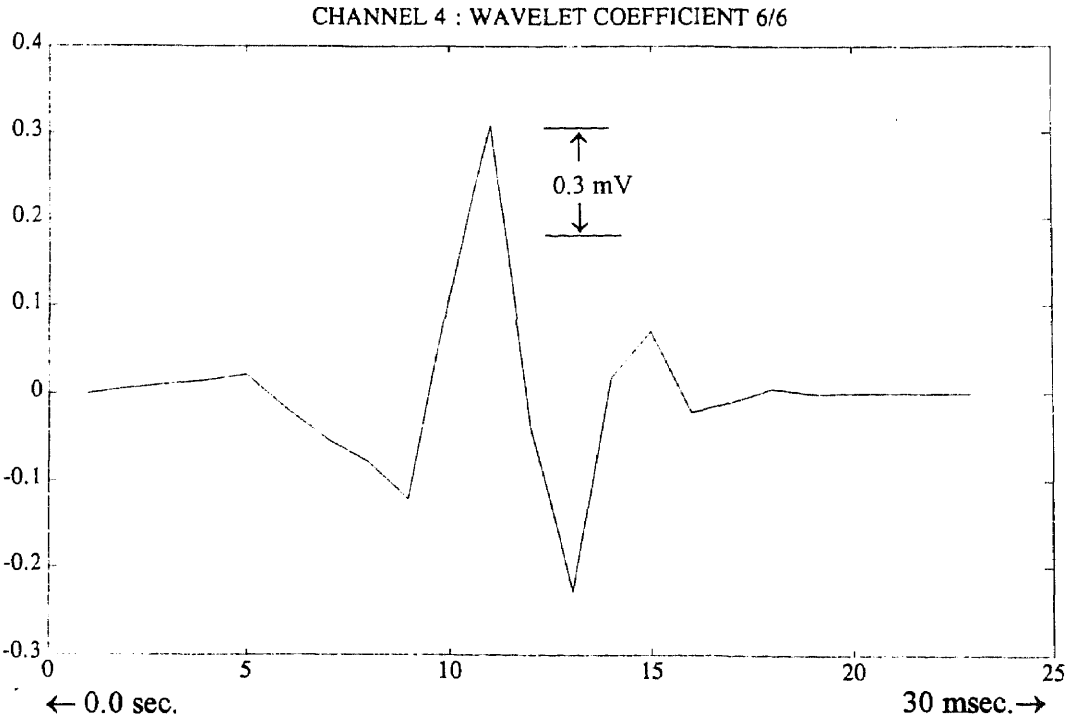

(b) Channel 4

Figure 2.4.14 Sixth level of MEP wavelet coefficients

APPENDIX F

FIGURES

Figure **Page**

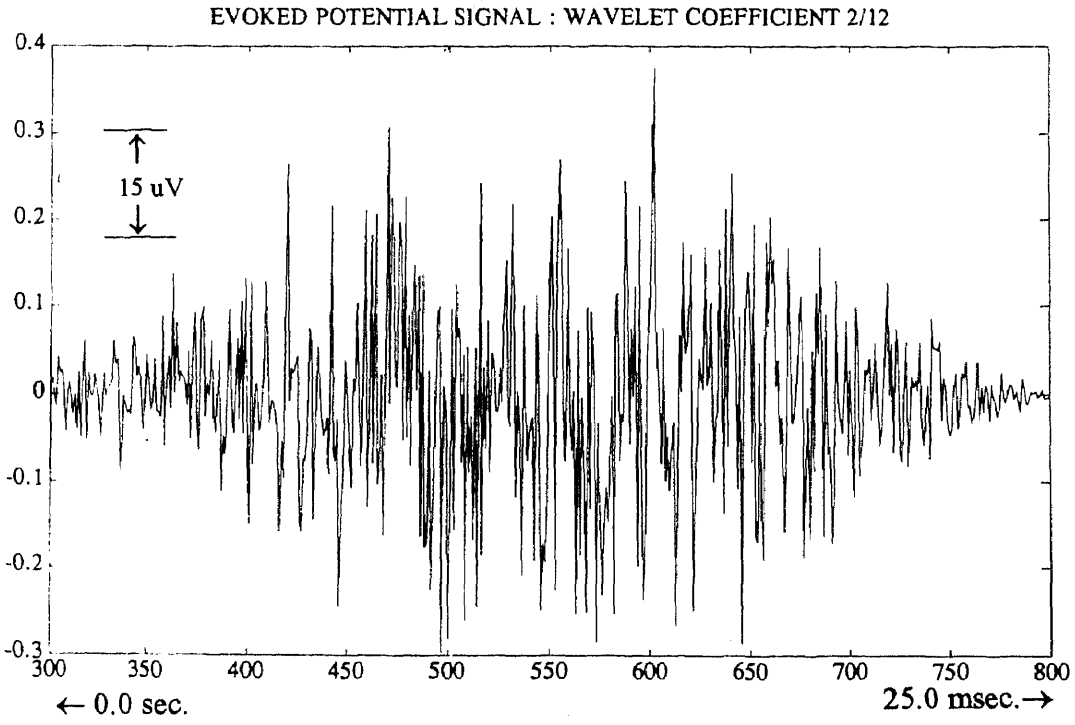

(a) Single EP

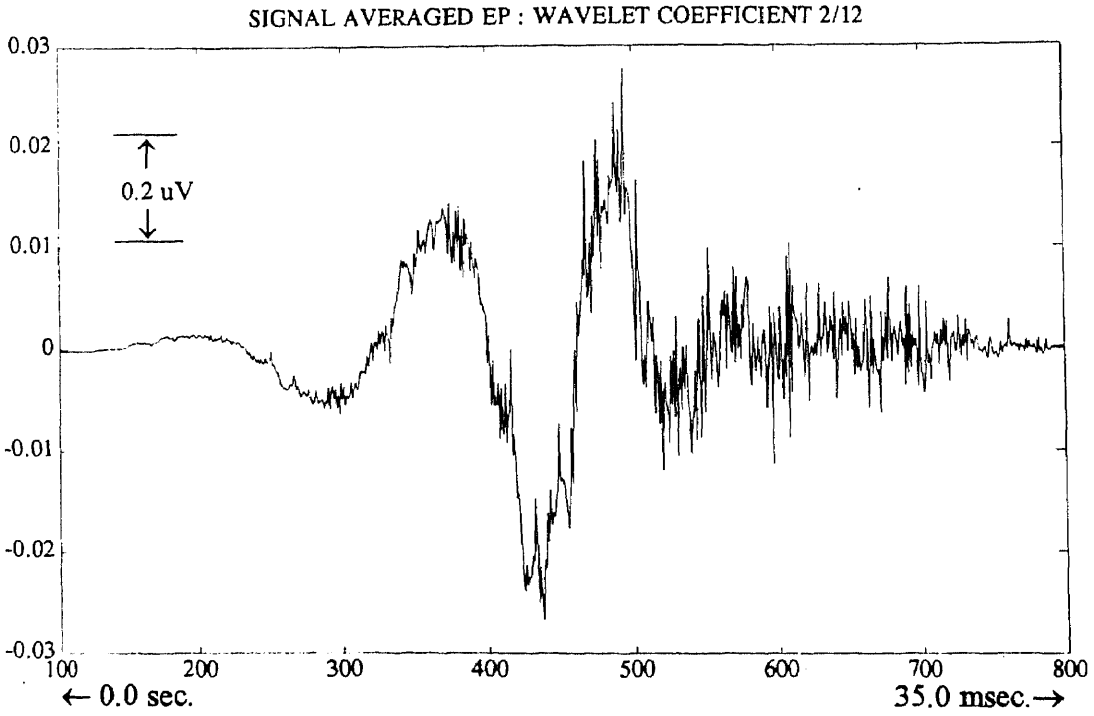

(b) Signal averaged EP

Figure 3.4.4 Second level of EP wavelet coefficients

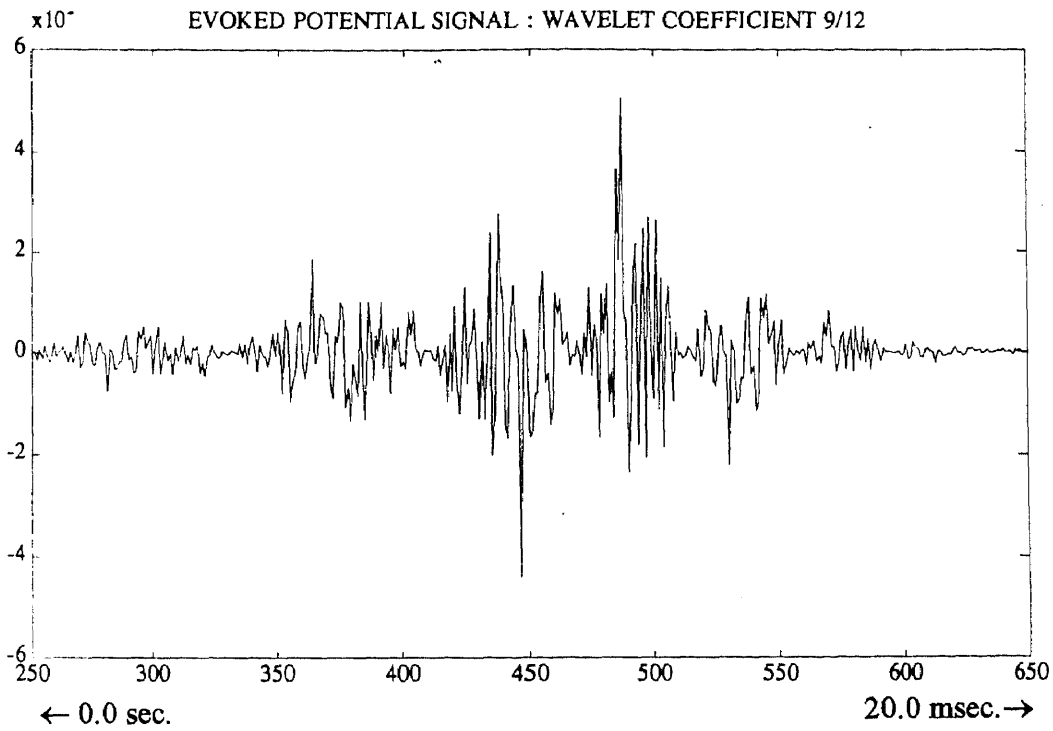

(a) Single EP

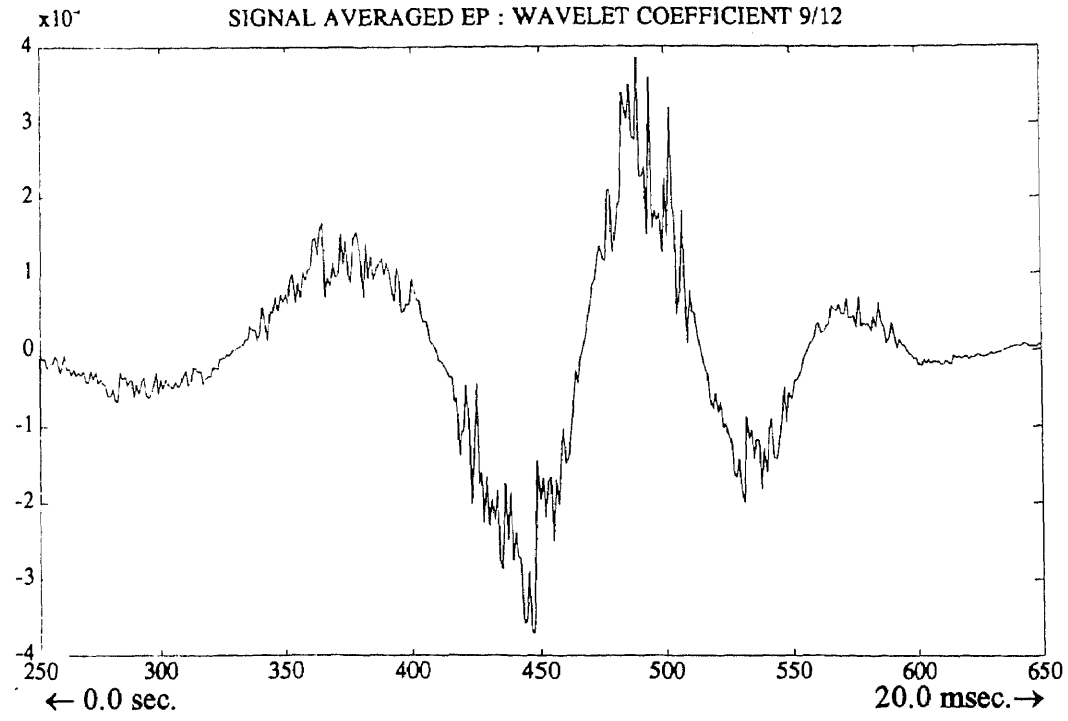

(b) Signal averaged EP

Figure 3.4.5 Ninth level of EP wavelet coefficients

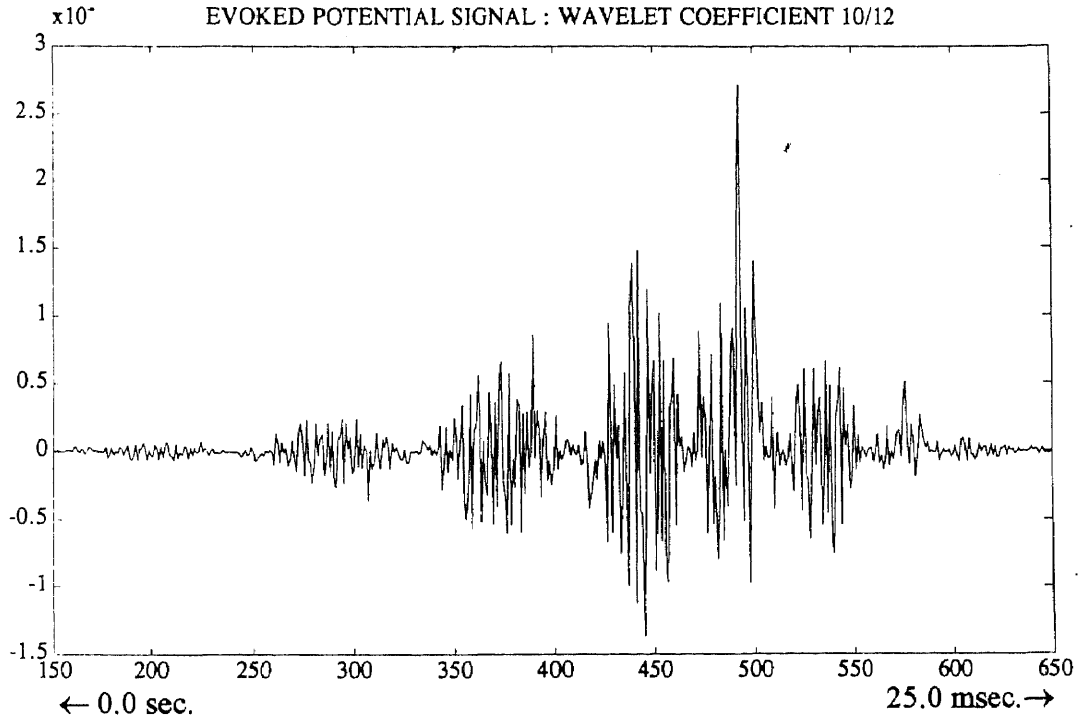

(a) Single EP

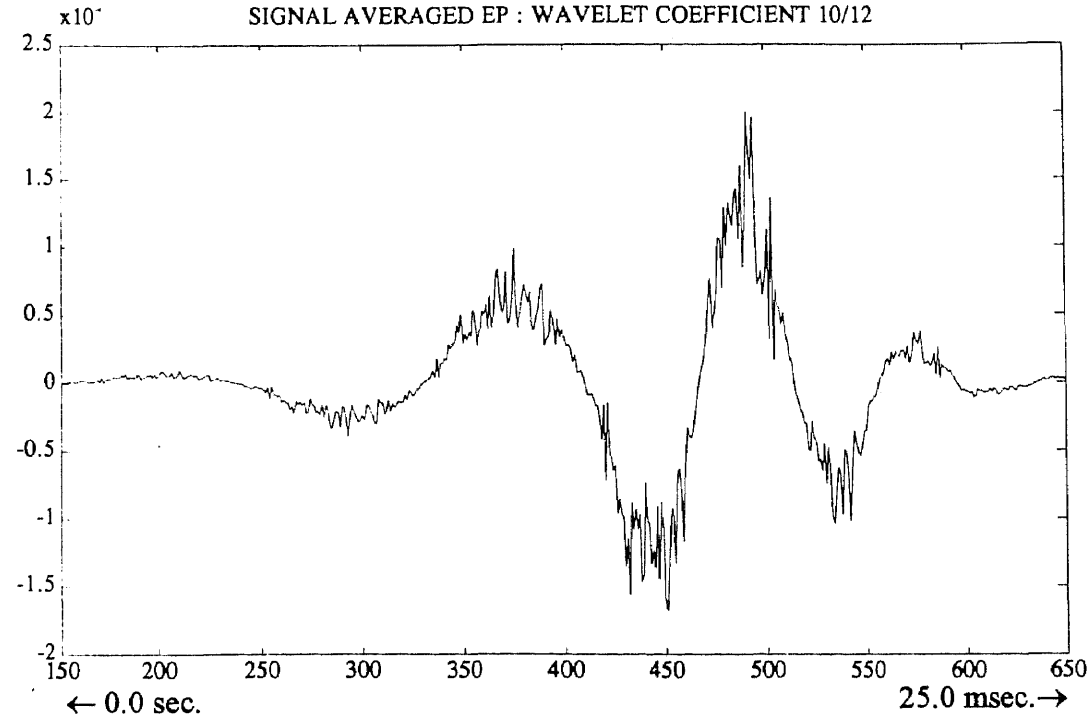

(b) Signal averaged EP

Figure 3.4.6 Tenth level of EP wavelet coefficients

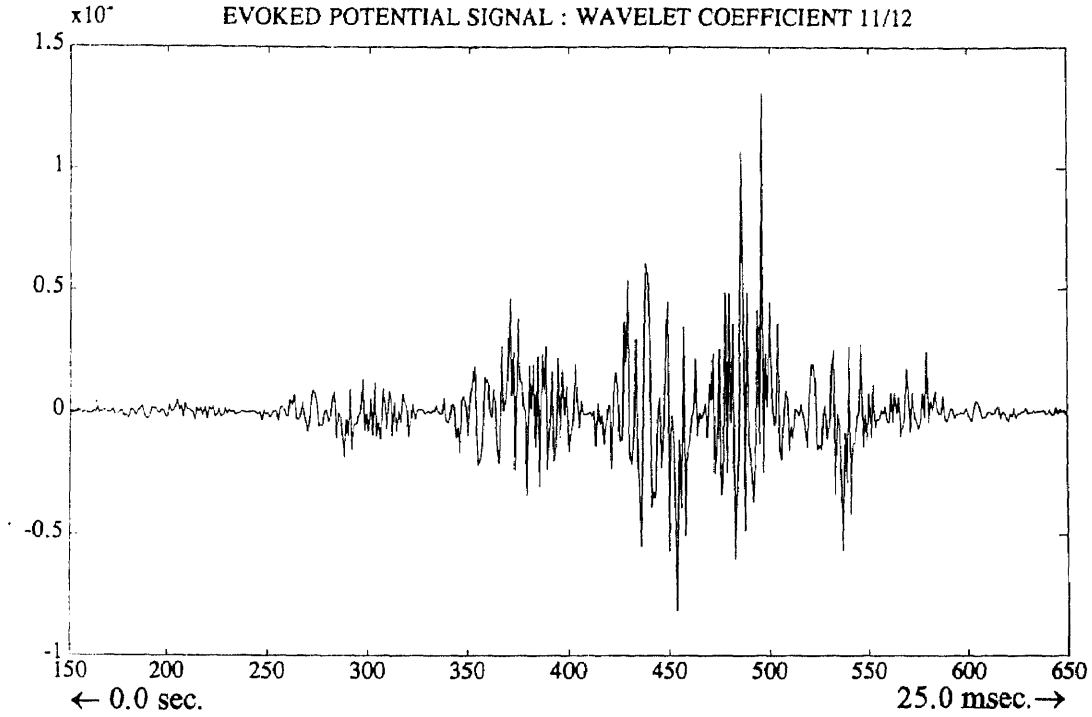

(a) Single EP

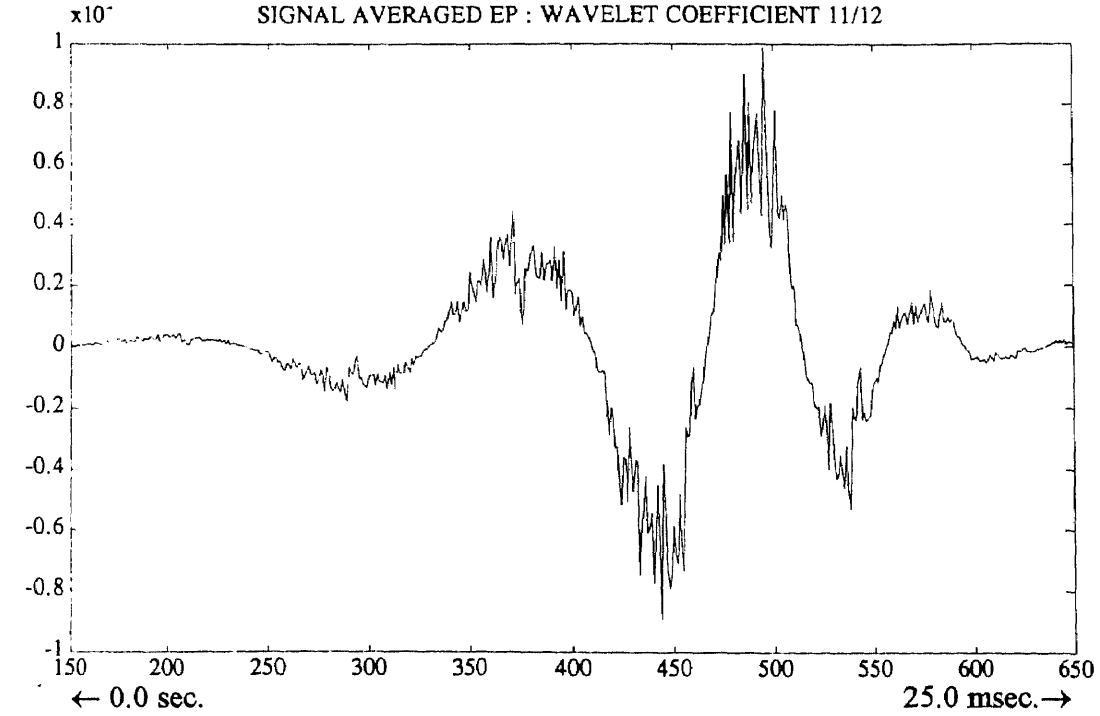

(b) Signal averaged EP

Figure 3.4.7 Eleventh level of EP wavelet coefficients

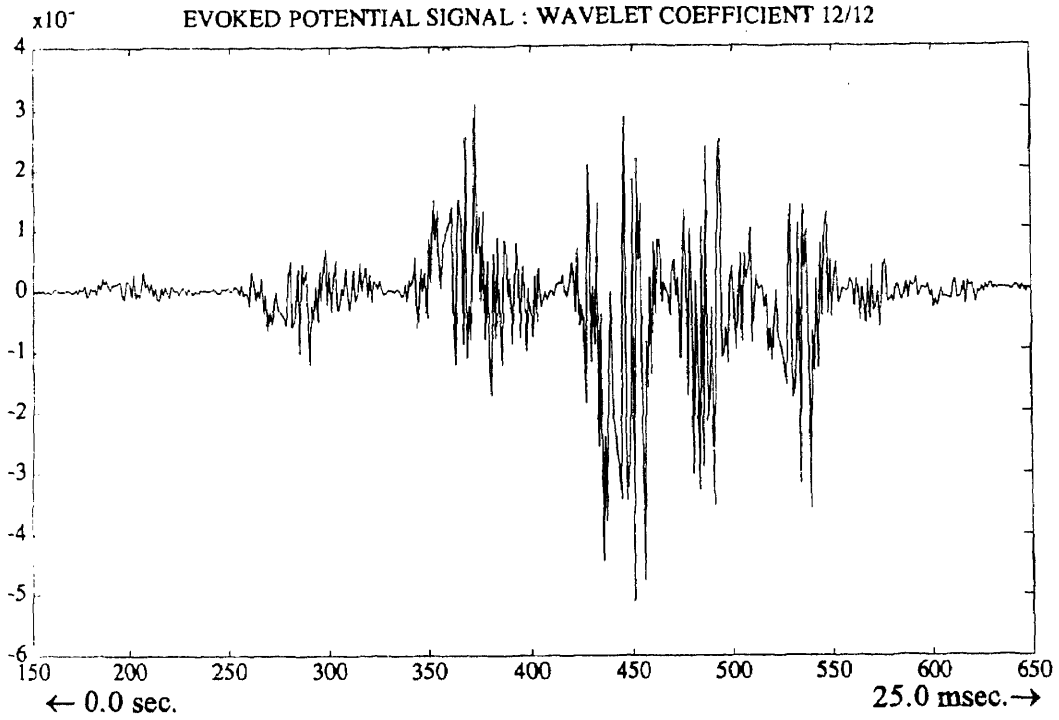

(a) Single EP

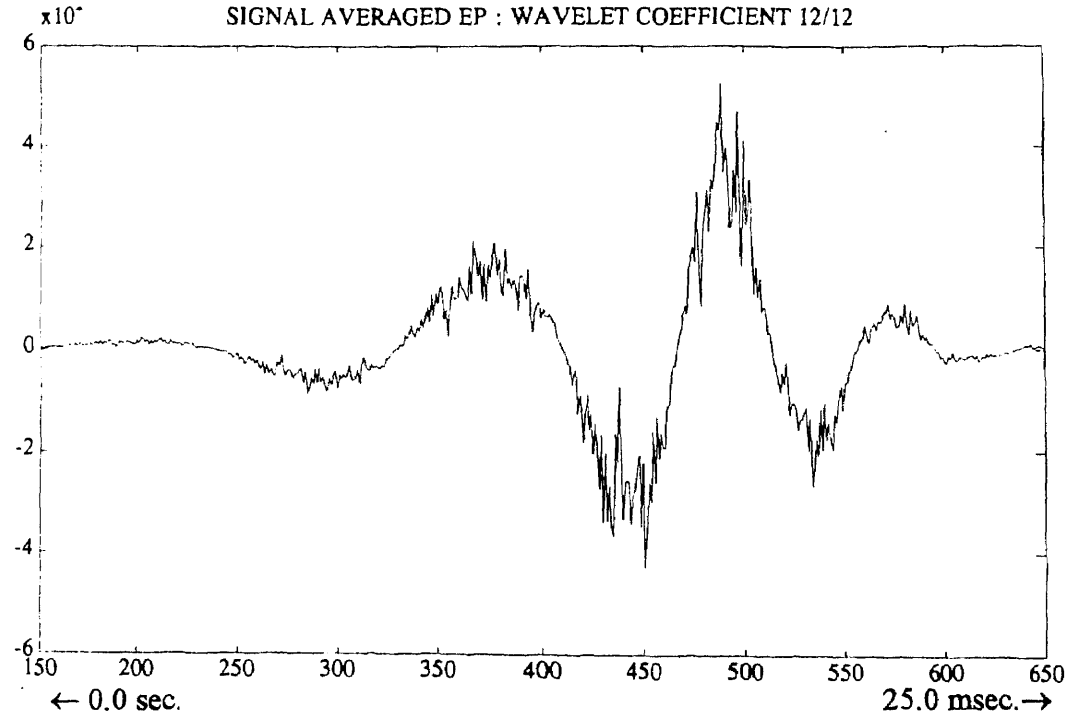

(b) Signal averaged EP

Figure 3.4.8 Twelfth level of EP wavelet coefficients

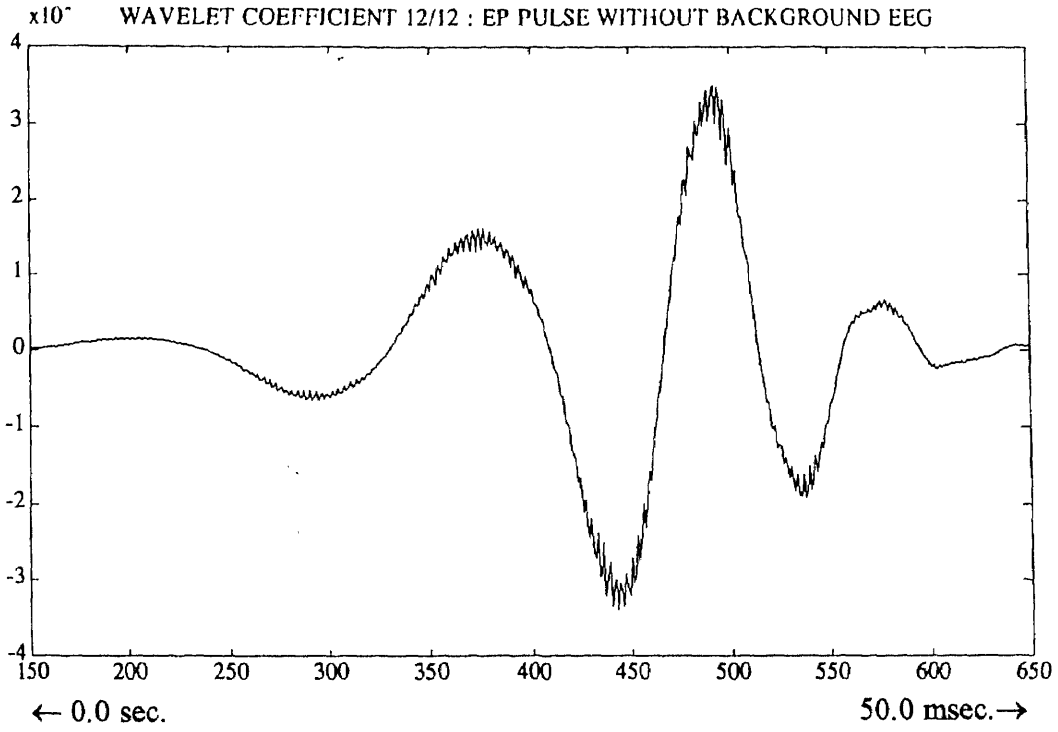

(a) EP pulse without background EEG

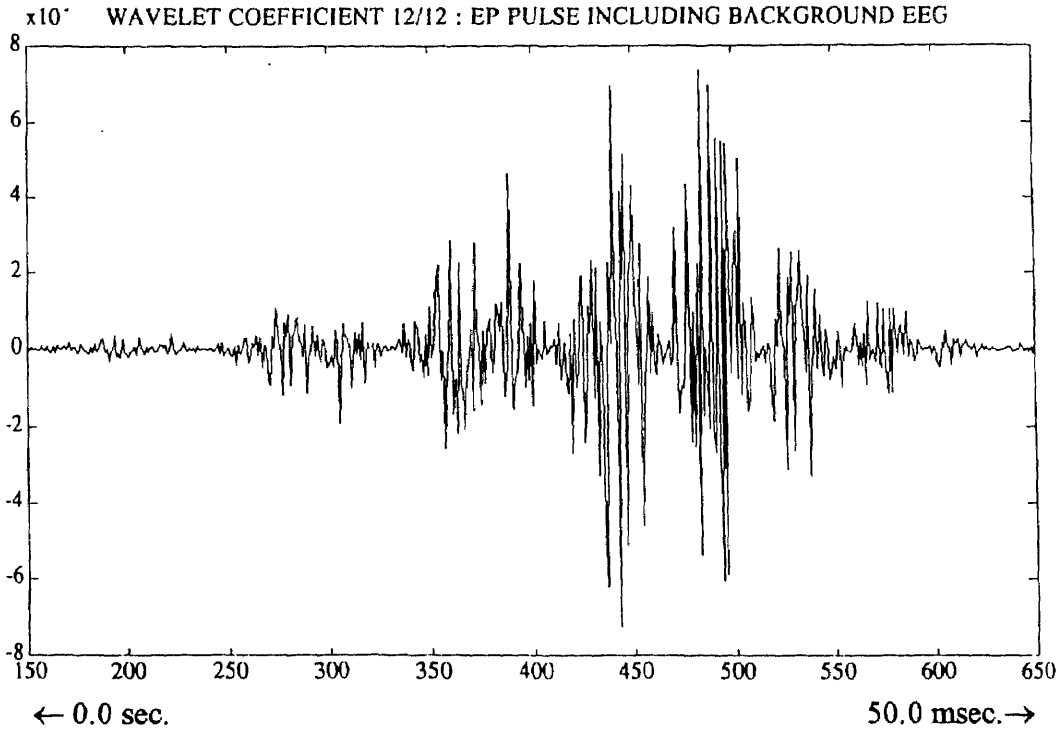

(b) EP pulse with background EEG

Figure 3.4.9 Twelfth level of single EP wavelet coefficients

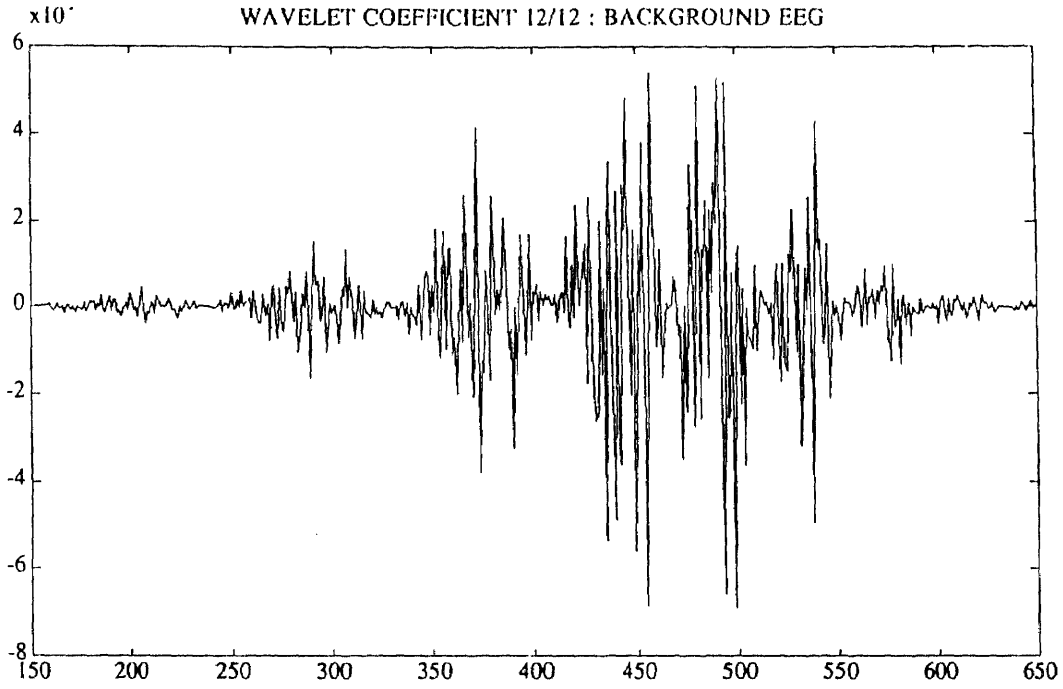

← 0.0 sec. 50.0 msec.→

(c) Background EEG

APPENDIX G

FIGURES

Figure **Page**

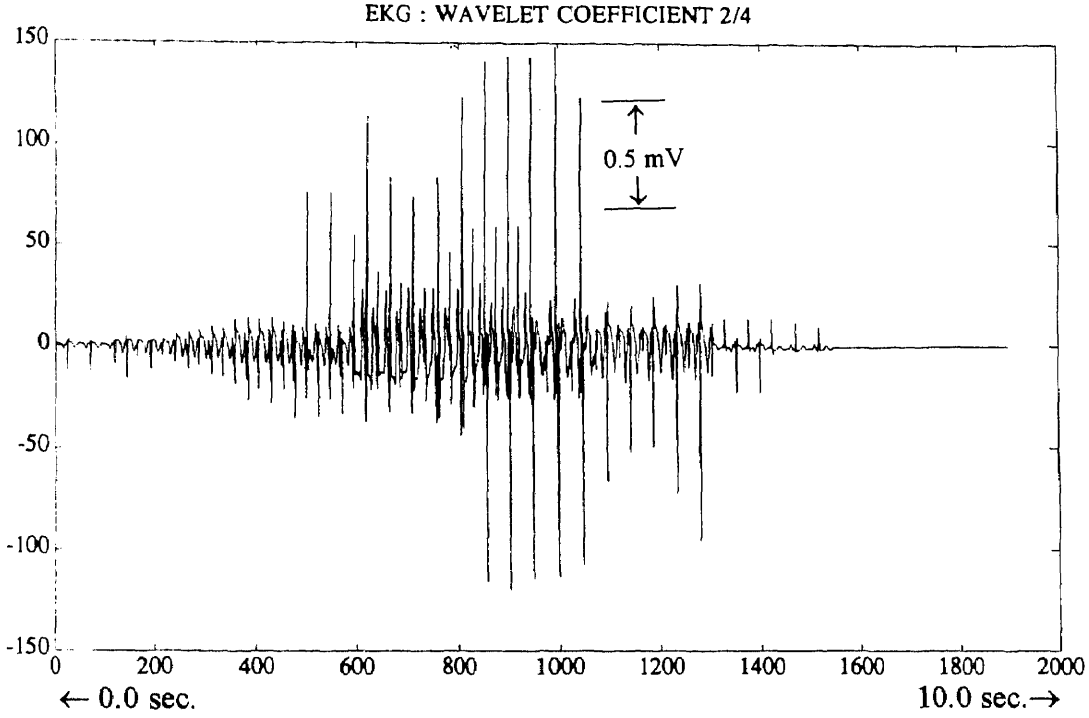

(a)

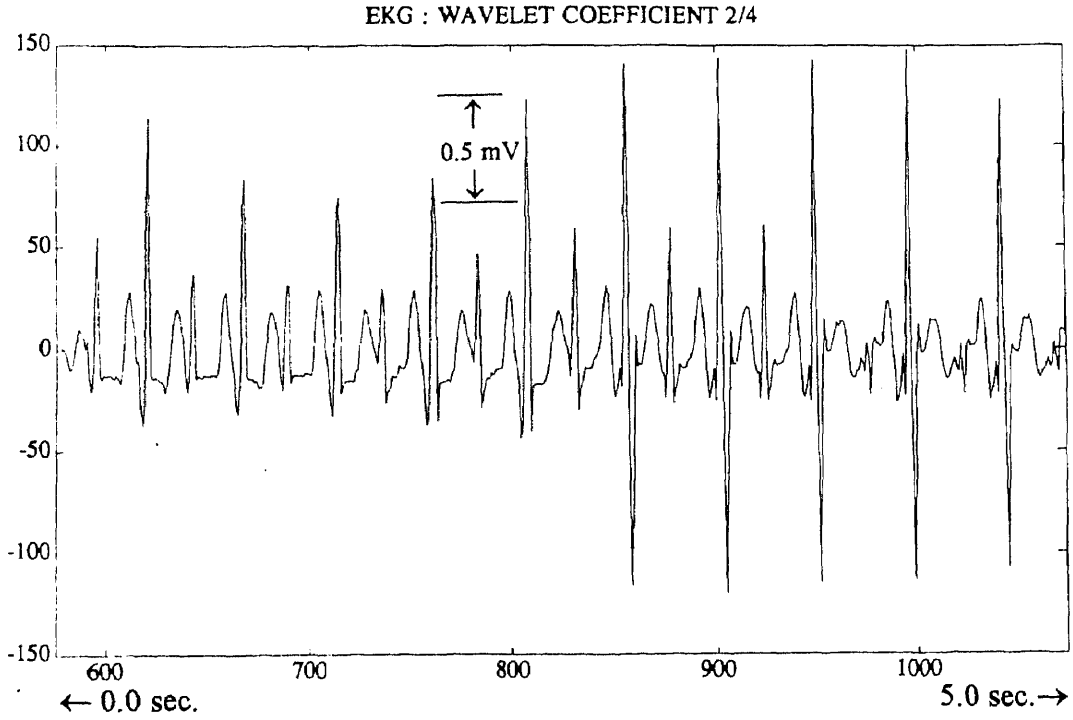

(b)

Figure 4.4.2 Normal EKG

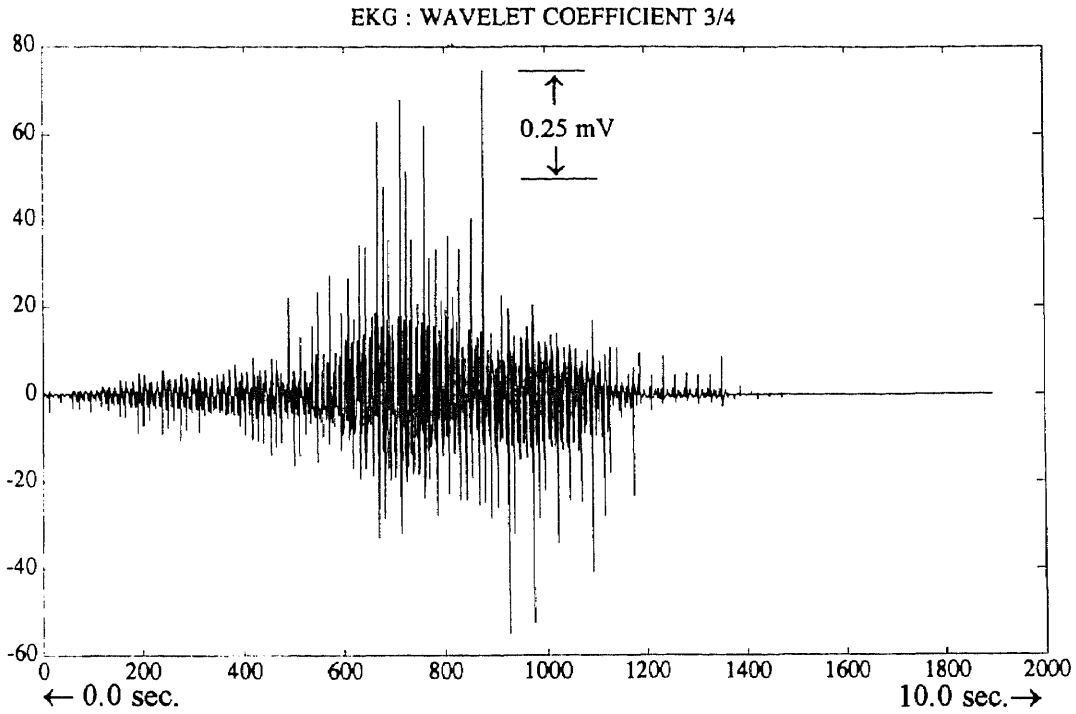

(a)

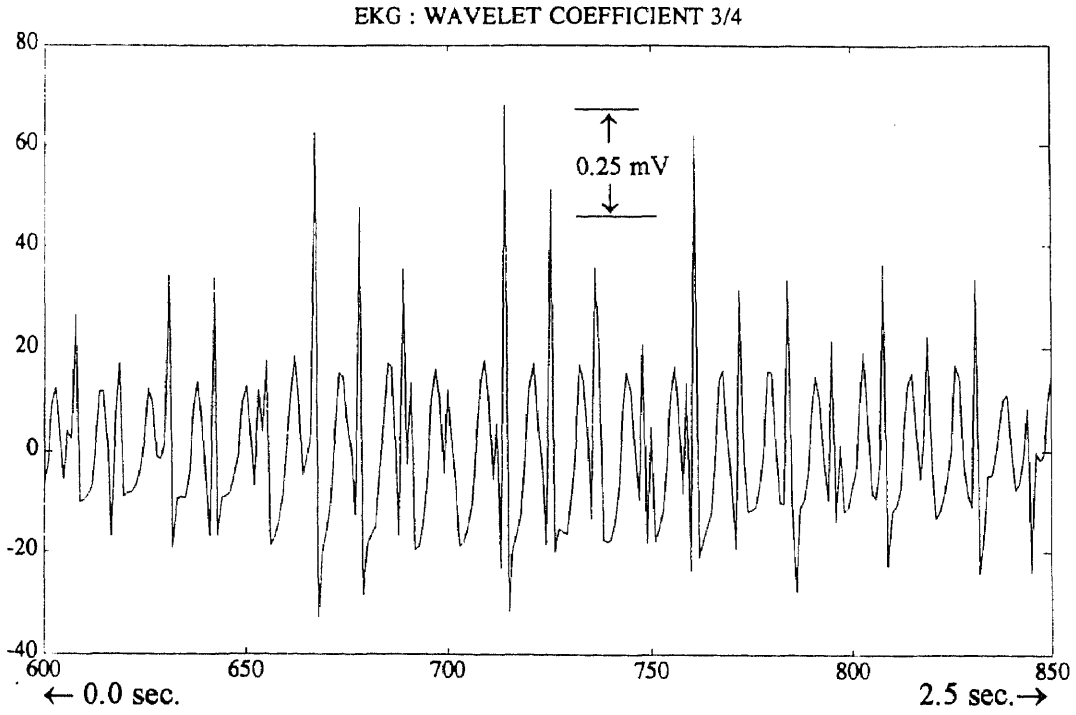

(b)

Figure 4.4.3 Normal EKG

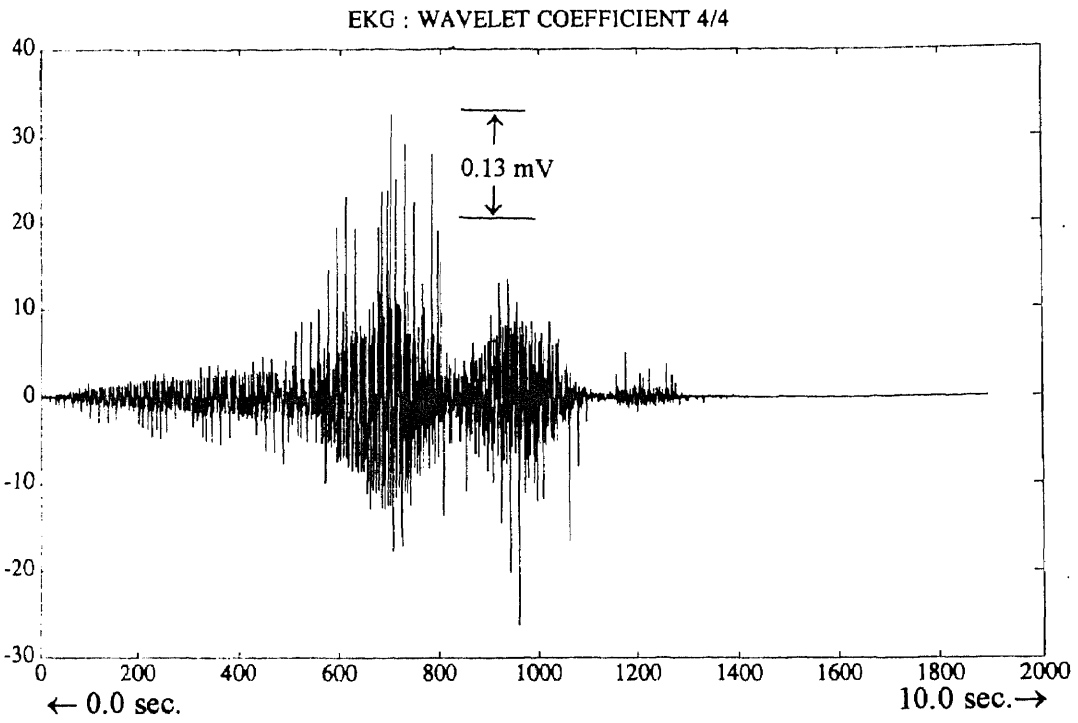

(a)

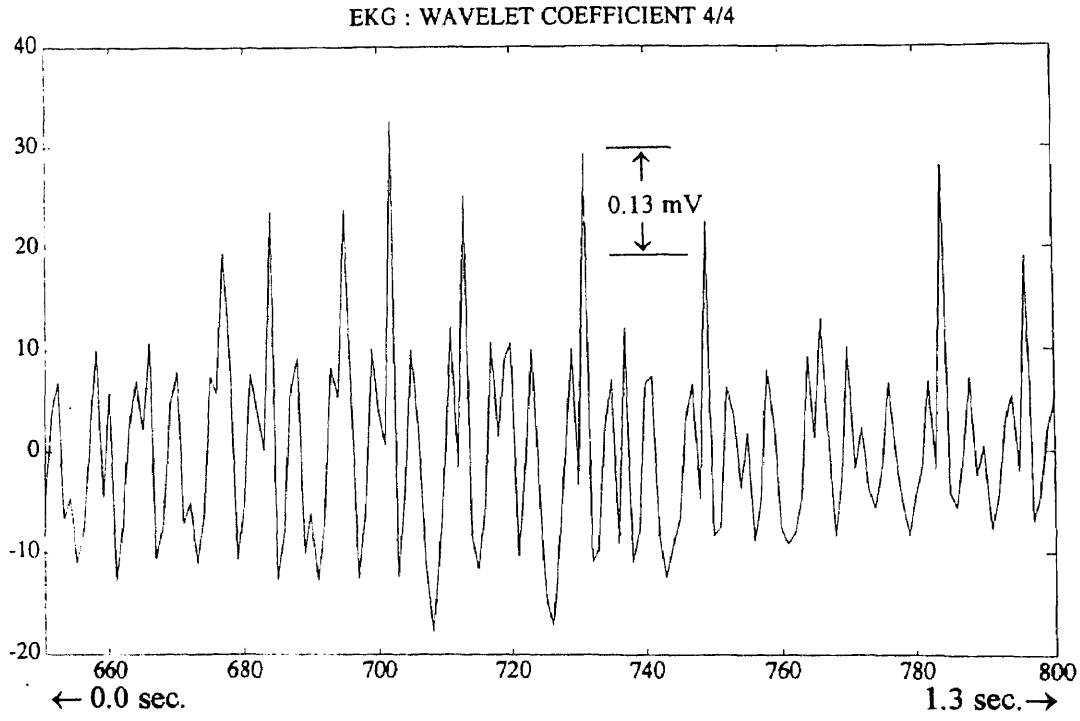

(b)

Figure 4.4.4 Normal EKG

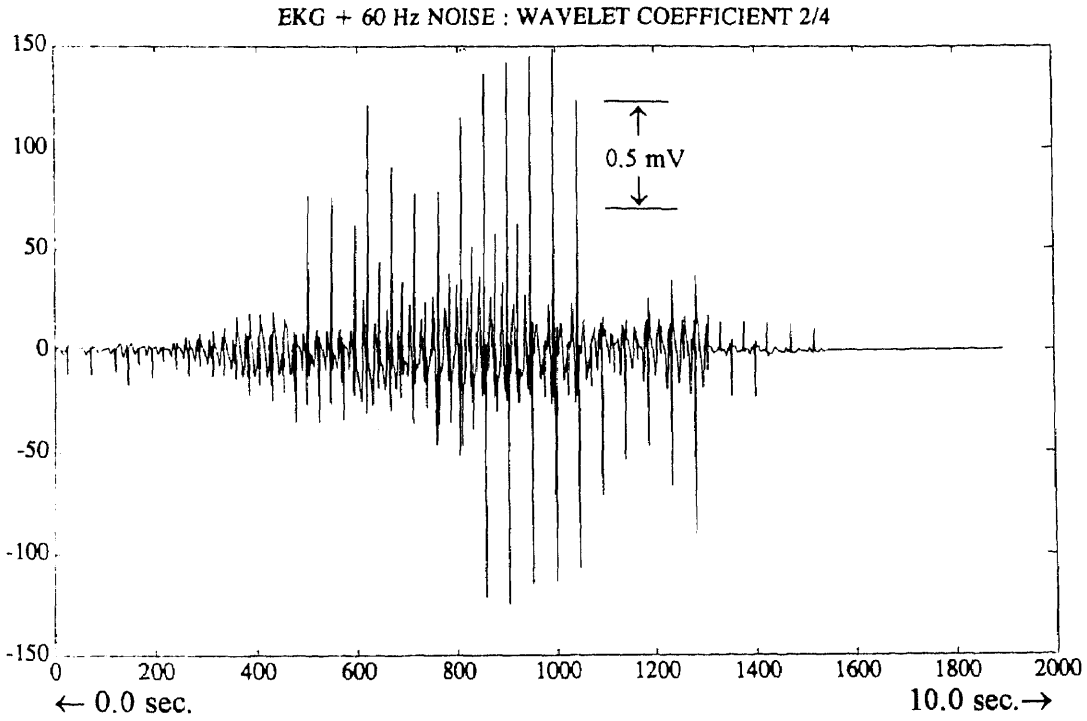

(a)

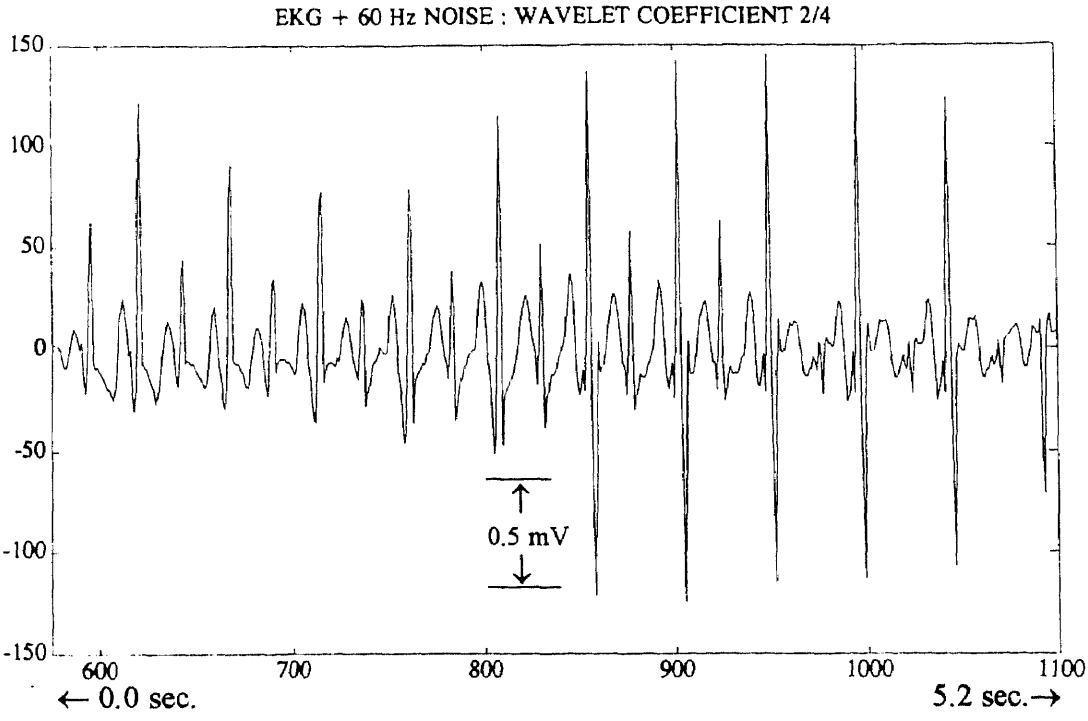

(b)

Figure 4.4.6 Normal EKG with 60 Hz noise added

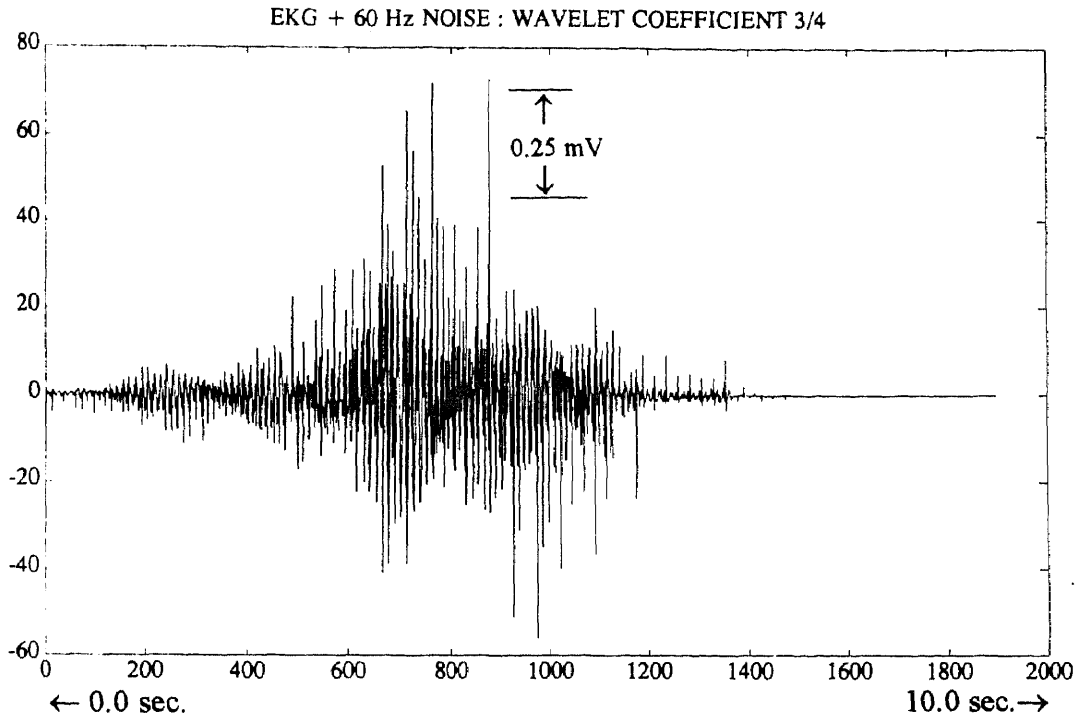

(a)

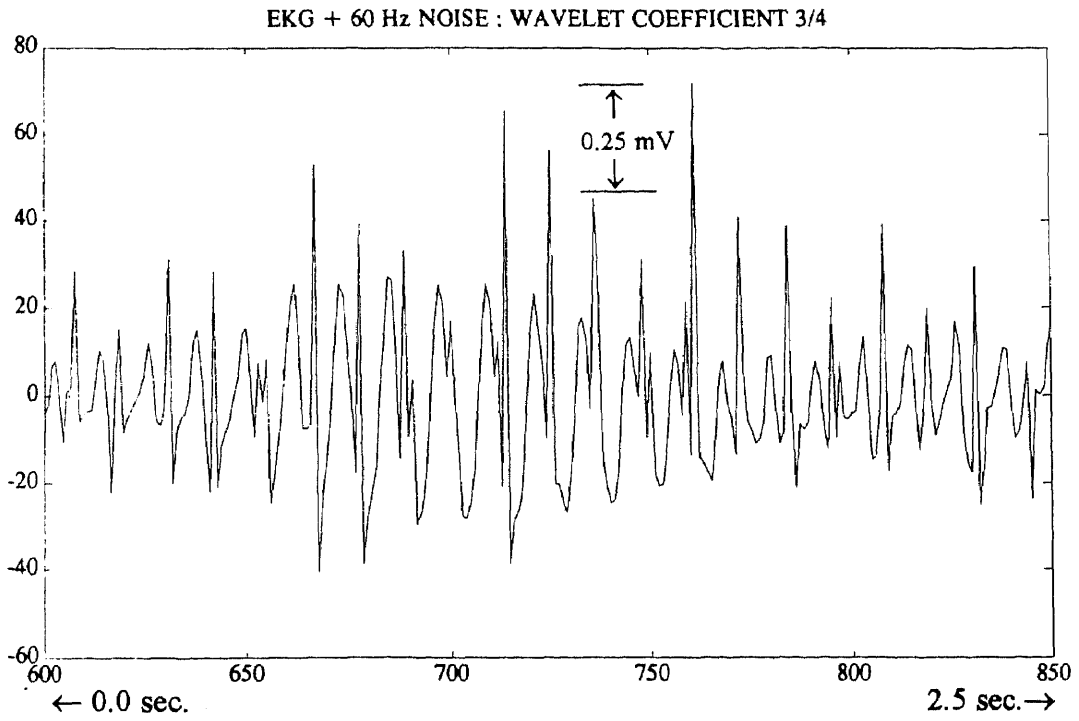

(b)

Figure 4.4.7 Normal EKG with 60 Hz noise added

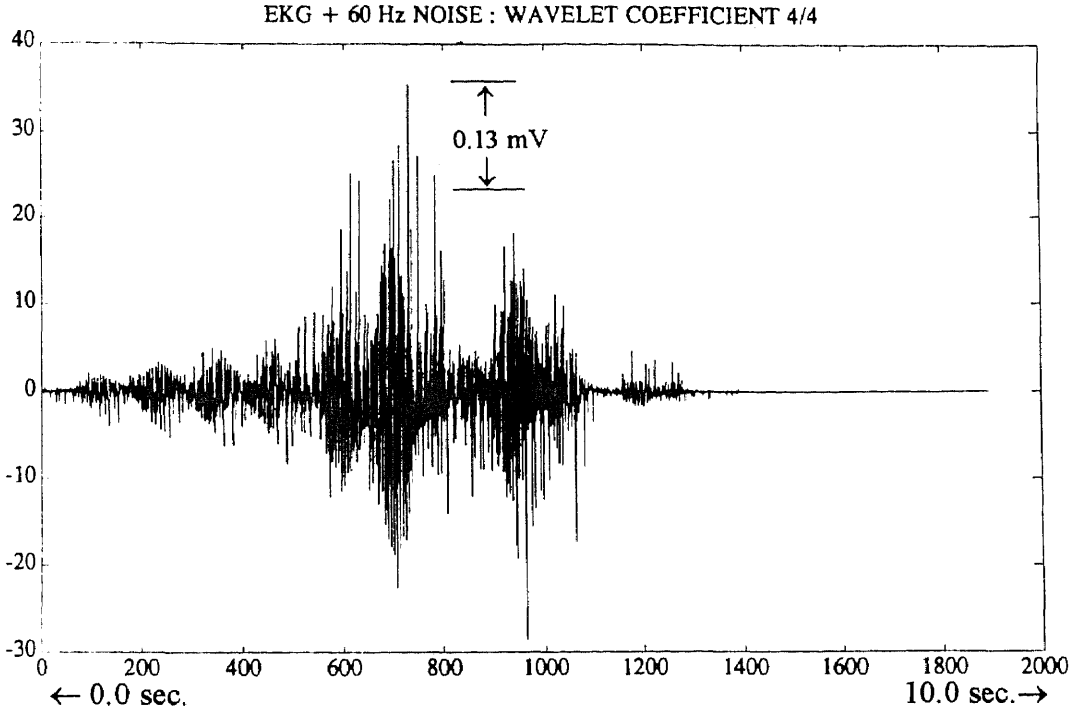

(a)

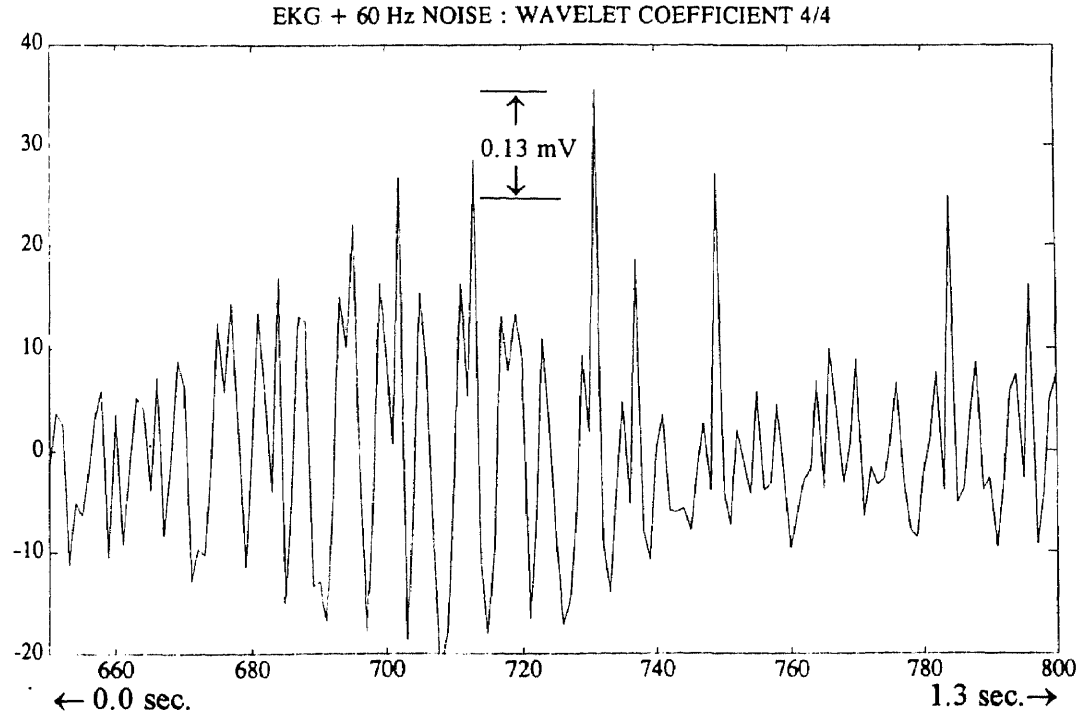

(b)

Figure 4.4.8 Normal EKG with 60 Hz noise added

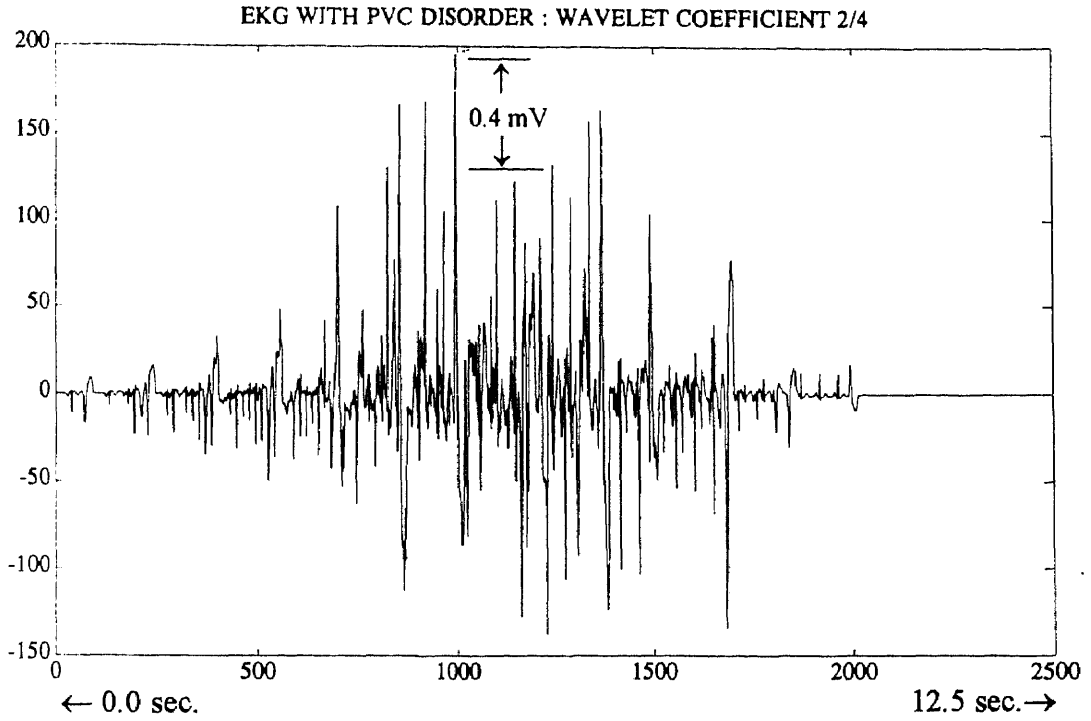

(a)

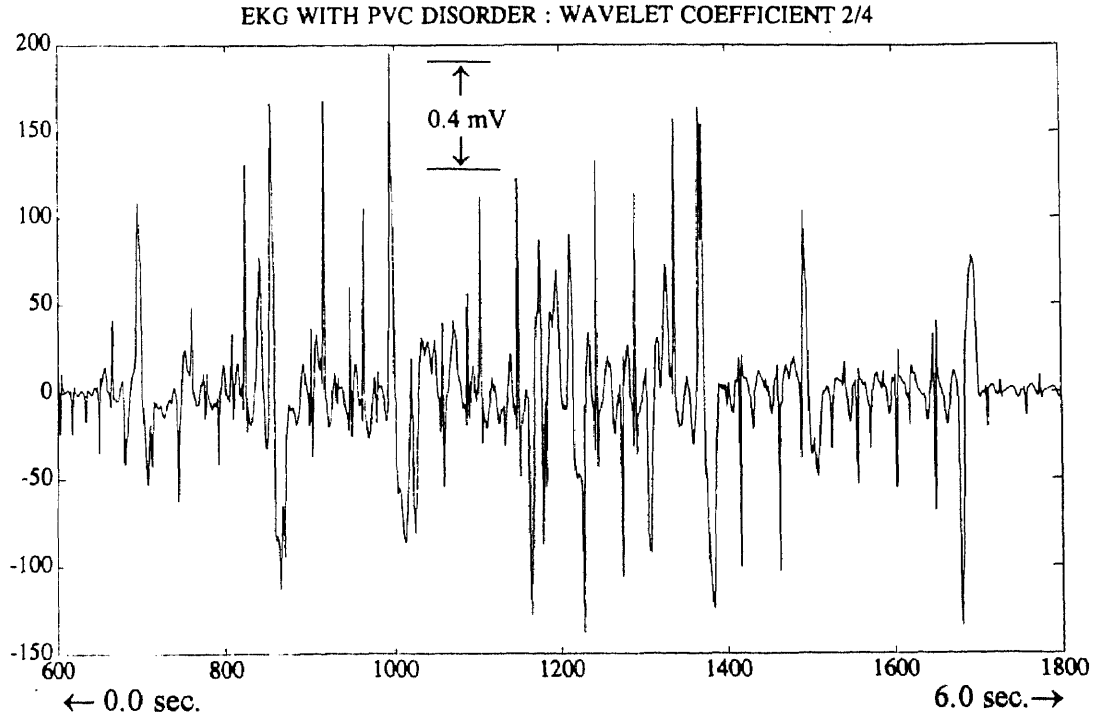

(b)

Figure 4.4.10 EKG with PVCs

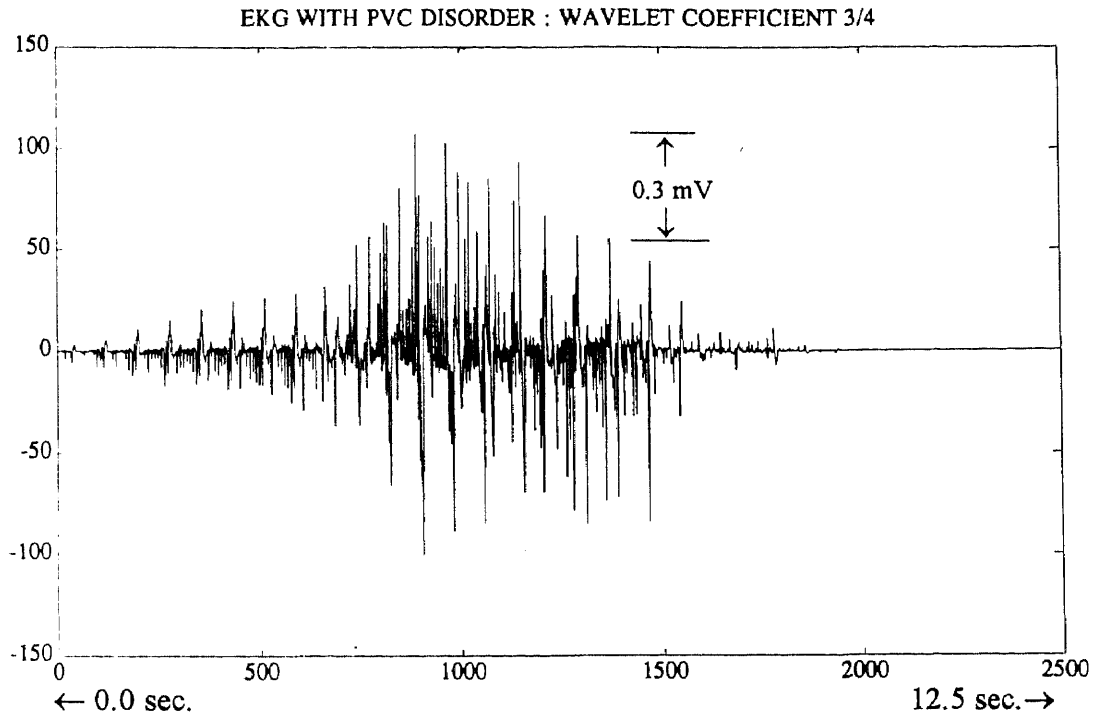

(a)

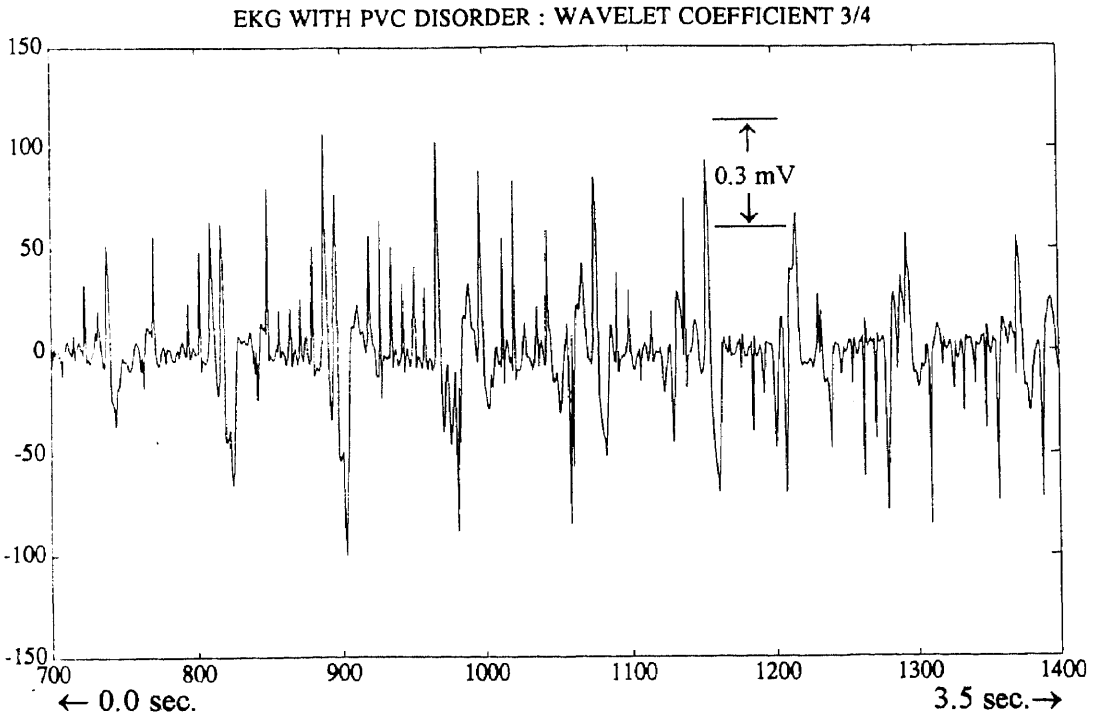

(b)

Figure 4.4.11 EKG with PVCs

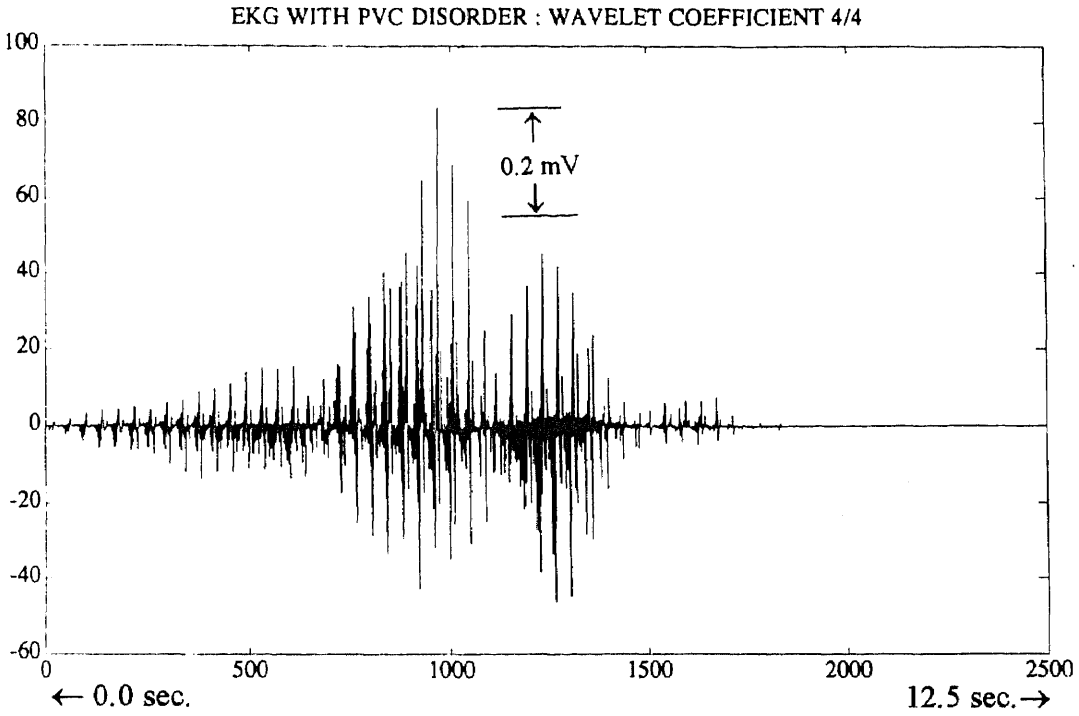

(a)

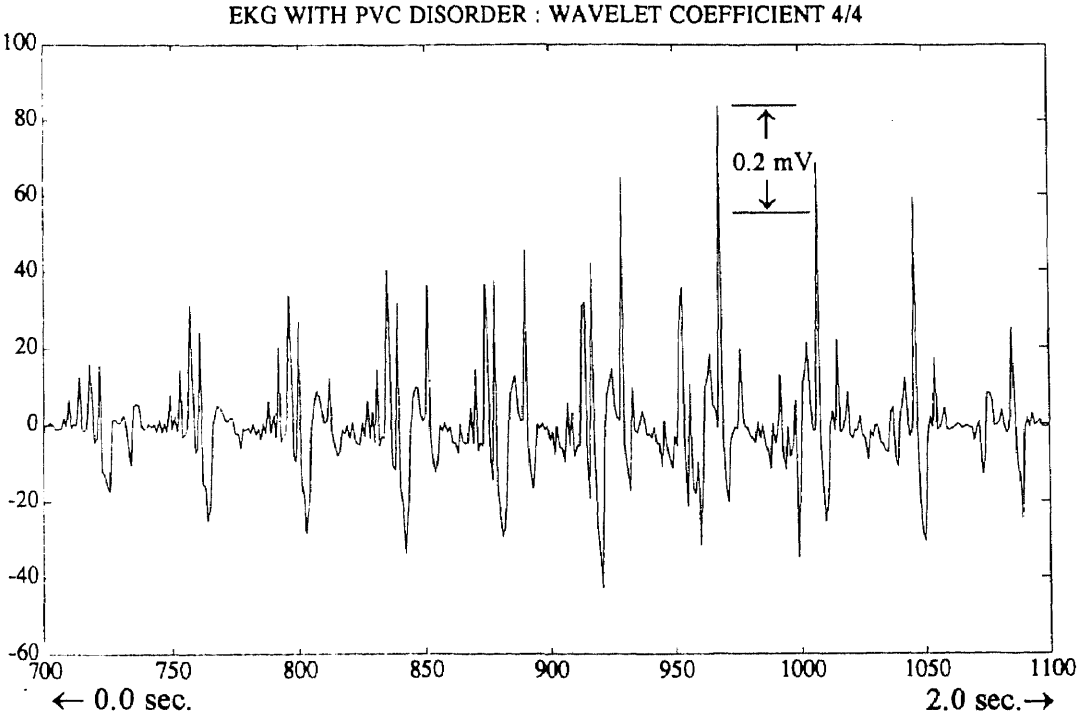

(b)

Figure 4.4.12 EKG with PVCs

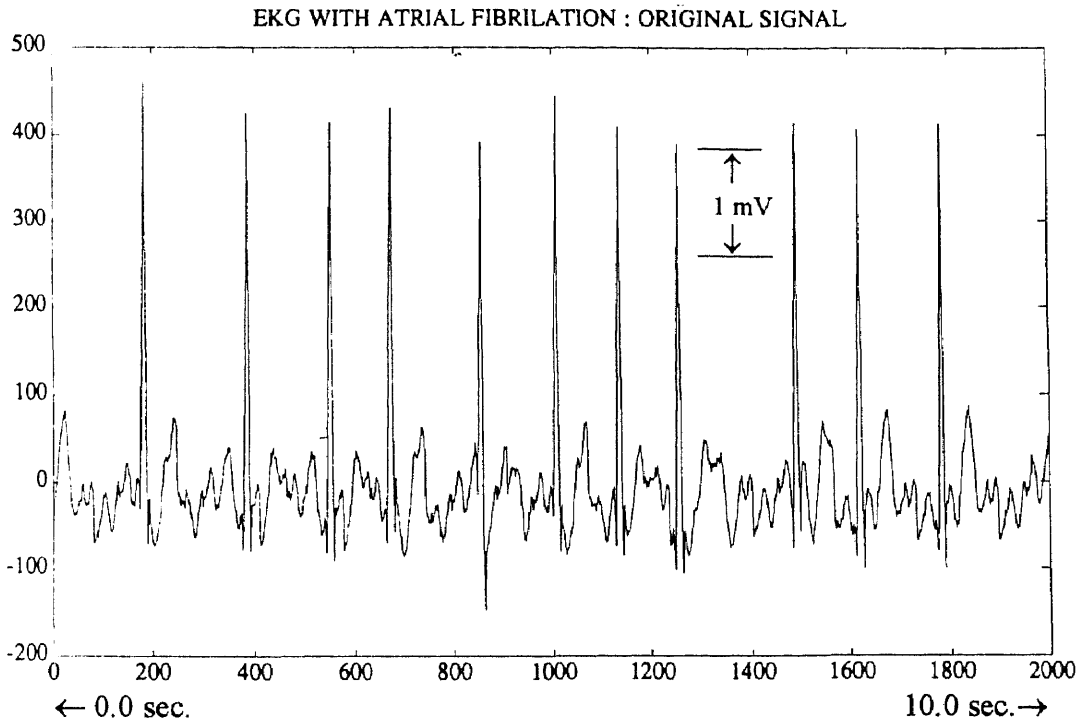

(a)

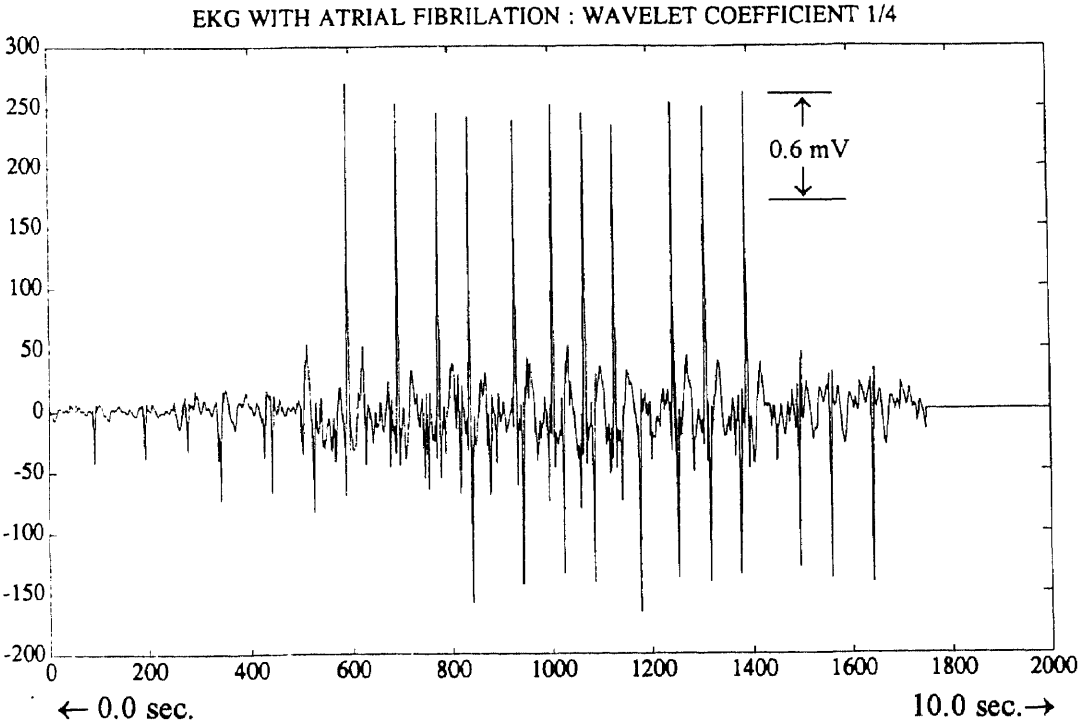

(b)

Figure 4.4.13 EKG with AFIBs

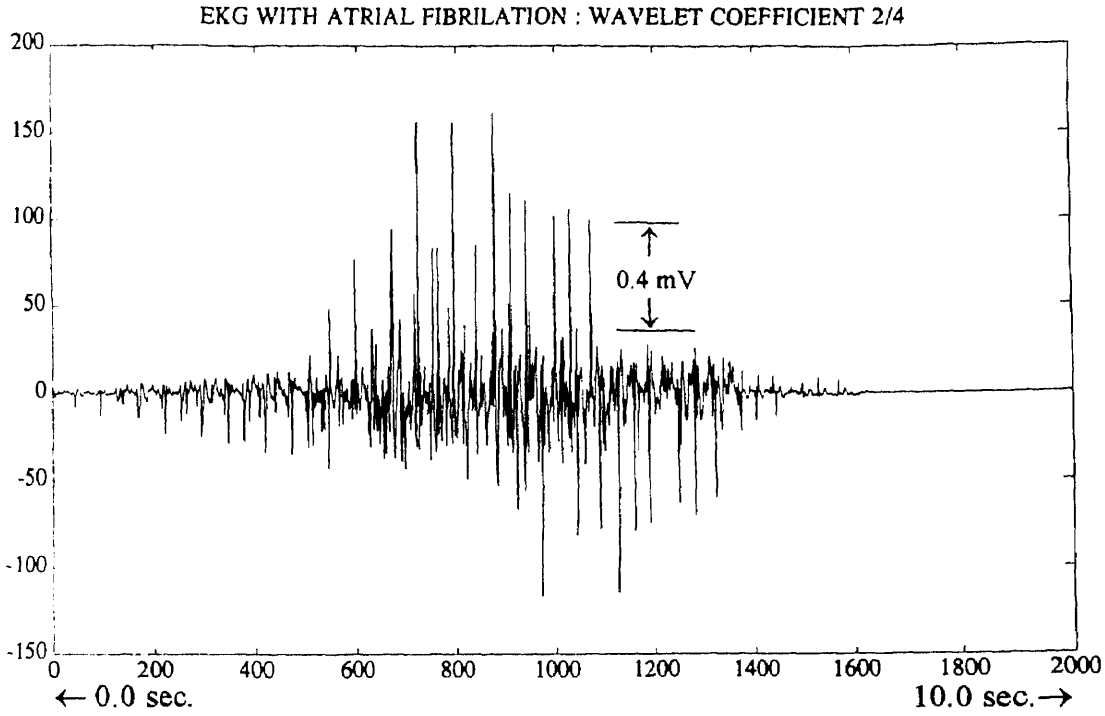

(a)

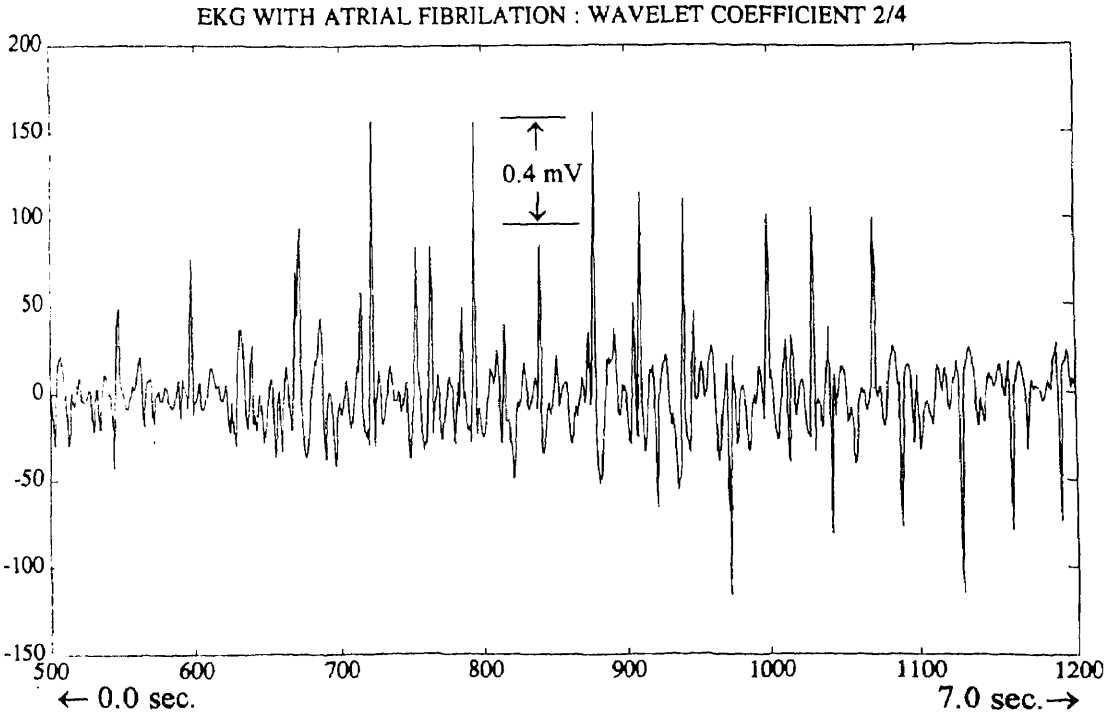

(b)

Figure 4.4.14 EKG with AFIBs

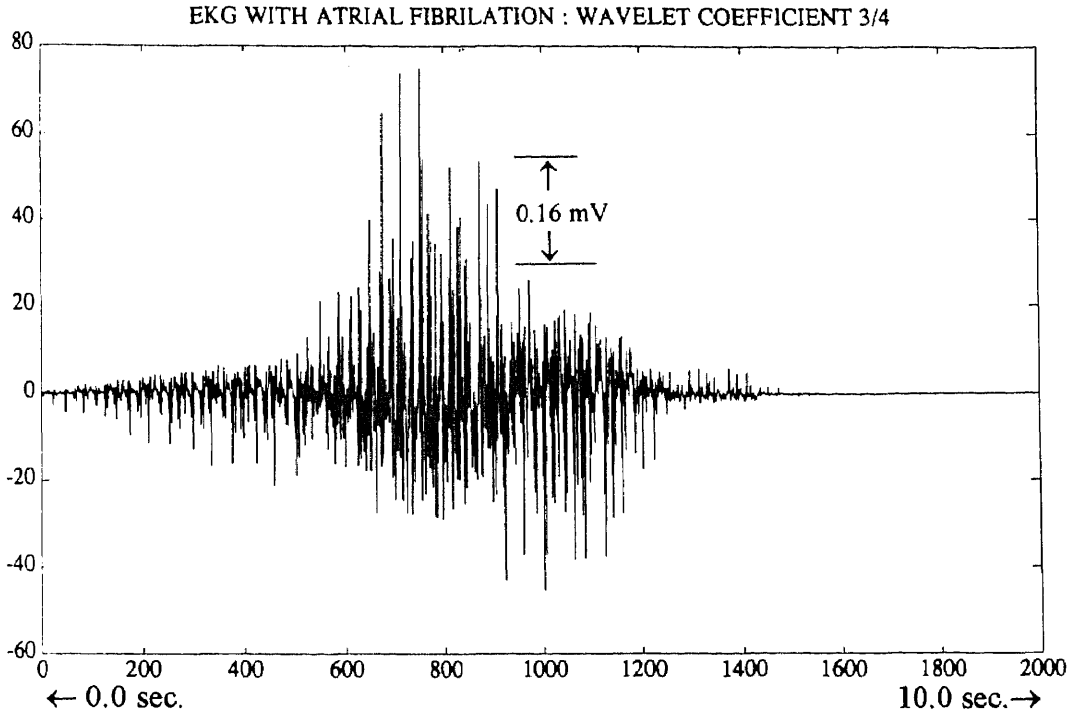

(a)

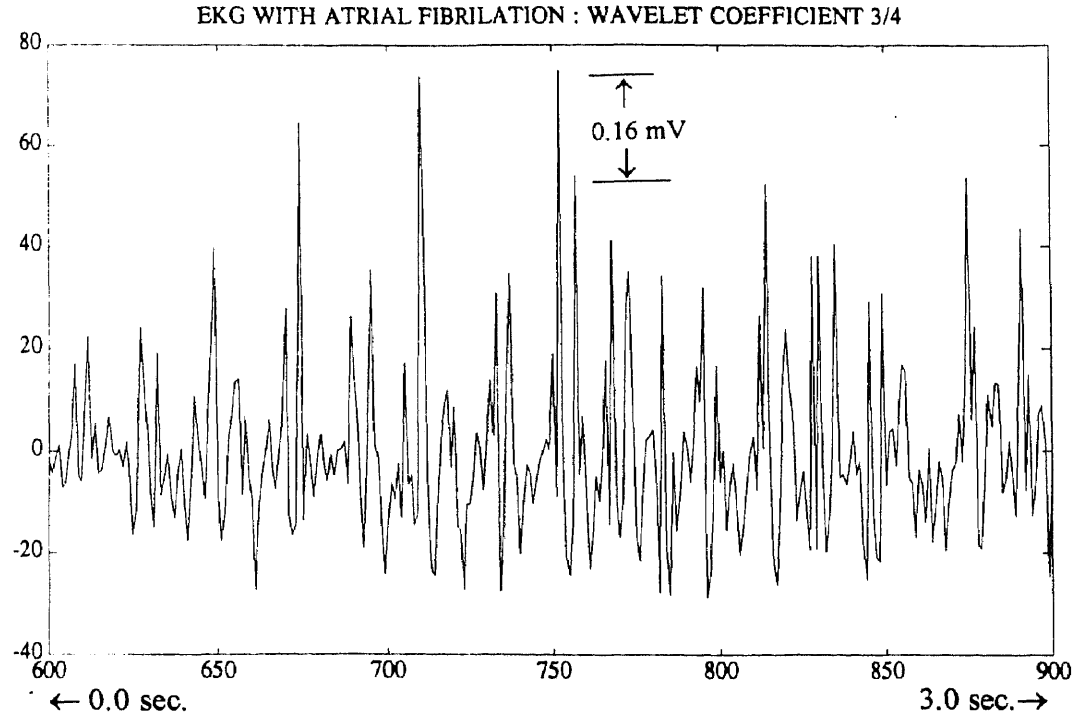

(b)

Figure 4.4.15 EKG with AFIBs

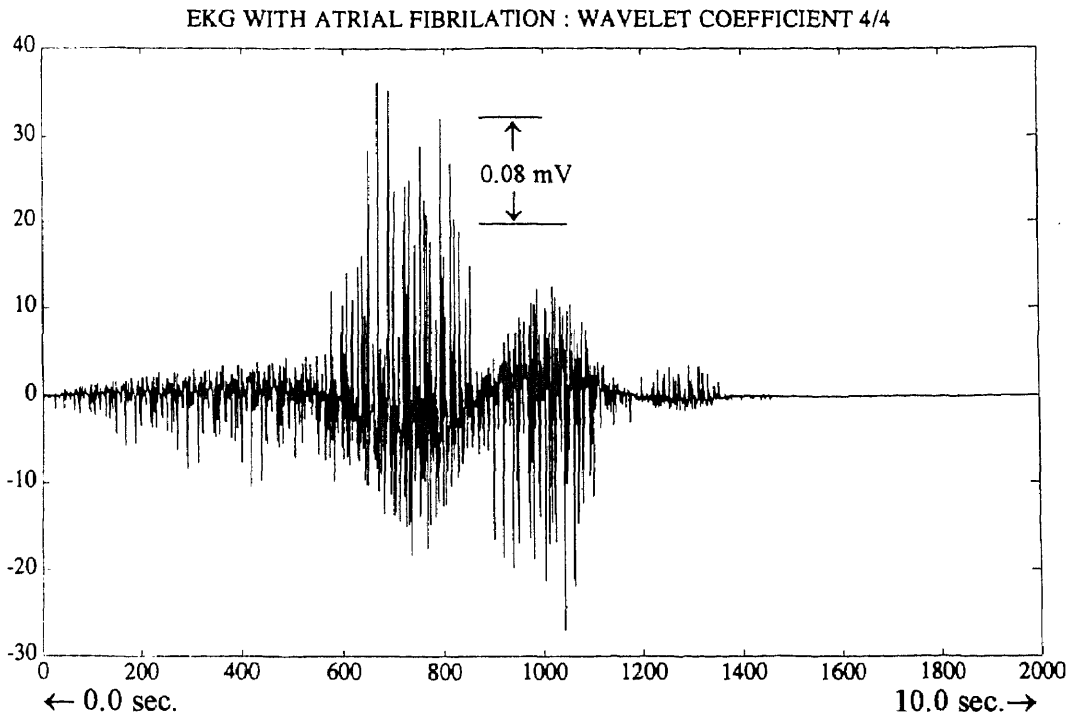

(a)

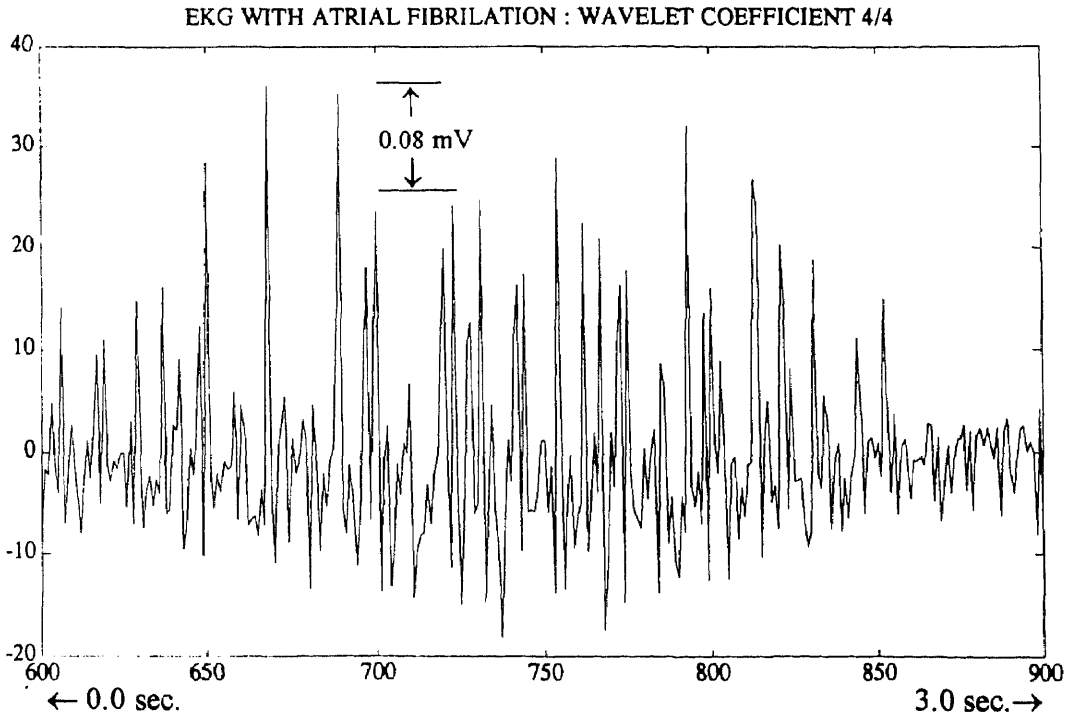

(b)

Figure 4.4.16 EKG with AFIBs

REFERENCES

1. Mark J. Shensa. "The Discrete Wavelet Transform: Wedding the A Trous and Mallat Algorithms." *IEEE Transactions on Signal Processing*, Vol. 40, No. 10, October 1992.

2. Martin Vetterli and Cormac Herley. "Wavelets and Filter Banks: Theory and, Design." *IEEE Transactions on Signal Processing*, Vol. 40, No. 9, September 1992.

3. Stephane G. Mallat. "A Theory for Multiresolution Signal Decomposition: The Wavelet Representation." *IEEE Transactions of Pattern Analysis and Machine Intelligence*, Vol. 11, NO. 7, July 1989.

4. Ahmed H. Tewfik, Deepen Sinha, and Paul Jorgensen. "On the Optimal Choice of a Wavelet for Signal Representation." *IEEE Transactions on Information Theory*, Vol. 38, No. 2, March 1992.

5. C.S. Burrus and R.A. Gopinath. "Introduction to Wavelets and Wavelet Transforms." ICASSP 93 Minneapolis, Minnesota, USA, April 26, 1993.

6. Sudhansu Chokroverty. Magnetic Stimulation in Clinical Neurophysiology. Butterworth Publishers, Stoneham, MA, 1990.

7. Ferdinando Grandori and Paolo Ravazzani. "Magnetic Stimulation of the Motor Cortex Theoretical Considerations." *IEEE Transactions on Biomedical Engineering*, Vol. 38, No. 2, February 1991.

8. A.T. Barker, B.Eng, Ph.D., IL. Freeston, R. Jalinous, and J.A. Jarratt, F.R.C.P. "Magnetic Stimulation of the Human Brain and Peripheral Nervous System: An Introduction and Results of an Initial Clinical Evaluation." *Congress of Neurological Surgeons*, Vol. 20, No. 1, U.S.A., 1987.

9. Leonardo G. Cohen, Bradley J. Roth, Jan Nillson, Nguyet Dang, Marcela Panizza, Stefania Bandinelli, Walter Friauf, and Mark Hallett. "Effects of coil design on delivery of focal magnetic stimulation. Technical considerations." Branch Division of Research Services, National Institute of Health, Bethesda, MD, August 9, 1989.

10. David B. Geselowitz. "On the Theory of the Electrocardiogram." *Proceedings of the IEEE*, Vol. 77, No. 6, June 1989.

11. Gerald J. Tortora and Nicholas P. Anagnostakos. Principles of Anatomy and Physiology, Sixth Edition. Harper and Row, Publishers, N.Y., N.Y., 1990.

12. John G. Webster. Medical Instrumentation, Application and Design, 2nd Edition. Houghton Mifflin Company, Boston, MA, 1992.

13. George M. Swisher. Introduction to Linear Systems Analysis. Matrix Publishers, Chesterland, OH, 1976.

14. Seymour Lipschutz. Schaum's Outline Series: Theory and Problems of Linear Algebra, 2nd Edition. McGraw-Hill Inc., N.Y., N.Y., 1991.

15. Michael Unser. "On the Asymptotic Convergence of B-Spline Wavelets to Gabor Functions." International Conference on Industrial and Applied Mathematics, Washington, DC, July 8, 1991.

16. Stephane G. Mallat. "A Theory for Multiresolution Signal Decomposition: The Wavelet Representation." *IEEE Transactions of Pattern Analysis and Machine Intelligence*, Vol. 11, No. 7, July 1989.

17. Roger Q. Cracco, M.D. and Ivan Bodis-Wollner, M.D. Evoked Potentials. Alan R. Liss Inc., N.Y., N.Y., 1986.

18. Keith H. Chia, P.P.A., M.D. Evoked Potentials in Clinical Medicine. Raven Press L.T.D., N.Y., N.Y., 1990.

19. Ali N. Akansu, Richard A Haddad, and Hakan Caglar. "The Binomial QMF-Wavelet Transform for Multiresolution Signal Decomposition." *IEEE Transactions on Signal Processing*, Vol. 41, No. 1, January 1993.

20. Hartmut Dickhaus, Labib Khadra, Alexandra Lipp, and Mark Schweizer. "Ventricular Late Potentials Studied by Nonstationary Signal Analysis."

21. L. Senhadji, G. Carrault, J.J. Bellanger, and G Passariello. "Some New Applications of the Wavelet Transforms."

22. Marc S. Fuller, Theodore Dustman, and Roger Freedman. "Wavelet Analysis of the Signal Averaged Electrocardiogram." Annual International conference of the IEEE Engineering in Medicine and Biology Society, Vol. 13, No. 2, 1991.

23. Jorge Bohorquez, Oliver Bertrand, Catherine Fischer, Patrick Bouchet, and Jacques Pernier. "Specific Time-Varying Digital Filtering Techniques for Intra-Operative Monitoring of Middle-Latency and Brainstem Auditory Evoked Potentials."

24. N.V. Thakor, H. Rix, and P. Caminal. "Wavelet Analysis of Evoked Potentials."

25. Gilbert Strang. "Wavelets and Dilation Equations: A Brief Introduction." *Society for Industrial and Applied Mathematics*, Vol. 21, No. 4, pp. 614-627, December 1989.

26. Iraj Sodagar, Kambiz Nayebi, and Thomas P. Barnwell, III. "A Class of Time-Varying Wavelet Transforms."

27. A. Grossman and J. Morlet. "Reading and Understanding Continuous Wavelet Transforms." Berlin Springer IPTI, 1989.

28. Paul Jorgensen. "Choosing Discrete Orthogonal Wavelets for Signal Analysis and Approximation."

29. Olivier Rioul and Pierre Duhamel. "Fast Algorithms for Discrete and Continuous Wavelet Transform." *IEEE Transactions on Information Theory*, Vol. 38, No. 2, March 1992.

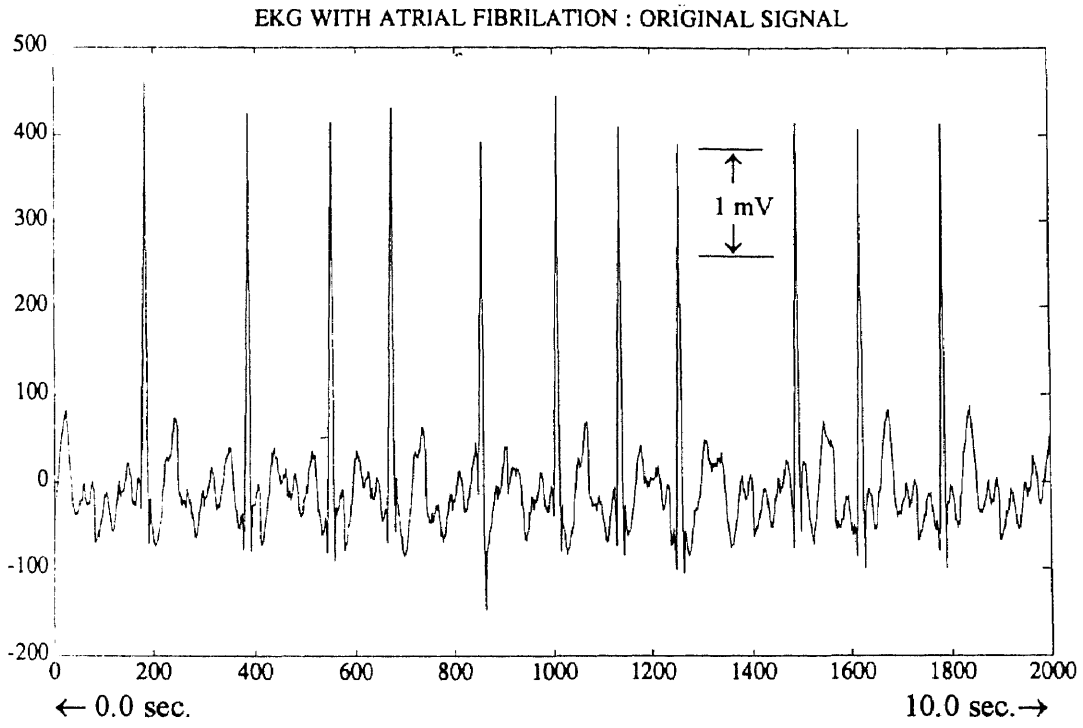

(a)

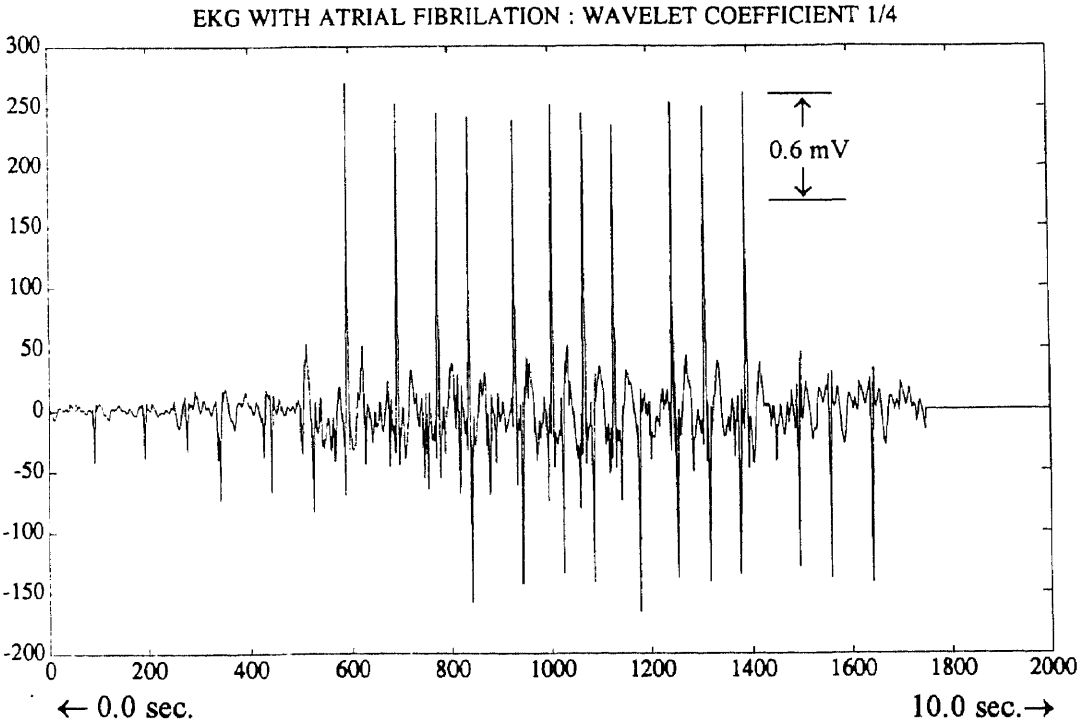

(b)

Figure 4.4.13 EKG with AFIBs

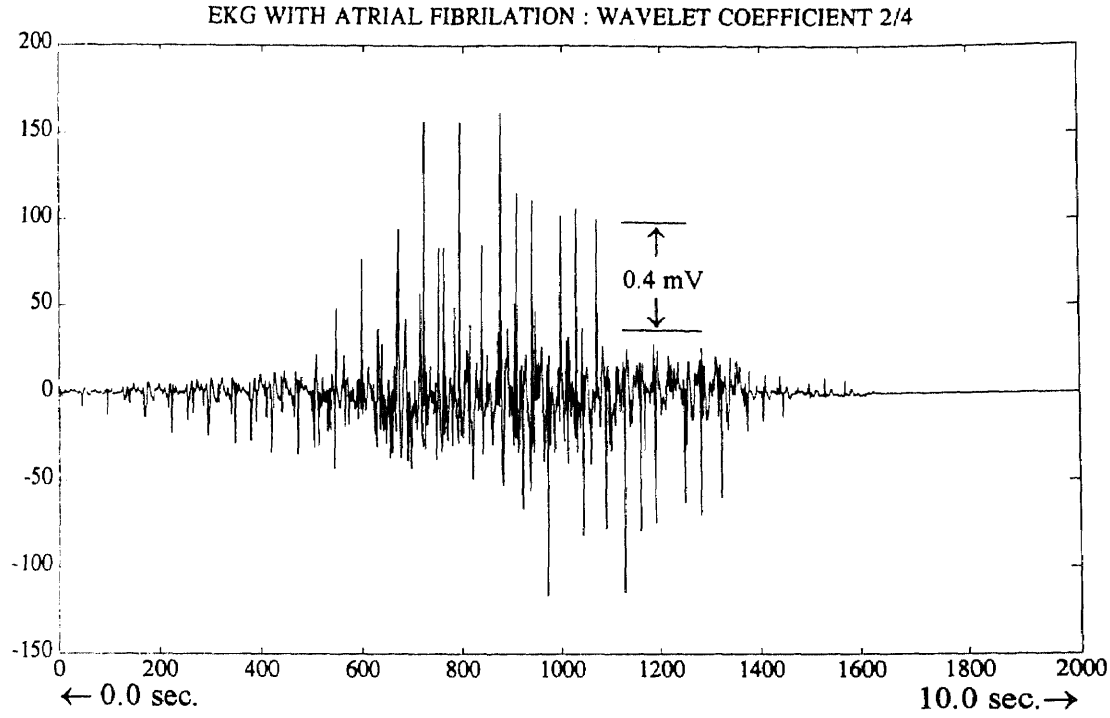

(a)

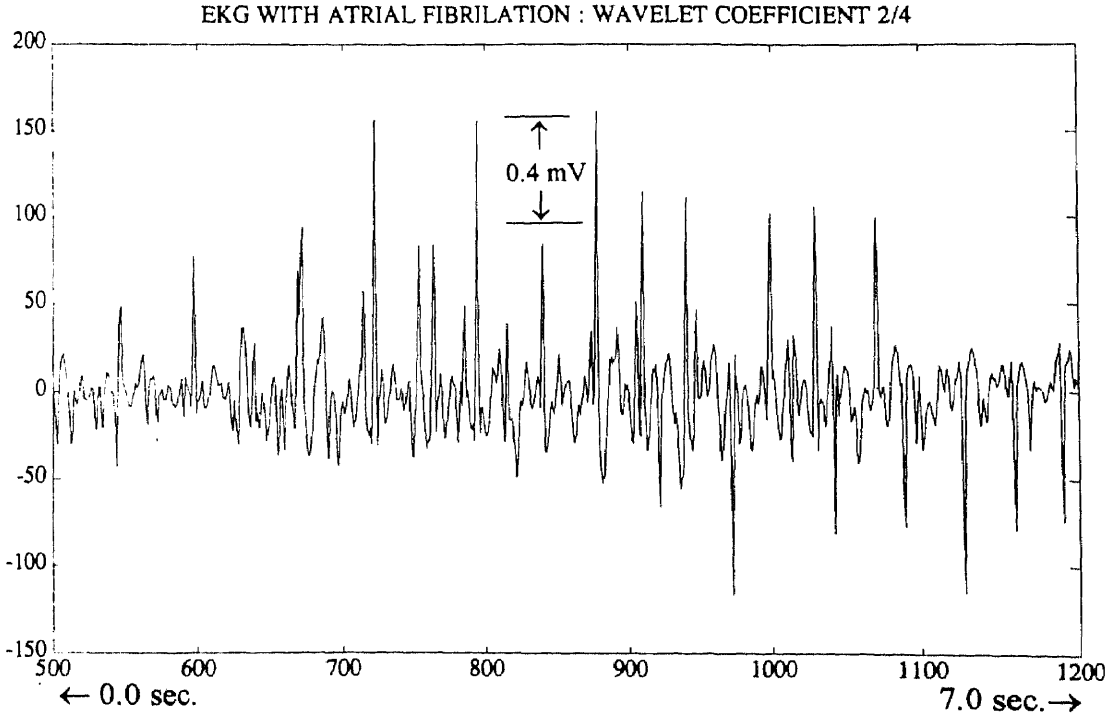

(b)

Figure 4.4.14 EKG with AFIBs

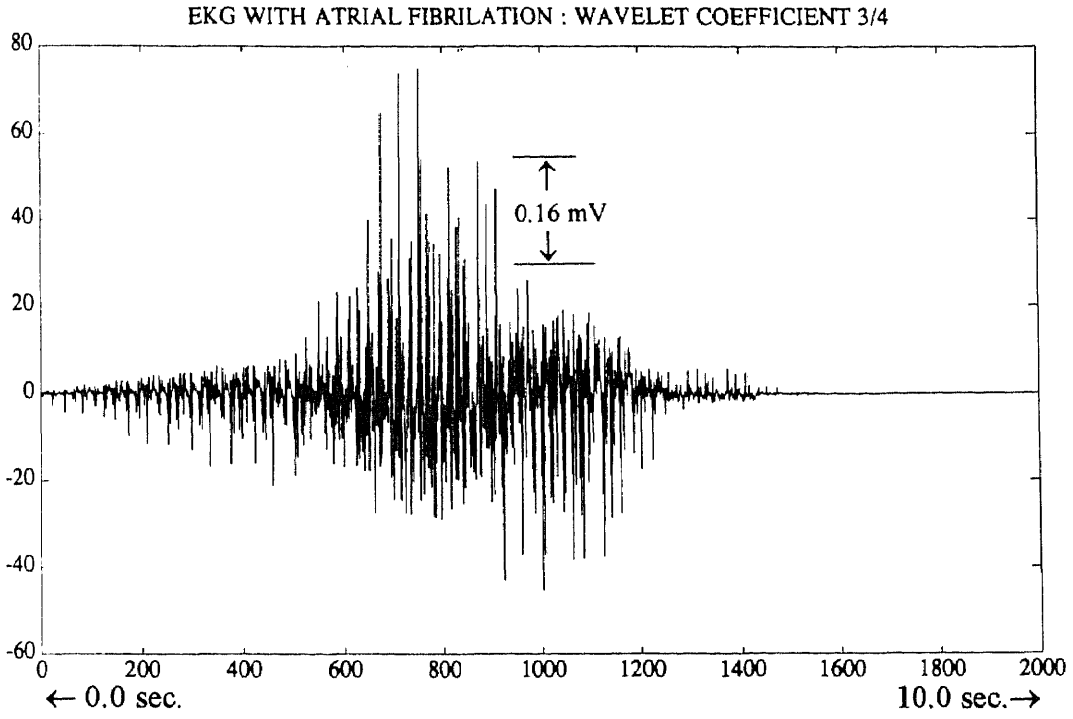

(a)

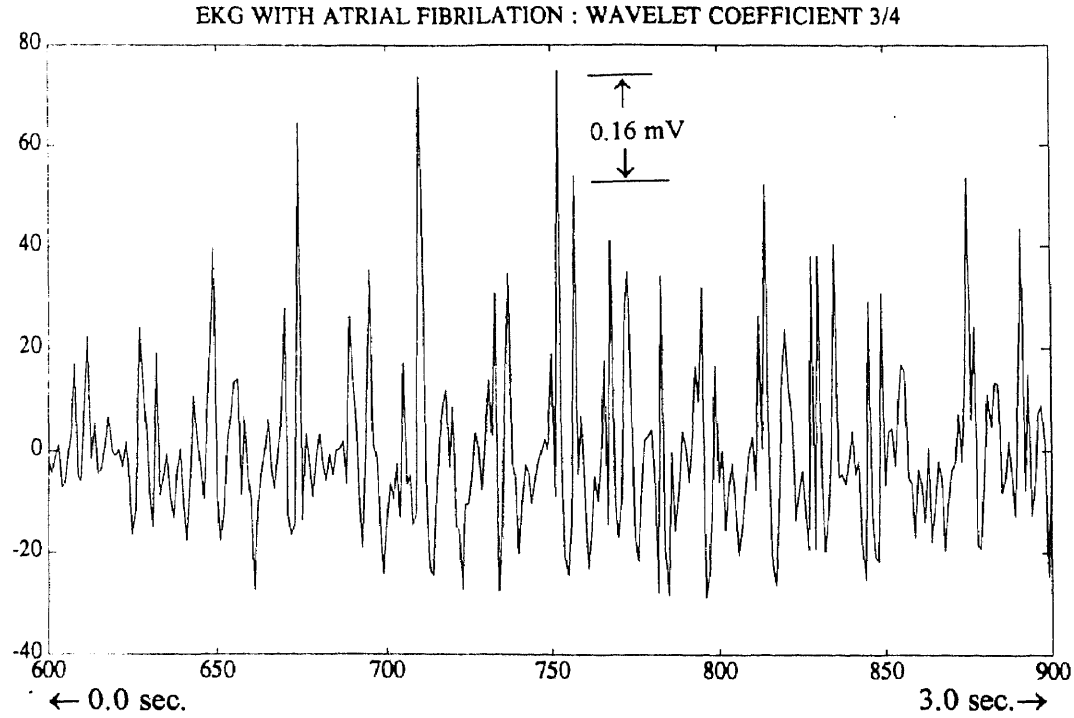

(b)

Figure 4.4.15 EKG with AFIBs

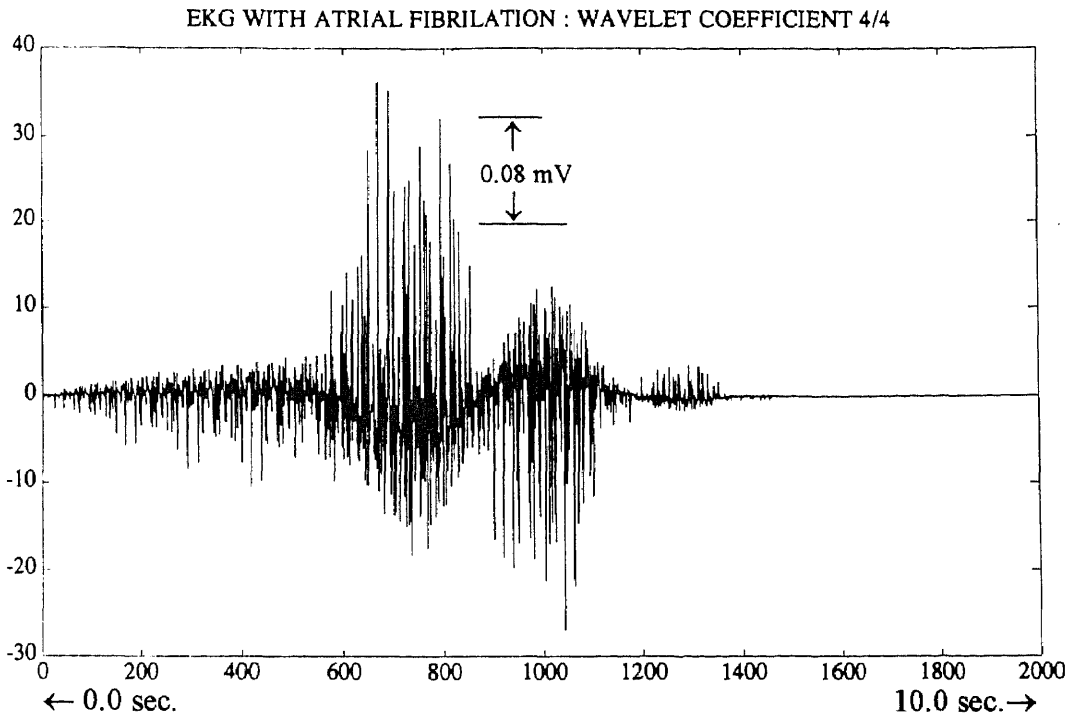

(a)

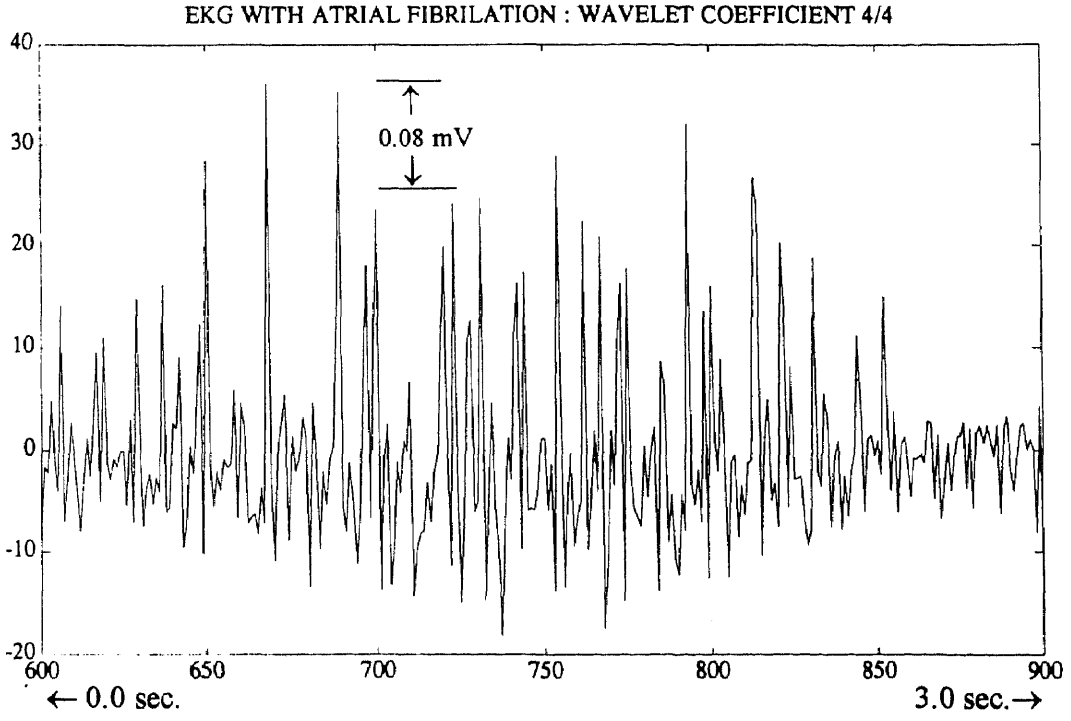

(b)

Figure 4.4.16 EKG with AFIBs

REFERENCES

1. Mark J. Shensa. "The Discrete Wavelet Transform: Wedding the A Trous and Mallat Algorithms." *IEEE Transactions on Signal Processing*, Vol. 40, No. 10, October 1992.

2. Martin Vetterli and Cormac Herley. "Wavelets and Filter Banks: Theory and, Design." *IEEE Transactions on Signal Processing*, Vol. 40, No. 9, September 1992.

3. Stephane G. Mallat. "A Theory for Multiresolution Signal Decomposition: The Wavelet Representation." *IEEE Transactions of Pattern Analysis and Machine Intelligence*, Vol. 11, NO. 7, July 1989.

4. Ahmed H. Tewfik, Deepen Sinha, and Paul Jorgensen. "On the Optimal Choice of a Wavelet for Signal Representation." *IEEE Transactions on Information Theory*, Vol. 38, No. 2, March 1992.

5. C.S. Burrus and R.A. Gopinath. "Introduction to Wavelets and Wavelet Transforms." ICASSP 93 Minneapolis, Minnesota, USA, April 26, 1993.

6. Sudhansu Chokroverty. Magnetic Stimulation in Clinical Neurophysiology. Butterworth Publishers, Stoneham, MA, 1990.

7. Ferdinando Grandori and Paolo Ravazzani. "Magnetic Stimulation of the Motor Cortex Theoretical Considerations." *IEEE Transactions on Biomedical Engineering*, Vol. 38, No. 2, February 1991.

8. A.T. Barker, B.Eng, Ph.D., IL. Freeston, R. Jalinous, and J.A. Jarratt, F.R.C.P. "Magnetic Stimulation of the Human Brain and Peripheral Nervous System: An Introduction and Results of an Initial Clinical Evaluation." *Congress of Neurological Surgeons*, Vol. 20, No. 1, U.S.A., 1987.

9. Leonardo G. Cohen, Bradley J. Roth, Jan Nillson, Nguyet Dang, Marcela Panizza, Stefania Bandinelli, Walter Friauf, and Mark Hallett. "Effects of coil design on delivery of focal magnetic stimulation. Technical considerations." Branch Division of Research Services, National Institute of Health, Bethesda, MD, August 9, 1989.

10. David B. Geselowitz. "On the Theory of the Electrocardiogram." *Proceedings of the IEEE*, Vol. 77, No. 6, June 1989.

11. Gerald J. Tortora and Nicholas P. Anagnostakos. Principles of Anatomy and Physiology, Sixth Edition. Harper and Row, Publishers, N.Y., N.Y., 1990.

12. John G. Webster. Medical Instrumentation, Application and Design, 2nd Edition. Houghton Mifflin Company, Boston, MA, 1992.

13. George M. Swisher. Introduction to Linear Systems Analysis. Matrix Publishers, Chesterland, OH, 1976.

14. Seymour Lipschutz. Schaum's Outline Series: Theory and Problems of Linear Algebra, 2nd Edition. McGraw-Hill Inc., N.Y., N.Y., 1991.

15. Michael Unser. "On the Asymptotic Convergence of B-Spline Wavelets to Gabor Functions." International Conference on Industrial and Applied Mathematics, Washington, DC, July 8, 1991.

16. Stephane G. Mallat. "A Theory for Multiresolution Signal Decomposition: The Wavelet Representation." *IEEE Transactions of Pattern Analysis and Machine Intelligence*, Vol. 11, No. 7, July 1989.

17. Roger Q. Cracco, M.D. and Ivan Bodis-Wollner, M.D. Evoked Potentials. Alan R. Liss Inc., N.Y., N.Y., 1986.

18. Keith H. Chia, P.P.A., M.D. Evoked Potentials in Clinical Medicine. Raven Press L.T.D., N.Y., N.Y., 1990.

19. Ali N. Akansu, Richard A Haddad, and Hakan Caglar. "The Binomial QMF-Wavelet Transform for Multiresolution Signal Decomposition." *IEEE Transactions on Signal Processing*, Vol. 41, No. 1, January 1993.

20. Hartmut Dickhaus, Labib Khadra, Alexandra Lipp, and Mark Schweizer. "Ventricular Late Potentials Studied by Nonstationary Signal Analysis."

21. L. Senhadji, G. Carrault, J.J. Bellanger, and G Passariello. "Some New Applications of the Wavelet Transforms."

22. Marc S. Fuller, Theodore Dustman, and Roger Freedman. "Wavelet Analysis of the Signal Averaged Electrocardiogram." Annual International conference of the IEEE Engineering in Medicine and Biology Society, Vol. 13, No. 2, 1991.

23. Jorge Bohorquez, Oliver Bertrand, Catherine Fischer, Patrick Bouchet, and Jacques Pernier. "Specific Time-Varying Digital Filtering Techniques for Intra-Operative Monitoring of Middle-Latency and Brainstem Auditory Evoked Potentials."

24. N.V. Thakor, H. Rix, and P. Caminal. "Wavelet Analysis of Evoked Potentials."

25. Gilbert Strang. "Wavelets and Dilation Equations: A Brief Introduction." *Society for Industrial and Applied Mathematics*, Vol. 21, No. 4, pp. 614-627, December 1989.

26. Iraj Sodagar, Kambiz Nayebi, and Thomas P. Barnwell, III. "A Class of Time-Varying Wavelet Transforms."

27. A. Grossman and J. Morlet. "Reading and Understanding Continuous Wavelet Transforms." Berlin Springer IPTI, 1989.

28. Paul Jorgensen. "Choosing Discrete Orthogonal Wavelets for Signal Analysis and Approximation."

29. Olivier Rioul and Pierre Duhamel. "Fast Algorithms for Discrete and Continuous Wavelet Transform." *IEEE Transactions on Information Theory*, Vol. 38, No. 2, March 1992.